



UNIVERSITAT DE
BARCELONA

Novel potential determinants in endoplasmic reticulum stress, inflammation and insulin resistance: Apo CIII and sAPP β

Gaia Botteri

ADVERTIMENT. La consulta d'aquesta tesi queda condicionada a l'acceptació de les següents condicions d'ús: La difusió d'aquesta tesi per mitjà del servei TDX (www.tdx.cat) i a través del Dipòsit Digital de la UB (diposit.ub.edu) ha estat autoritzada pels titulars dels drets de propietat intel·lectual únicament per a usos privats emmarcats en activitats d'investigació i docència. No s'autoritza la seva reproducció amb finalitats de lucre ni la seva difusió i posada a disposició des d'un lloc aliè al servei TDX ni al Dipòsit Digital de la UB. No s'autoritza la presentació del seu contingut en una finestra o marc aliè a TDX o al Dipòsit Digital de la UB (framing). Aquesta reserva de drets afecta tant al resum de presentació de la tesi com als seus continguts. En la utilització o cita de parts de la tesi és obligat indicar el nom de la persona autora.

ADVERTENCIA. La consulta de esta tesis queda condicionada a la aceptación de las siguientes condiciones de uso: La difusión de esta tesis por medio del servicio TDR (www.tdx.cat) y a través del Repositorio Digital de la UB (diposit.ub.edu) ha sido autorizada por los titulares de los derechos de propiedad intelectual únicamente para usos privados enmarcados en actividades de investigación y docencia. No se autoriza su reproducción con finalidades de lucro ni su difusión y puesta a disposición desde un sitio ajeno al servicio TDR o al Repositorio Digital de la UB. No se autoriza la presentación de su contenido en una ventana o marco ajeno a TDR o al Repositorio Digital de la UB (framing). Esta reserva de derechos afecta tanto al resumen de presentación de la tesis como a sus contenidos. En la utilización o cita de partes de la tesis es obligado indicar el nombre de la persona autora.

WARNING. On having consulted this thesis you're accepting the following use conditions: Spreading this thesis by the TDX (www.tdx.cat) service and by the UB Digital Repository (diposit.ub.edu) has been authorized by the titular of the intellectual property rights only for private uses placed in investigation and teaching activities. Reproduction with lucrative aims is not authorized nor its spreading and availability from a site foreign to the TDX service or to the UB Digital Repository. Introducing its content in a window or frame foreign to the TDX service or to the UB Digital Repository is not authorized (framing). Those rights affect to the presentation summary of the thesis as well as to its contents. In the using or citation of parts of the thesis it's obliged to indicate the name of the author.

VLDL and apolipoprotein CIII induce ER stress and inflammation and attenuate insulin signalling via Toll-like receptor 2 in mouse skeletal muscle cells

Gaia Botteri^{1,2,3} · Marta Montori^{1,2,3} · Anna Gumà^{2,4} · Javier Pizarro^{1,2,3} · Lidia Cedó^{2,5} · Joan Carles Escolà-Gil^{2,5,6} · Diana Li⁷ · Emma Barroso^{1,2,3} · Xavier Palomer^{1,2,3} · Alison B. Kohan⁷ · Manuel Vázquez-Carrera^{1,2,3}

Received: 15 May 2017 / Accepted: 30 June 2017 / Published online: 23 August 2017
© Springer-Verlag GmbH Germany 2017

Abstract

Aim/hypothesis Here, our aim was to examine whether VLDL and apolipoprotein (apo) CIII induce endoplasmic reticulum (ER) stress, inflammation and insulin resistance in skeletal muscle.

Methods Studies were conducted in mouse C2C12 myotubes, isolated skeletal muscle and skeletal muscle from transgenic mice overexpressing apoCIII.

Results C2C12 myotubes exposed to VLDL showed increased levels of ER stress and inflammatory markers whereas peroxisome proliferator-activated receptor γ co-activator 1 α

(PGC-1 α) and AMP-activated protein kinase (AMPK) levels were reduced and the insulin signalling pathway was attenuated. The effects of VLDL were also observed in isolated skeletal muscle incubated with VLDL. The changes caused by VLDL were dependent on extracellular signal-regulated kinase (ERK) 1/2 since they were prevented by the ERK1/2 inhibitor U0126 or by knockdown of this kinase by siRNA transfection. ApoCIII mimicked the effects of VLDL and its effects were also blocked by ERK1/2 inhibition, suggesting that this apolipoprotein was responsible for the effects of VLDL. Skeletal muscle from transgenic mice overexpressing apoCIII showed increased levels of some ER stress and inflammatory markers and increased phosphorylated ERK1/2 levels, whereas PGC-1 α levels were reduced, confirming apoCIII effects in vivo. Finally, incubation of myotubes with a neutralising antibody against Toll-like receptor 2 abolished the effects of apoCIII on ER stress, inflammation and insulin resistance, indicating that the effects of apoCIII were mediated by this receptor.

Conclusions/interpretation These results imply that elevated VLDL in diabetic states can contribute to the exacerbation of insulin resistance by activating ERK1/2 through Toll-like receptor 2.

Keywords AMPK · apoCIII · ERK1/2 · TLR2 · VLDL

Electronic supplementary material The online version of this article (doi:10.1007/s00125-017-4401-5) contains peer-reviewed but unedited supplementary material, which is available to authorised users.

✉ Manuel Vázquez-Carrera
mvazquezcarrera@ub.edu

¹ Pharmacology Unit, Department of Pharmacology, Toxicology and Therapeutic Chemistry, Faculty of Pharmacy and Food Sciences, Institut de Biomedicina de la Universidad de Barcelona (IBUB), University of Barcelona, Diagonal 643, E-08028 Barcelona, Spain

² Centro de Investigación Biomédica en Red de Diabetes y Enfermedades Metabólicas Asociadas (CIBERDEM), Instituto de Salud Carlos III, Barcelona, Spain

³ Institut de Recerca Sant Joan de Déu (IR-SJD), Esplugues de Llobregat, Barcelona, Spain

⁴ Department of Biochemistry and Molecular Biology and IBUB, University of Barcelona, Barcelona, Spain

⁵ Institut d'Investigacions Biomèdiques (IIB) Sant Pau, Barcelona, Spain

⁶ Department of Biochemistry and Molecular Biology, Autonomous University of Barcelona, Barcelona, Spain

⁷ Department of Nutritional Sciences, University of Connecticut, Storrs, CT, USA

Abbreviations

ACC	Acetyl-CoA carboxylase
AMPK	AMP-activated protein kinase
Apo	Apolipoprotein
apoCIII Tg	Transgenic mice overexpressing human apoCIII
BiP	Binding immunoglobulin protein
CPT-1	Carnitine palmitoyltransferase 1

CHOP	CCAAT-enhancer-binding protein homologous protein
eIF2 α	Eukaryotic initiation factor 2 α
EMSA	Electrophoretic mobility shift assay
ER	Endoplasmic reticulum
ERK	Extracellular signal-regulated kinase
FAO	Fatty acid oxidation
GRP78	Glucose-regulated protein 78
I κ B	Inhibitor of κ B
IKK- β	I κ B kinase β
IR β	Insulin receptor β -subunit
IRE-1 α	Inositol-requiring 1 transmembrane kinase/endonuclease-1 α
MAPK	Mitogen-activated protein kinase
MCAD	Medium chain acyl-CoA dehydrogenase
MCP-1	Monocyte chemoattractant protein 1
MEK	MAPK–ERK
NRF1	Nuclear respiratory factor 1
NRF2	Nuclear factor-E2-related factor 2
OXPHOS	Oxidative phosphorylation
PERK	Eukaryotic translation initiation factor-2 α kinase 3
PGC-1 α	Peroxisome proliferator-activated receptor γ co-activator 1 α
PPAR	Peroxisome proliferator-activated receptor
SOCS	Suppressor of cytokine signalling 3
STAT3	Signal transducer and activator of transcription 3
TLR	Toll-like receptor
TRB3	Tribbles 3
UPR	Unfolded protein response
XBP1	X-box binding protein-1

Introduction

Insulin resistance and type 2 diabetes mellitus are characterised by the presence of atherogenic dyslipidaemia, which includes the following cluster of abnormalities: high levels of triacylglycerols, low levels of HDL-cholesterol and the appearance of small, dense LDLs [1]. Atherogenic dyslipidaemia frequently precedes type 2 diabetes mellitus by several years, indicating that derangement of lipid metabolism is an early event in the development of this disease [2]. It is now well accepted that the different components of atherogenic dyslipidaemia are closely linked and are initiated by insulin resistance through overproduction of triacylglycerol-rich VLDL [1, 2]. In addition to triacylglycerols, VLDLs also contain apolipoproteins, of which apolipoprotein (apo) CIII is one of the most abundant [3] with levels that are closely correlated with serum triacylglycerol levels [4]. Plasma apoCIII increases plasma triacylglycerols predominantly through the inhibition of VLDL hydrolysis by lipoprotein lipase and by

inhibiting chylomicron and VLDL clearance by the liver [5], but it also causes inflammation in endothelial cells [6]. Furthermore, some studies have associated elevated circulating apoCIII with insulin resistance [7], although others did not find a relationship [8].

Whereas the effects of insulin resistance on lipoprotein metabolism have been studied extensively [1, 2], little is known about the effects of elevated VLDL and apoCIII on the molecular mechanism of insulin resistance in skeletal muscle cells. This is important, since the primary site of insulin-stimulated glucose disposal is skeletal muscle and this can account for up to 90% of glucose clearance [9]. As a result, loss of skeletal muscle insulin sensitivity is believed to be critical in the pathogenesis of type 2 diabetes [10]. The mechanisms involved in the development of insulin resistance are currently unclear, but accumulating evidence points to the presence of a chronic low-level inflammatory process [11]. Among other mechanisms, endoplasmic reticulum (ER) stress [12] and Toll-like receptors (TLRs) [13] can activate proinflammatory signalling pathways, including inhibitor of κ B (I κ B) kinase β (IKK- β)–NF- κ B. Thus, IKK- β phosphorylates IRS-1 on serine residues, attenuating the insulin signalling pathway whereas, once activated, NF- κ B regulates the expression of multiple inflammatory mediators, which also contribute to insulin resistance [11].

In the present study, we examined whether VLDL and apoCIII induce ER stress, inflammation and insulin resistance in skeletal muscle cells.

Methods

Materials *Escherichia coli* (K12 strain) lipopolysaccharide (ultrapure) and PAM3CSK4 (tripalmitoylated cysteine-, serine- and lysine-containing peptide) were purchased from InvivoGen (San Diego, CA, USA). LDH Cytotoxicity Assay Kit (88953) was from Thermo Scientific (Waltham, MA, USA) and the Elisa kit for measuring IL-6 secretion (Novex, KMC0061) was from Life Technologies (Carlsbad, CA, USA).

Plasma VLDL isolation VLDL particles (< 1.006 g/ml) were isolated by ultracentrifugation at 100,000g for 24 h from normolipidaemic human plasma obtained in EDTA-containing vacutainer tubes (total cholesterol \leq 5.2 mmol/l, triacylglycerols \leq 1 mmol/l). To obtain VLDL particles containing low or high amounts of apoCIII, we further isolated light VLDL (Svedberg flotation units 60–400) from normolipidaemic and hypertriacylglycerolaemic (triacylglycerols \geq 2.5 mmol/l) human plasma by ultracentrifugation at 56,000g for 1 h. VLDL preparations were extensively dialysed in PBS and then triacylglycerol and apoB concentrations were measured using a commercial kit adapted to a

COBAS c501 autoanalyser (Roche Diagnostics, Rotkreuz, Switzerland). ApoB/triacylglycerol ratios were similar in both light VLDL preparations. ApoCIII levels were determined using a nephelometric commercial kit (Kamiya Biomedical Company, Seattle, WA, USA) adapted to COBAS c501 autoanalyser. Cells were treated with 300 $\mu\text{g/ml}$ of filtered VLDL, based on triacylglycerol concentration, as previously described [14].

Cell culture Mouse mycoplasma free C2C12 cells (ATCC, Manassas, VA, USA) were maintained, grown and differentiated to myotubes as previously described [15]. ATCC provided authentication of the cells. Where indicated, cells were treated with 10 $\mu\text{mol/l}$ U0126, 100 $\mu\text{g/ml}$ apoCIII (purity > 95%) (Abcam, Cambridge, UK), 50 $\mu\text{g/ml}$ TLR2 neutralising antibody (InvivoGen) or control non-immune IgG for 24 h. Cells were transiently transfected with 50 nmol/l siRNA against extracellular signal-regulated kinase (ERK) 1/2 (Santa Cruz, Dallas, TX, USA) and siRNA control using Lipofectamine 2000 (Life Technologies) according to the manufacturer's instructions.

Animals Skeletal muscle (gastrocnemius) samples from male wild-type and transgenic mice overexpressing human apoCIII (apoCIII Tg; C57BL/6J background) were frozen in liquid nitrogen and then stored at -80°C . For ex vivo experiments,

skeletal muscles were isolated from male C57BL/6J mice (6–8 weeks old) and mounted in an incubation bath as previously described [16] in the presence or absence of 500 $\mu\text{g/ml}$ VLDL. Experimenters were not blind to group assignment or outcome assessment. For further details, please refer to the electronic supplementary material (ESM) **Methods**.

RNA preparation and quantitative RT-PCR Relative levels of specific mRNAs were assessed by real-time PCR, as previously described [15]. For details, see ESM **Methods**. The primer sequences used are shown in ESM Table 1.

Immunoblotting Isolation of total and nuclear protein extracts was performed as described elsewhere [15]. Western blot analysis was performed using antibodies against total (1:1000, 9272) and phospho-Akt (Ser⁴⁷³) (1:1000, 9271), glucose-regulated protein78 (GRP78)/binding immunoglobulin protein (BiP) (1:1000, 3177), insulin receptor β -subunit (IR β) (1:1000, 3020), CCAT-enhancer-binding protein homologous protein (CHOP) (1:1000, 5554), total eukaryotic initiation factor 2 α (eIF2 α) (1:1000, 9722) and phospho-eIF2 α (Ser⁵¹) (1:1000, 9721S), total signal transducer and activator of transcription 3 (STAT3) (1:1000, 9132) and phospho-STAT3 (Tyr⁷⁰⁵) (1:1000, 9131), total extracellular signal-regulated kinase (ERK) 1/2 (1:1000, 9102) and phospho-ERK1/2 (Thr²⁰²/Tyr²⁰⁴) (1:1000, 9101), total

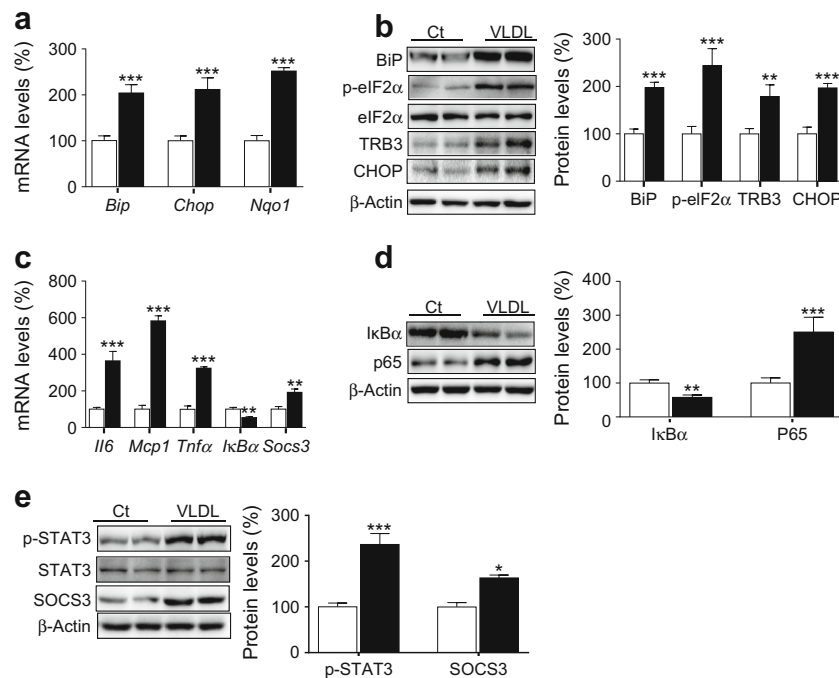


Fig. 1 VLDL induces ER stress and inflammation. Mouse C2C12 myotubes were incubated in the presence (black bars) or absence (control, Ct, white bars) of 300 $\mu\text{g/ml}$ VLDL for 24 h. **(a)** mRNA abundance of *Bip*, *Chop* and *Nqo1*. mRNA levels are normalised to *Apr1* ($n = 8-10$, five independent C2C12 cultures were used). **(b)** BiP, phospho-eIF2 α (Ser⁵¹), TRB3, CHOP and β -actin protein levels. **(c)**, mRNA abundance of *Il6*,

Mcp1, *Tnf α* , *I κ B α* and *Socs3*. **(d)** I κ B α , p65 and β -actin protein levels. **(e)** Phospho-STAT3 (Tyr⁷⁰⁵), SOCS3 and β -actin protein levels. The graphs show quantification expressed as a percentage of control samples. Data are means \pm SD of five independent experiments and were compared by Student's *t* test. * $p < 0.05$, ** $p < 0.01$ and *** $p < 0.001$ vs control

acetyl-CoA carboxylase (ACC) (1:1000, 3662) and phospho-ACC (Ser⁷⁹) (1:1000, 3661), NQO1 (1:500, 62,262), nuclear respiratory factor 1 (NRF1) (1:500, 12,381), nuclear factor-E2-related factor 2 (NRF2) (1:500, 4399), phospho-IRS-1 (Ser³⁰⁷) (1:500, 2381), I κ B α (1:500, 9242), p65 (1:500, 3034), total AMP-activated protein kinase (AMPK) (1:1000, 2532) and phospho-AMPK (Thr¹⁷²) (1:1000, 2531) (all from Cell Signaling Technology, Danvers, MA, USA; numbers indicate catalogue number), oxidative phosphorylation (1:1000, ab110413) (OXPHOS), peroxisome proliferator-activated receptor γ co-activator 1 α (PGC-1 α ; (1:1000, ab54481) (Abcam), OCT-1 (1:500, sc-8024X), peroxisome proliferator-activated receptor (PPAR) β/δ (1:500, sc-7197), prohibitin (1:500, sc-377037), suppressor of cytokine signaling 3 (SOCS3) (1:500, sc-51699), Tribbles 3 (TRB3) (1:500, sc-365842), glyceraldehyde 3-phosphate dehydrogenase (1:500, sc-32233), total IRS-1 (1:500, sc-560) and β -actin (1:500, sc-47778) (all from Santa Cruz; numbers indicate catalogue number). Detection was achieved using the Western Lightning Plus-ECL chemiluminescence kit (PerkinElmer, Waltham, MA, USA). The equal loading of proteins was assessed by Ponceau S staining. For validation, we used a protein marker (Precision Plus Protein Dual Color Standards 1610374; Bio-Rad, Hercules, CA, USA), on the same blots. All of these commercially available antibodies showed a single distinct band at the molecular weight indicated in the datasheets.

Electrophoretic mobility shift assay The electrophoretic mobility shift assay (EMSA) was performed as described in ESM Methods.

2-Deoxy-D-(1,2-[³H]N)glucose uptake Glucose uptake experiments were performed as described in ESM Methods.

Image analysis The chemiluminescent blots were imaged using the ChemiDoc MP imager (Bio-Rad). Image acquisition and subsequent densitometric analysis of the corresponding blots were performed using ImageLab software version 4.1 (Bio-Rad). For further details, see ESM Methods.

Statistical analyses Results were normalised to levels in control groups and are expressed as mean \pm SD. Significant differences were established by either Student's *t* test or two-way ANOVA, according to the number of groups compared, using GraphPad Prism V4.03 software (GraphPad Software, San Diego, CA, USA). When significant variations were found by two-way ANOVA, the Tukey–Kramer multiple comparison post hoc test was performed. Differences were considered significant at $p < 0.05$.

Results

VLDL induces ER stress, inflammation and insulin resistance in myotubes VLDL exposure significantly increased expression of the ER stress markers *Bip* (also known as *Hspa5*), *Chop* (*Ddit3*) and *Nqo1*, the latter being an NRF2-target gene activated by ER stress (Fig. 1a). Consistent with

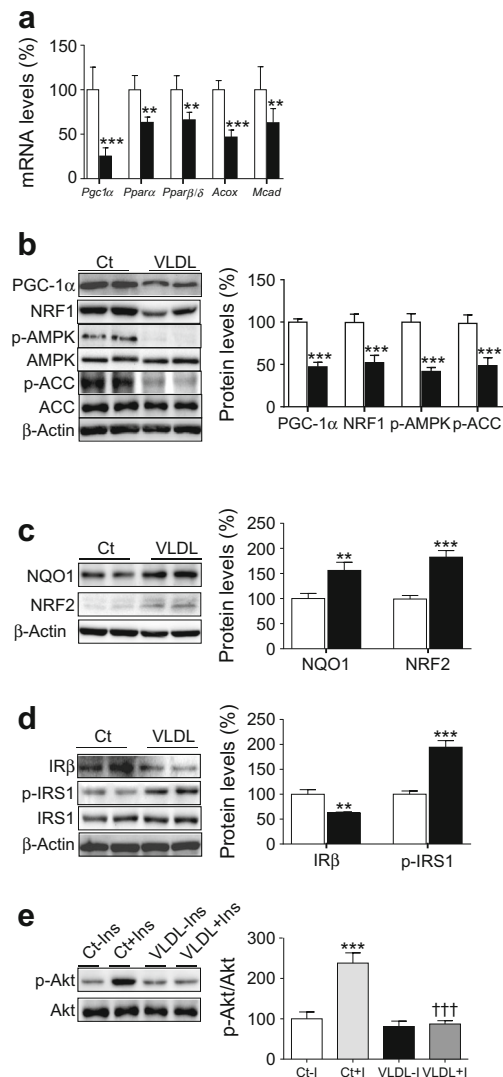


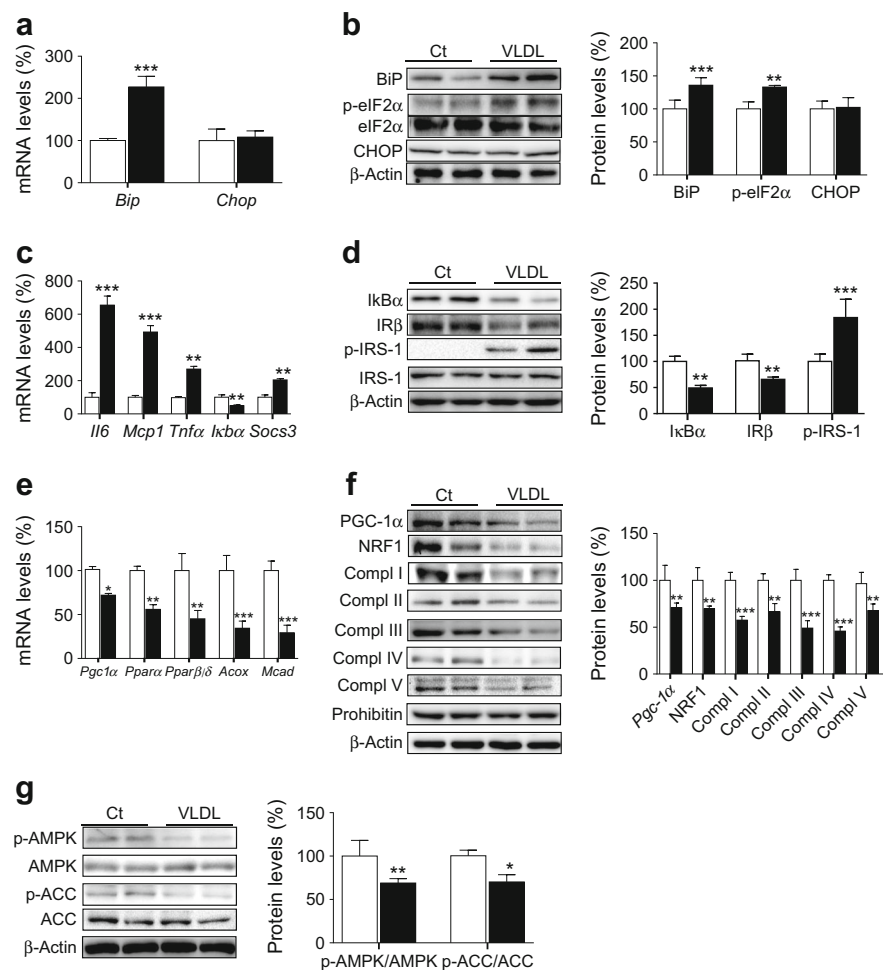
Fig. 2 VLDL reduces PGC-1 α and AMPK levels and induces insulin resistance. Mouse C2C12 myotubes were incubated in the presence (black bars) or absence (control, Ct, white bars) of 300 μ g/ml VLDL for 24 h. (a) *Pgc1α*, *Pparα* (*Ppara*), *Pparβ/δ* (*Pparb/Ppard*), *Acox* and *Mcad* mRNA levels ($n = 8–10$, five independent C2C12 cultures were used). (b) PGC-1 α , NRF1, phospho-AMPK (Thr¹⁷²), phospho-ACC (Ser⁷⁹) and β -actin protein levels. (c) NQO1, NRF2 and β -actin protein levels. (d) IR β , phospho-IRS-1 (Ser³⁰⁷), and β -actin protein levels. (e) Phospho-Akt (Ser⁴⁷³) protein levels. Where indicated, cells were incubated with 100 nmol/l insulin (Ins, I) for the last 10 min. The graphs show quantification expressed as a percentage of control samples. Data are means \pm SD of five independent experiments and compared by Student's *t* test (a–d) or two-way ANOVA followed by Tukey post hoc test (e). ** $p < 0.01$ and *** $p < 0.001$ vs control; ††† $p < 0.001$ vs control cells incubated with insulin

the presence of VLDL-induced ER stress, the protein levels of BiP, phospho-eIF2 α , CHOP and TRB3, a pseudokinase that mediates ER stress-induced insulin resistance in myotubes [17], were increased by VLDL (Fig. 1b). VLDL exposure also increased the mRNA levels of inflammatory genes such as *Il6*, *Mcp1* (also known as *Ccl2*) and *Tnf α* (*Tnf*), whereas the mRNA expression of the NF- κ B inhibitor *I κ B α* (*Nfkbia*) was reduced (Fig. 1c). IL-6 induces insulin resistance by activating STAT3, which in turn upregulates the transcription of SOCS3. SOCS3 inhibits insulin signalling through several distinct mechanisms, including IRS degradation [18]. In agreement with the increase in IL-6 expression, the mRNA levels of *Socs3* were also increased after VLDL exposure (Fig. 1c). The potential activation of the NF- κ B pathway by VLDL was confirmed by the presence of reduced protein levels of *I κ B α* and enhanced levels of the p65 subunit of NF- κ B (Fig. 1d). Similarly, increased protein levels of phospho-STAT3 (phosphorylated at Tyr⁷⁰⁵) and SOCS3 demonstrated the activation of the STAT3–SOCS3 pathway by VLDL (Fig. 1e).

Mitochondrial function is transcriptionally controlled by PGC-1 α [19], which plays a critical role in skeletal muscle metabolic function. In fact, some studies indicate that the

reported reduction in PGC-1 α expression and/or function in the skeletal muscle of individuals who have diabetes or are at risk for diabetes [20, 21] induces insulin resistance by reducing oxidative phosphorylation and lipid oxidation, leading to accumulation of lipid derivatives in skeletal muscle [22]. Myotubes exposed to VLDL showed a reduction in the mRNA expression of *Pgc1 α* (also known as *Ppargc1a*) (Fig. 2a). This transcriptional co-activator regulates the activity of several transcription factors, including PPAR α and PPAR β/δ , which control the expression/function of genes involved in fatty acid oxidation (FAO) [23]. The expression of these transcription factors and that of their target genes involved in FAO, such as those encoding acyl-coA oxidase (*Acox*, also known as *Acox1*) and medium chain acyl-CoA dehydrogenase (*Mcad*, also known as *Acadm*), was also decreased by VLDL (Fig. 2a). In addition, PGC-1 α protein levels were downregulated by VLDL and, consistent with this reduction, the protein levels of its downstream transcription factor NRF1 [24] were also reduced (Fig. 2b). FAO is also under the control of AMPK, whose activation exerts multiple protective effects, including inhibition of inflammation and insulin resistance [25]. Activation of this kinase upregulates PGC-1 α levels and

Fig. 3 VLDL induces ER stress and inflammation, reduces the levels of mitochondrial proteins and attenuates the insulin signalling pathway in isolated skeletal muscle. Mouse gastrocnemius muscles were incubated in the presence (black bars) or absence (control, Ct, white bars) of 500 μ g/ml VLDL for 6 h. **(a)** mRNA abundance of *Bip* and *Chop*. **(b)** BiP, Phospho-eIF2 α (Ser⁵¹), CHOP and β -actin protein levels. **(c)** mRNA abundance of *Il6*, *Mcp1*, *Tnf α* , *I κ B α* and *Socs3*. **(d)** *I κ B α* , IR β , phospho-IRS-1 (Ser³⁰⁷), and β -actin protein levels. **(e)** *Pgc1 α* , *Ppar α* , *Ppar β/δ* , *Acox* and *Mcad* mRNA levels. **(f)** PGC-1 α , NRF1, OXPHOS complexes (Compl), prohibitin and β -actin protein levels. **(g)** Phospho-AMPK (Thr¹⁷²), phospho-ACC (Ser⁷⁹) and β -actin protein levels. The graphs show quantification expressed as a percentage of control. Data are means \pm SD of five independent experiments and were compared by Student's *t* test. **p* < 0.05. ***p* < 0.01 and ****p* < 0.001 and vs control



increases FAO by phosphorylating ACC at Ser⁷⁹, leading to inhibition of ACC's activity and decreased malonyl-CoA content, which inhibits carnitine palmitoyltransferase (CPT-1), the rate-limiting step in FAO in mitochondria [25]. VLDL reduced the levels of both phospho-AMPK and phospho-ACC in myotubes (Fig. 2b), whereas it increased the protein levels of the redox transcription factor NRF2 and the protein encoded by its target gene *Nqo1* (Fig. 2c).

When we examined proteins involved in the insulin signaling pathway, we observed that in agreement with a previous study reporting that ER stress reduced insulin receptor levels in adipocytes [26], protein levels of IR β were reduced in VLDL-exposed cells (Fig. 2d). In addition, VLDL increased IRS-1 phosphorylation at Ser³⁰⁷ (Fig. 2d) and blunted insulin-stimulated Akt phosphorylation (Fig. 2e).

VLDL increases ER stress, mitochondrial dysfunction and inflammation in isolated skeletal muscle Next, we examined the effects of VLDL on skeletal muscle. Gastrocnemius muscles isolated from mice were incubated with VLDL for 6 h, which resulted in an increase in the mRNA expression

and protein levels of BiP and phospho-eIF2 α , whereas no changes were observed in CHOP (Fig. 3a, b). Muscles exposed to VLDL also showed a significant increase in the mRNA levels of *Il6*, *Mcp1* and *Tnf α* (Fig. 3c), consistent with the reduction in I κ B α (Fig. 3d). VLDL also reduced IR β protein levels and increased IRS phosphorylation at Ser³⁰⁷ (Fig. 3d). Similar to what we observed in vitro, VLDL caused a marked reduction in the expression of *Pgc1 α* , *Ppar α* , *Ppar β/δ* , and their target genes involved in FAO (Fig. 3e). Consistent with the reported regulation of mitochondrial OXPHOS genes [27] and NRF1 [24] by PGC-1 α , the reduction in the protein levels of this transcriptional co-activator caused by VLDL was accompanied by a reduction in NRF1 and the different OXPHOS complexes (Fig. 3f). In addition, a reduction was detected in phospho-AMPK and phospho-ACC in muscles exposed to VLDL (Fig. 3g).

ERK1/2 inhibition prevents the effects of VLDL Interestingly, TLR-mediated NF- κ B activation requires mitogen-activated protein kinase (MAPK)–ERK (MEK) 1/2 [28] and activation of both MEK1/2 and NF- κ B results in the

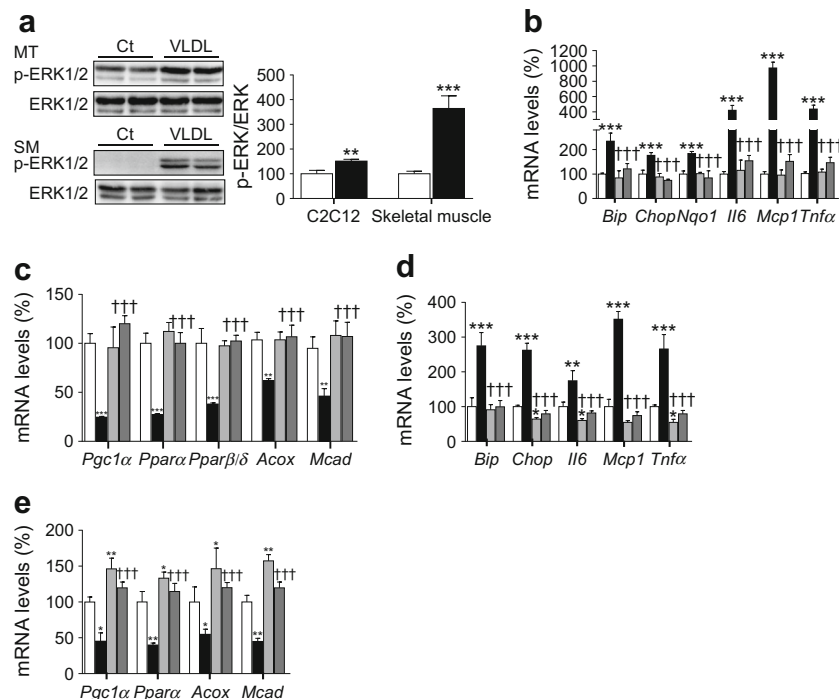


Fig. 4 ERK1/2 inhibition and knockdown prevents the effects of VLDL. (a) C2C12 myotubes (MT) and isolated skeletal muscles (SM) were incubated in the presence (black bars) or absence (control, Ct, white bars) of 300 μ g/ml VLDL (myotubes) or 500 μ g/ml VLDL (muscle) and the protein levels of phospho-ERK1/2 (Thr²⁰²/Tyr²⁰⁴) were analysed. (b, c) C2C12 myotubes were incubated in the presence (black bars) or absence (control, white bars) of 300 μ g/ml VLDL for 24 h; 10 μ mol/l U0126 was added to control (light grey bars) or VLDL-treated (dark grey bars) myotubes and the mRNA abundance of *Bip*, *Chop*, *Nqo1*, *Il6*, *Mcp1* and *Tnf α* (b) and *Pgc1 α* , *Ppar α* , *Ppar β/δ* , *Acox* and *Mcad* (c) was evaluated. (d, e) C2C12 cells were transfected with control siRNA or ERK1/2

siRNA and incubated in the presence or absence of 300 μ g/ml VLDL. The mRNA abundance of *Bip*, *Chop*, *Il6*, *Mcp1* and *Tnf α* (d) and *Pgc1 α* , *Ppar α* , *Acox* and *Mcad* (e) was evaluated. White bars, control siRNA; light grey bars ERK1/2 siRNA; black bars VLDL + control siRNA; dark grey bars VLDL+ERK1/2 siRNA. The graphs show quantification expressed as a percentage of control. Data are means \pm SD of five independent experiments and were compared by Student's *t* test (a) or two-way ANOVA followed by Tukey post hoc test (b–e). **p* < 0.05, ***p* < 0.01 and ****p* < 0.001 vs control; †††*p* < 0.001 vs VLDL-exposed cells

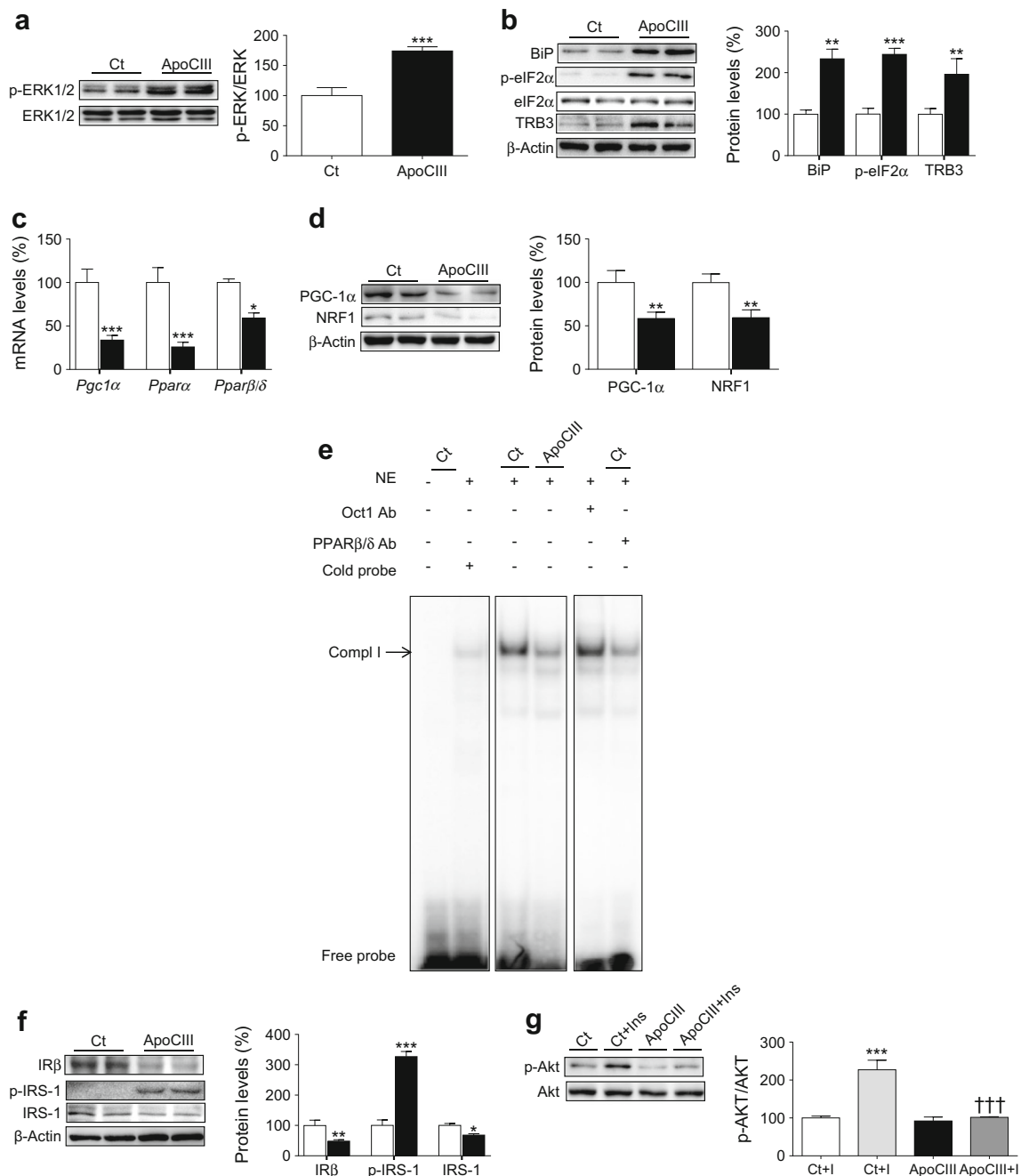


Fig. 5 ApoCIII activates ERK1/2 and induces ER stress, inflammation and insulin resistance. C2C12 myotubes were incubated in the presence (black bars) or absence (control, Ct, white bars) of 100 μ g/ml apoCIII for 24 h. **(a)** Phospho-ERK1/2 (Thr²⁰²/Tyr²⁰⁴) protein levels. **(b)** BiP, phospho-eIF2 α (Ser⁵¹), TRB3 and β -actin protein levels. **(c)** mRNA abundance of *Pgc1 α* , *Ppara* and *Ppar β / δ* . **(d)** PGC-1 α , NRF1 and β -actin protein levels. **(e)** Autoradiograph of EMSA performed with a ³²P-labelled PPAR nucleotide and crude nuclear protein extract (NE) from C2C12 myotubes. One main specific complex (Comp I) based on competition with a molar excess of unlabelled probe is shown. The supershift

assay performed by incubating NE with an antibody (Ab) directed against PPAR β / δ shows a reduction in the band, whereas the band is unchanged by an unrelated antibody against Oct1. **(f)** IR β , phospho-IRS-1 (Ser³⁰⁷) and β -actin protein levels. **(g)** Phosphorylated Akt (Ser⁴⁷³) protein levels. Where indicated, cells were incubated with 100 nmol/l insulin (Ins, I) for the last 10 min. The graphs show quantification expressed as a percentage of control. Data are means \pm SD of five independent experiments and were compared by Student's *t* test (**a–f**) or two-way ANOVA followed by Tukey post hoc test (**g**). **p* < 0.05, ***p* < 0.01 and ****p* < 0.001 vs control; †††*p* < 0.001 vs control cells incubated with insulin

downregulation of PGC-1 α in myotubes [29]. Similarly, an inhibitory crosstalk between AMPK and ERK1/2 has been reported and inhibition of ERK1/2 was found to improve

AMPK and Akt pathways and to reverse ER stress-induced insulin resistance in myotubes [30]. These data prompted us to investigate whether the ERK–MAPK cascade was involved in

the effects mediated by VLDL. This possibility was supported by the fact that VLDL increased phospho-ERK1/2 levels in both cultured myotubes and isolated muscle (Fig. 4a). Next, we used U0126, a potent and specific ERK1/2 inhibitor that binds to MEK, thereby inhibiting its catalytic activity and phosphorylation of ERK1/2, to investigate whether inhibition of this kinase prevented the effects caused by VLDL. U0126 prevented the increase in the expression of ER stress and inflammatory markers (Fig. 4b) and the reduction in genes involved in FAO (Fig. 4c). Knockdown of ERK1/2 by siRNA transfection (ESM Fig. 1) confirmed that this kinase was responsible for the effects of VLDL on ER stress and inflammation (Fig. 4d) and the reduction in genes involved in FAO (Fig. 4e).

ApoCIII mimics the effects of VLDL through TLR2 Given that apoCIII is the most abundant apolipoprotein in VLDL in individuals with diabetes [3], we next investigated whether this apolipoprotein was responsible for the effects of VLDL in myotubes. Exposure of myotubes to light VLDL with high or low apoCIII content isolated from

plasma of hypertriacylglycerolaemia or normolipidaemic individuals, respectively, showed that light VLDL with low levels of apoCIII did not cause the effects observed with VLDL with high apoCIII content (ESM Fig. 2a,b). Incubation of myotubes with apoCIII did not cause toxicity (ESM Fig. 2c) and led to a significant increase in phospho-ERK1/2 (Fig. 5a), TRB3, phospho-eIF2 α and BiP protein levels (Fig. 5b), as well as secretion of IL-6 (ESM Fig. 2d), indicating that this apolipoprotein induces ER stress and inflammation. In contrast, apoCIII exposure reduced the expression of *Pgc1 α* , *Ppar α* and *Ppar β/δ* (Fig. 5c) and reduced the protein levels of PGC-1 α and NRF1 (Fig. 5d). In agreement with this, apoCIII reduced the DNA-binding activity of PPAR β/δ (Fig. 5e). Moreover, the effects of apoCIII were concentration dependent (ESM Fig. 3). The induction of ER stress caused by apoCIII was accompanied by a reduction in the protein levels of IR β and an increase in IRS-1 phosphorylated at Ser³⁰⁷ (Fig. 5f), whereas insulin-stimulated Akt phosphorylation was mitigated (Fig. 5g). No changes were observed in ER stress and inflammatory markers or in the protein levels of PGC-1 α and phospho-

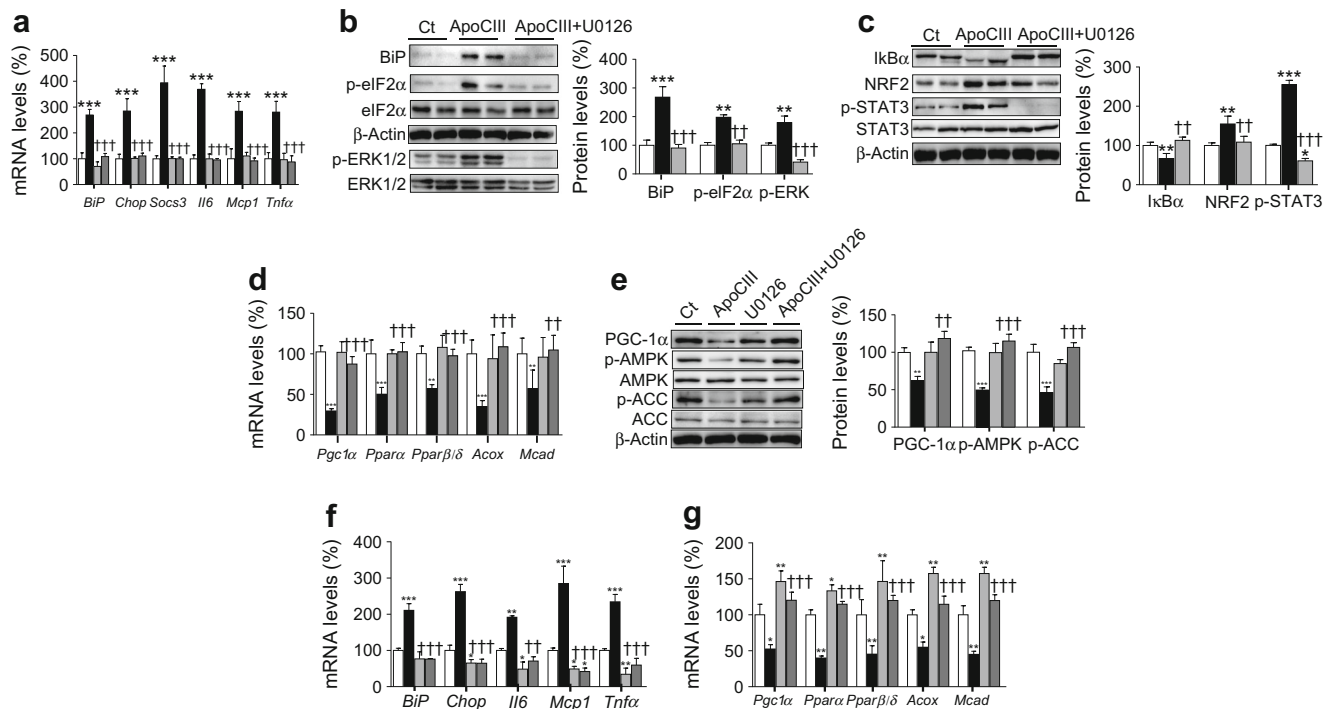


Fig. 6 ERK1/2 inhibition prevents the effects of apoCIII on ER stress and inflammation. (a–e) C2C12 myotubes were incubated in the presence (black bars) or absence (control, Ct, white bars) of 100 $\mu\text{g/ml}$ apoCIII for 24 h; 10 $\mu\text{mol/l}$ U0126 was added to control myotubes (light grey bars) or apoCIII-treated myotubes (dark grey bars). (a) mRNA abundance of *Bip*, *Chop*, *Socs3*, *Il6*, *Mcp1* and *Tnfa*. (b) BiP, phospho-eIF2 α (Ser⁵¹), phospho-ERK1/2 (Thr²⁰²/Tyr²⁰⁴) and β -actin protein levels. (c) I κ B α , NRF2, phospho-STAT3 (Tyr⁷⁰⁵) and β -actin protein levels. (d) mRNA abundance of *Pgc1 α* , *Ppar α* , *Ppar β/δ* , *Acox* and *Mcad*. (e) PGC-1 α , phospho-AMPK (Thr¹⁷²), phospho-ACC (Ser⁷⁹) and β -actin protein levels. (f, g) C2C12 myotubes were transfected with control or ERK1/2

siRNA and incubated in the presence or absence of 100 $\mu\text{g/ml}$ apoCIII for 24 h. The mRNA abundance of *Bip*, *Chop*, *Il6*, *Mcp1* and *Tnfa* (f) and *Pgc1 α* , *Ppar α* , *Ppar β/δ* , *Acox* and *Mcad* (g) was evaluated. White bars, control siRNA; light grey bars ERK1/2 siRNA; black bars, apoCIII+control siRNA; dark grey bars, apoCIII+ERK1/2 siRNA. The graphs show quantification expressed as a percentage of control. Data are means \pm SD of five independent experiments and were compared by two-way ANOVA followed by Tukey post hoc test. * $p < 0.05$, ** $p < 0.01$ and *** $p < 0.001$ vs control; † $p < 0.01$ and †† $p < 0.001$ vs apoCIII-exposed cells

ERK1/2 when cells were incubated with apoCI, indicating that the effects of apoCIII were specific (ESM Fig. 4a,b). In addition, VLDL and apoCIII reduced insulin-stimulated glucose uptake, whereas light VLDL low in apoCIII did not (ESM Fig. 4c). Moreover, apoCIII intensified the effects of the saturated fatty acid palmitate on the levels of ER stress markers, ERK1/2 phosphorylation, PGC-1 α and insulin signalling pathway (ESM Fig. 4d), indicating that the increase in apoCIII might exacerbate the effects of lipids on insulin resistance.

The increase in the expression of ER stress and inflammatory markers caused by apoCIII was blunted by co-incubation with U0126 (Fig. 6a). Likewise, U0126 prevented the increase in the protein levels of BiP, phospho-eIF2 α and phospho-ERK1/2 caused by apoCIII (Fig. 6b). Inhibition of the MAPK–ERK1/2 pathway also prevented the reduction in I κ B α and the increase in the DNA-binding activity of NF- κ B (ESM Fig. 5a) and the increase in NRF2 and phospho-STAT3 (Tyr⁷⁰⁵) (Fig. 6c) observed in cells exposed only to apoCIII. ApoCIII also reduced the expression of *Pgc1 α* , *Ppar α* and *Ppar β/δ* and their target genes involved in FAO—changes that were abolished by U0126 (Fig. 6d). Additionally, the reduction in the protein levels of PGC-1 α , phospho-AMPK and phospho-ACC was reversed by U0126 (Fig. 6e). siRNA knockdown of ERK1/2 confirmed that this kinase was responsible for the increase in ER stress and inflammation (Fig. 6f) and the reduction in FAO genes (Fig. 6g) caused by apoCIII.

Next, we examined whether some of the changes caused by apoCIII in vitro were observed in skeletal muscle of transgenic mice with human apoCIII overexpression (apoCIII Tg) (Fig. 7a). These mice have marked elevations in plasma triacylglycerols but no impairment of glucose tolerance [31]. However, apoCIII Tg mice fed a high-fat diet show hepatic insulin resistance [7] and are more susceptible to development of diabetes [32]. In skeletal muscle of apoCIII Tg mice fed a standard diet, increased *Chop*, *Il6* and *Tnf α* expression was detected when these mice were compared with non-transgenic littermates, whereas no changes were observed in *Bip* mRNA levels (Fig. 7b). Moreover, the marked increase in the protein levels of phospho-ERK1/2 in skeletal muscle from apoCIII Tg mice was accompanied by a reduction in PGC-1 α protein levels (Fig. 7c, d).

Since TLRs activate ERK1/2 and cause inflammation [28], we examined whether apoCIII acted through these receptors. We incubated mouse C2C12 myotubes exposed to apoCIII with a selective neutralising antibody against either TLR2 or IgG (ESM Fig. 5b). In the presence of this neutralising antibody, the increase in phospho-ERK1/2 levels caused by apoCIII alone was blunted (Fig. 8a). Consistent with a crucial role for ERK1/2 in the effects caused by apoCIII, the TLR2 neutralising antibody prevented the apoCIII-induced changes in the mRNA (Fig. 8b) and protein (Fig. 8c) levels of ER stress

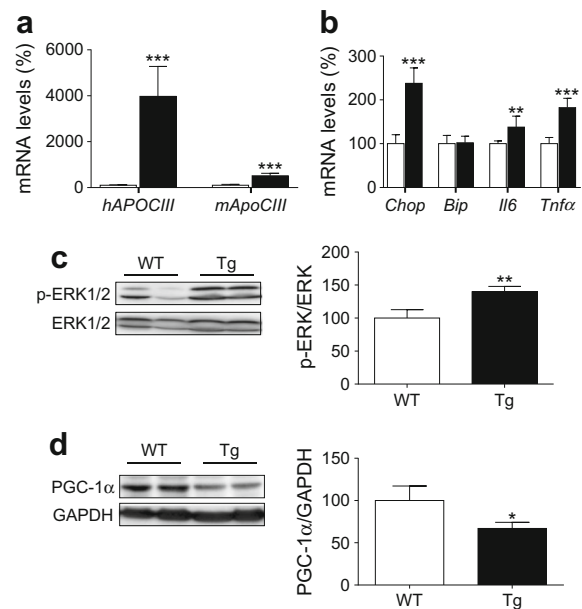


Fig. 7 Skeletal muscle from apoCIII Tg mice shows increased levels of phospho-ERK1/2. Skeletal muscle from male non-transgenic (WT, white bars) and apoCIII Tg mice (Tg, black bars) was used. **(a)** mRNA abundance of human *APOCIII* and mouse *ApoCIII* (*ApoC3*). **(b)** mRNA abundance of *Chop*, *Bip*, *Il6* and *Tnf α* . **(c)** Phospho-ERK1/2 (Thr²⁰²/Tyr²⁰⁴) protein level. **(d)** PGC-1 α protein levels. The graphs show quantification expressed as a percentage of WT value. Data are means \pm SD ($n = 5$ per group) and were compared by Student's *t* test. * $p < 0.05$, ** $p < 0.01$ and *** $p < 0.001$ vs WT mice

and inflammatory markers. Likewise, TLR2 neutralisation partially reversed the reduction in the protein levels of IR β (Fig. 8d), blunted the increase in phospho-IRS-1 (Ser³⁰⁷) (Fig. 8d) and prevented the reduction in PGC-1 α and NRF1 (Fig. 8e). Blocking TLR2 also prevented the apoCIII-induced reduction in the expression of genes involved in FAO (Fig. 8f).

Discussion

Although it is well established that insulin resistance drives atherogenic dyslipidaemia, there is little evidence on whether the increase in VLDL particles associated with insulin-resistant states exacerbates the insulin resistance. Our findings demonstrate that exposure of myotubes and isolated skeletal muscle to VLDL increases the levels of ER stress and inflammatory markers and attenuates the insulin signalling pathway. These data indicate that increased levels of VLDL particles may contribute towards exacerbation of insulin resistance. Our findings also demonstrate that apoCIII may be the VLDL component responsible for the changes caused by VLDL exposure. This is interesting, since apoCIII expression is increased by insulin deficiency, insulin resistance [33, 34] and hyperglycaemia [35], converting apoCIII into the most abundant VLDL apolipoprotein in individuals with diabetes [3], suggesting that the increase in apoCIII levels in diabetic

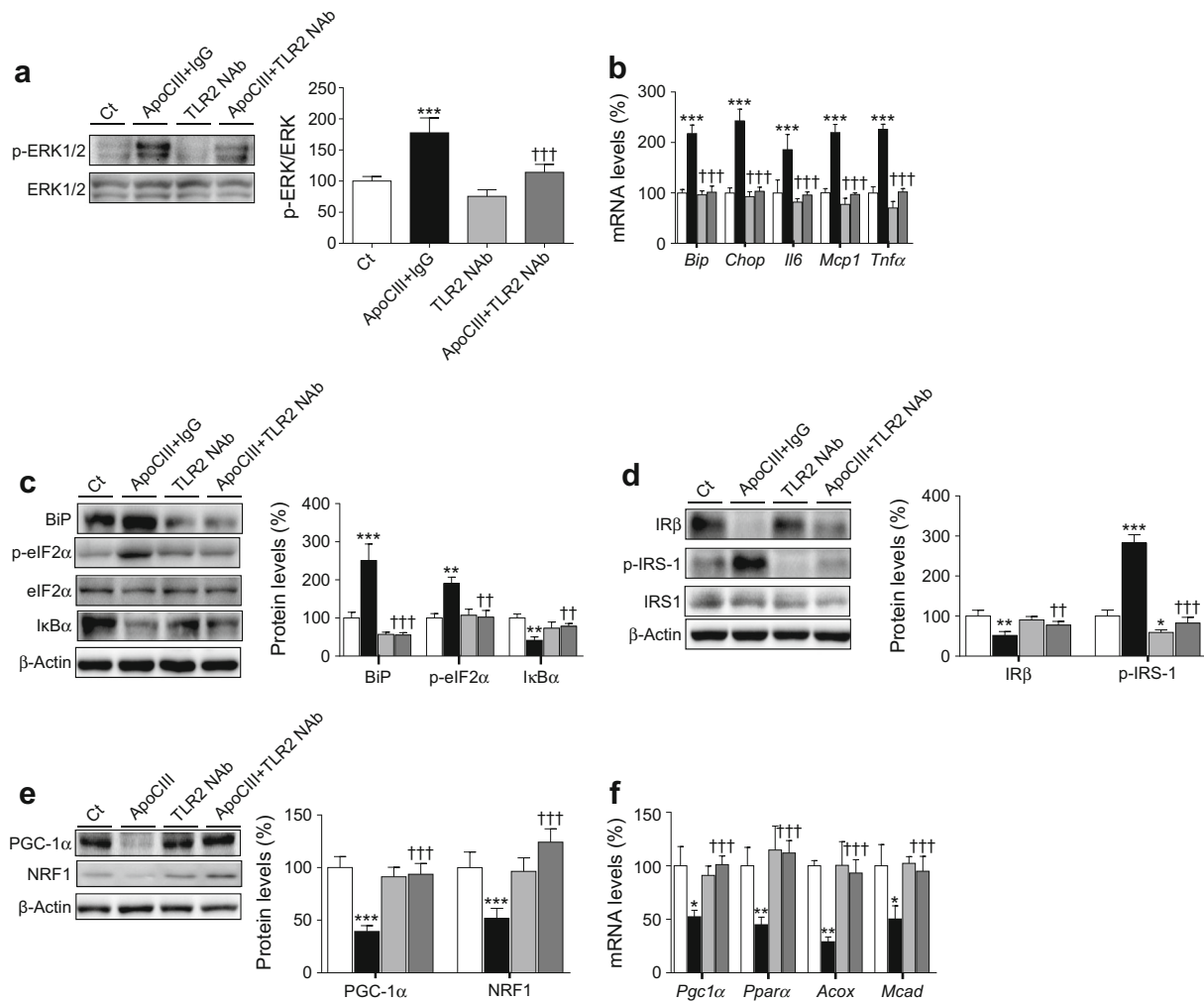


Fig. 8 TLR2 mediates the effects of apoCIII on ERK1/2, ER stress and inflammation. Mouse C2C12 myotubes were incubated in the presence or absence (control, Ct, white bars) of 100 $\mu\text{g}/\text{ml}$ apoCIII for 24 h; 50 $\mu\text{g}/\text{ml}$ of IgG was added to apoCIII-treated myotubes (black bars) or 50 $\mu\text{g}/\text{ml}$ of the neutralising antibody against TLR2 (TLR2NAb) was added to the control (light grey bars) or apoCIII-treated (dark grey bars) myotubes. **(a)** Phospho-ERK1/2 (Thr²⁰²/Tyr²⁰⁴) protein levels. **(b)** mRNA abundance of *Bip*, *Chop*, *Il6*, *Mcp1* and *Tnfα*. **(c)** BiP, phospho-eIF2 α

(Ser⁵¹), I κ B α , and β -actin protein levels. **(d)** IR β , phospho-IRS-1 (Ser³⁰⁷) and β -actin protein levels. **(e)** PGC-1 α , NRF1 and β -actin protein levels. **(f)** mRNA abundance of *Pgc1α*, *Ppara*, *Acox* and *Mcad* mRNA. The graphs show quantification expressed as a percentage of control. Data are means \pm SD of five independent experiments and were compared by two-way ANOVA followed by Tukey post hoc test. * $p < 0.05$, ** $p < 0.01$ and *** $p < 0.001$ vs control; † $p < 0.01$ and †† $p < 0.001$ vs apoCIII-exposed cells

states may contribute to exacerbation of these conditions. In this regard, it is interesting to note that humans with a mutation in the *APOCIII* gene (also known as *APOC3*) that results in a reduction in the half-life of apoCIII, show a favourable lipoprotein pattern, increased insulin sensitivity and longevity and protection against cardiovascular diseases [36, 37]. Recent evidence seems to confirm that apoCIII plays a key role in diabetes. Thus, decreasing apoCIII in mice results in improved glucose tolerance [38]. In agreement with this, antisense-mediated lowering of plasma apoCIII improves dyslipidaemia and insulin sensitivity in humans with type 2 diabetes [39] and a null mutation in human *APOCIII* confers a favourable plasma lipid profile, although it does not improve insulin sensitivity [8].

The mechanism by which VLDL and apoCIII increase ER stress and inflammation and attenuate insulin signalling in myotubes seems to involve ERK1/2 activation. This kinase has been implicated in the development of insulin resistance associated with obesity and type 2 diabetes [40]. In fact, *Erk1*^{-/-} mice (also known as *Mapk3*^{-/-} mice) challenged with a high-fat diet are resistant to obesity and are protected from insulin resistance [41]. In addition, hyperinsulinaemic–euglycaemic clamp studies have demonstrated an increase in whole-body insulin sensitivity in *ob/ob-Erk1*^{-/-} mice associated with an increase in both insulin-stimulated glucose disposal in skeletal muscles and adipose tissue insulin sensitivity [42].

In the present study, apoCIII-induced ERK1/2 activation was accompanied by a reduction in AMPK activity. An

inhibitory crosstalk exists between AMPK and ERK1/2 and activation of ERK1/2 inhibits AMPK and promotes ER stress-induced insulin resistance in skeletal muscle cells [14, 29]. Hence, VLDL and apoCIII-induced ER stress might be a result of the reduction in AMPK activity. In fact, AMPK activation inhibits ER stress [14, 43], whereas the reduction in its activity promotes ER stress [44]. Moreover, VLDL- and apoCIII-induced ER stress ultimately results in activation of the IKK β -NF- κ B pathway, which attenuates the insulin signalling pathway by phosphorylating IRS-1 in serine residues and increases the transcription of inflammatory genes. In agreement with this, we found that ERK1/2 inhibition or knockdown prevented the changes in ER stress and inflammation and the attenuation of the insulin signalling pathway caused by VLDL. Moreover, ERK1/2 inhibition prevented the reduction in AMPK caused by apoCIII, confirming the negative crosstalk between ERK1/2 and AMPK.

Similarly, the reduction in AMPK caused by apoCIII-induced ERK1/2 activation may contribute to reduced PGC-1 α levels, since PGC-1 α is an important mediator of AMPK-induced gene expression and AMPK activation regulates PGC-1 α transcription [45]. Given the key role of PGC-1 α in regulating the activity of transcription factors involved in FAO, such as PPARs [22], the reduction in PGC-1 α following treatment with VLDL or apoCIII leads to a decrease in the expression of genes involved in FAO, suggesting that it can promote the deleterious effects of saturated fatty acids [11].

VLDLs also bind to the VLDL receptor, which is a determinant factor in adipose tissue inflammation and adipocyte macrophage infiltration when stimulated with VLDL from hyperlipidaemic mice [13]. Although we cannot discount a role for this receptor, the fact that the effects of VLDL from normolipidaemic individuals are mimicked by apoCIII seems to suggest that most of the effects of these lipoproteins are caused by the presence of apoCIII in these particles.

Interestingly, our findings indicate that the effects of apoCIII are mediated by TLR2. TLR2 not only recognises numerous lipid-containing molecules but also it recognises endogenous proteins [46]. It is expressed in skeletal muscle cells and is involved in fatty acid-induced insulin resistance [47]. Moreover, activation of the TLR2 pathway ultimately leads to NF- κ B and ERK1/2 activation [48]. Likewise, TLR2 deficiency improves insulin sensitivity and attenuates cytokine expression [49]. Our findings confirm the importance of TLR2 in insulin resistance and indicate that its activation by VLDL and apoCIII induces ER stress, inflammation and insulin resistance.

In conclusion, our findings show that VLDL- and apoCIII-induced TLR2 activation results in ER stress, inflammation and insulin resistance by activating ERK1/2 in skeletal muscle cells. These results imply that elevated VLDL in diabetic states can contribute to the exacerbation of insulin resistance.

Acknowledgements We thank the University of Barcelona's Language Advisory Service for revising the manuscript.

Data availability Data are available on request from the authors.

Funding This study was partly supported by funds from the Spanish Ministerio de Economía y Competitividad (SAF2012-30708 and SAF2015-64146-R to MVC), the Generalitat de Catalunya (2014SGR-0013 to MVC), NIH NIDDK (DK101663 to ABK), USDA NIFA (11874590 to ABK) and USDA NIFA Hatch Formula Funds (2015-31200-06009 to ABK), an Instituto de Salud Carlos III grant (PI16-00139 to JCE-G) and European Union ERDF funds. CIBER de Diabetes y Enfermedades Metabólicas Asociadas (CIBERDEM) is an Instituto de Salud Carlos III project (Grant CB07/08/0003 to MVC). GB was supported by an FPI grant from the Spanish Ministerio de Economía y Competitividad.

Duality of interest The authors declare that there is no duality of interest associated with this manuscript.

Contribution statement All authors processed the samples, analysed and prepared the data and were involved in drafting the article. GB, AG, JCEG, XP and ABK contributed to data interpretation and revised the article. MVC designed the experiments, interpreted the data and was primarily responsible for writing the manuscript. All authors approved the final version of the manuscript. MVC is the guarantor of this work.

References

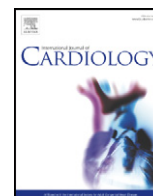
- Xiao C, Dash S, Morgantini C, Hegele RA, Lewis GF (2016) Pharmacological targeting of the atherogenic dyslipidemia complex: the next frontier in CVD prevention beyond lowering LDL cholesterol. *Diabetes* 65:1767–1778
- Adiels M, Olofsson SO, Taskinen MR, Borén J (2008) Overproduction of very low-density lipoproteins is the hallmark of the dyslipidemia in the metabolic syndrome. *Arterioscler Thromb Vasc Biol* 28:1225–1236
- Hiukka A, Fruchart-Najib J, Leinonen E, Hilden H, Fruchart JC, Taskinen MR (2005) Alterations of lipids and apolipoprotein CIII in very low density lipoprotein subspecies in type 2 diabetes. *Diabetologia* 48:1207–1215
- Campos H, Perlov D, Khoo C, Sacks FM (2001) Distinct patterns of lipoproteins with apoB defined by presence of apoE or apoC-III in hypercholesterolemia and hypertriglyceridemia. *J Lipid Res* 42:1239–1249
- Aalto-Setälä K, Fisher EA, Chen X et al (1992) Mechanism of hypertriglyceridemia in human apolipoprotein (apo) CIII transgenic mice. Diminished very low density lipoprotein fractional catabolic rate associated with increased apo CIII and reduced apo E on the particles. *J Clin Invest* 90:1889–1900
- Kawakami A, Aikawa M, Alcaide P, Lusinskas FW, Libby P, Sacks FM (2006) Apolipoprotein CIII induces expression of vascular cell adhesion molecule-1 in vascular endothelial cells and increases adhesion of monocytic cells. *Circulation* 114:681–687
- Lee HY, Birkenfeld AL, Jornayvaz FR et al (2011) Apolipoprotein CIII overexpressing mice are predisposed to diet-induced hepatic steatosis and hepatic insulin resistance. *Hepatology* 54:1650–1660
- Pollin TI, Damcott CM, Shen H et al (2008) A null mutation in human APOC3 confers a favorable plasma lipid profile and apparent cardioprotection. *Science* 332:1702–1705

9. DeFronzo RA, Gunnarsson R, Björkman O, Olsson M, Wahren J (1985) Effects of insulin on peripheral and splanchnic glucose metabolism in noninsulin-dependent (type II) diabetes mellitus. *J Clin Invest* 76:149–155
10. Abdul-Ghani MA, DeFronzo RA (2010) Pathogenesis of insulin resistance in skeletal muscle. *J Biomed Biotechnol* 2010:476279
11. Schenk S, Saberi M, Olefsky JM (2008) Insulin sensitivity: modulation by nutrients and inflammation. *J Clin Invest* 118:2992–3002
12. Salvadó L, Palomer X, Barroso E, Vázquez-Carrera M (2015) Targeting endoplasmic reticulum stress in insulin resistance. *Trends Endocrinol Metab* 26:438–448
13. Könnér AC, Brüning JC (2011) Toll-like receptors: linking inflammation to metabolism. *Trends Endocrinol Metab* 22:16–23
14. Nguyen A, Tao H, Mettrione M, Hajri T (2014) Very low density lipoprotein receptor (VLDLR) expression is a determinant factor in adipose tissue inflammation and adipocyte-macrophage interaction. *J Biol Chem* 289:1688–1703
15. Salvadó L, Barroso E, Gómez-Foix AM et al (2014) PPAR β/δ prevents endoplasmic reticulum stress-associated inflammation and insulin resistance in skeletal muscle cells through an AMPK-dependent mechanism. *Diabetologia* 57:2126–2135
16. Alkhateeb H, Chabowski A, Bonen A (2006) Viability of the isolated soleus muscle during long-term incubation. *Appl Physiol Nutr Metab* 31:467–476
17. Koh HJ, Toyoda T, Didesch MM et al (2013) Tribbles 3 mediates endoplasmic reticulum stress-induced insulin resistance in skeletal muscle. *Nat Commun* 4:1871
18. Howard JK, Flier JS (2006) Attenuation of leptin and insulin signaling by SOCS proteins. *Trends Endocrinol Metab* 17:365–371
19. Handschin C, Spiegelman BM (2006) Peroxisome proliferator-activated receptor gamma coactivator 1 coactivators, energy homeostasis, and metabolism. *Endocr Rev* 27:728–735
20. Patti ME, Butte AJ, Crunkhorn S et al (2003) Coordinated reduction of genes of oxidative metabolism in humans with insulin resistance and diabetes: potential role of *PGC1* and *NRF1*. *Proc Natl Acad Sci U S A* 100:8466–8471
21. Mootha VK, Lindgren CM, Eriksson KF et al (2003) PGC-1 α -responsive genes involved in oxidative phosphorylation are coordinately downregulated in human diabetes. *Nat Genet* 34:267–273
22. Miura S, Kai Y, Ono M, Ezaki O (2003) Overexpression of peroxisome proliferator-activated receptor γ coactivator-1 α down-regulates GLUT4 mRNA in skeletal muscles. *J Biol Chem* 278:31385–31390
23. Vega RB, Huss JM, Kelly DP (2000) The coactivator PGC-1 cooperates with peroxisome proliferator-activated receptor α in transcriptional control of nuclear genes encoding mitochondrial fatty acid oxidation enzymes. *Mol Cell Biol* 20:1868–1876
24. Wu Z, Puigserver P, Andersson U et al (1999) Mechanisms controlling mitochondrial biogenesis and respiration through the thermogenic coactivator PGC-1. *Cell* 98:115–124
25. Zhang BB, Zhou G, Li C (2009) AMPK: an emerging drug target for diabetes and the metabolic syndrome. *Cell Metab* 9:407–416
26. Zhou L, Zhang J, Fang Q et al (2009) Autophagy-mediated insulin receptor down-regulation contributes to endoplasmic reticulum stress-induced insulin resistance. *Mol Pharmacol* 76:596–603
27. Wenz T, Rossi SG, Rotundo RL, Spiegelman BM, Moraes CT (2009) Increased muscle PGC-1 α expression protects from sarcopenia and metabolic disease during aging. *Proc Natl Acad Sci U S A* 106:20405–20410
28. Chung S, Lapoint K, Martinez K et al (2006) Preadipocytes mediate lipopolysaccharide-induced inflammation and insulin resistance in primary cultures of newly differentiated human adipocytes. *Endocrinology* 147:5340–5351
29. Coll T, Jové M, Rodríguez-Calvo R et al (2006) Palmitate-mediated downregulation of peroxisome proliferator-activated receptor-gamma coactivator 1 α in skeletal muscle cells involves MEK1/2 and nuclear factor- κ B activation. *Diabetes* 55:2779–2787
30. Hwang SL, Jeong YT, Li X et al (2013) Inhibitory cross-talk between the AMPK and ERK pathways mediates endoplasmic reticulum stress-induced insulin resistance in skeletal muscle. *Br J Pharmacol* 169:69–81
31. Reaven GM, Mondon CE, Chen YD, Breslow JL (1994) Hypertriglyceridemic mice transgenic for the human apolipoprotein C-III gene are neither insulin resistant nor hyperinsulinemic. *J Lipid Res* 35:820–824
32. Salerno AG, Silva TR, Amaral ME et al (2007) Overexpression of apolipoprotein CIII increases and CETP reverses diet-induced obesity in transgenic mice. *Int J Obes* 31:1586–1595
33. Chen M, Breslow JL, Li W, Leff T (1994) Transcriptional regulation of the apoC-III gene by insulin in diabetic mice: correlation with changes in plasma triglyceride levels. *J Lipid Res* 35:1918–1924
34. Altomonte J, Cong L, Harbaran S et al (2004) Foxo1 mediates insulin action on apoC-III and triglyceride metabolism. *J Clin Invest* 114:1493–1503
35. Caron S, Verrijken A, Mertens I et al (2011) Transcriptional activation of apolipoprotein CIII expression by glucose may contribute to diabetic dyslipidemia. *Arterioscler Thromb Vasc Biol* 31:513–519
36. Atzmon G, Rincon M, Schechter CB et al (2006) Lipoprotein genotype and conserved pathway for exceptional longevity in humans. *PLoS Biol* 4:e113
37. Jørgensen AB, Frikke-Schmidt R, Nordestgaard BG, Tybjaerg-Hansen A (2014) Loss-of-function mutations in *APOC3* and risk of ischemic vascular disease. *N Engl J Med* 371:32–41
38. Åvall K, Ali Y, Leibiger IB et al (2015) Apolipoprotein CIII links islet insulin resistance to β -cell failure in diabetes. *Proc Natl Acad Sci U S A* 112:E2611–E2619
39. Digenio A, Dunbar RL, Alexander VJ et al (2016) Antisense-mediated lowering of plasma apolipoprotein C-III by volanesorsen improves dyslipidemia and insulin sensitivity in type 2 diabetes. *Diabetes Care* 39:1408–1415
40. Ozaki KI, Awazu M, Tamiya M et al (2016) Targeting the ERK signaling pathway as a potential treatment for insulin resistance and type 2 diabetes. *Am J Physiol Endocrinol Metab* 310:E643–E651
41. Bost F, Aouadi M, Caron L et al (2005) The extracellular signal-regulated kinase isoform ERK1 is specifically required for in vitro and in vivo adipogenesis. *Diabetes* 54:402–411
42. Jager J, Corcelle V, Grémeaux T et al (2011) Deficiency in the extracellular signal-regulated kinase 1 (ERK1) protects leptin-deficient mice from insulin resistance without affecting obesity. *Diabetologia* 54:180–189
43. Dong Y, Zhang M, Wang S et al (2010) Activation of AMP-activated protein kinase inhibits oxidized LDL-triggered endoplasmic reticulum stress in vivo. *Diabetes* 59:1386–1396
44. Dong Y, Zhang M, Liang B et al (2010) Reduction of AMP-activated protein kinase α 2 increases endoplasmic reticulum stress and atherosclerosis in vivo. *Circulation* 121:792–803
45. Cantó C, Auwerx J (2009) PGC-1 α , SIRT1 and AMPK, an energy sensing network that controls energy expenditure. *Curr Opin Lipidol* 20:98–105
46. Rubartelli A, Lotze MT (2007) Inside, outside, upside down: damage-associated molecular-pattern molecules (DAMPs) and redox. *Trends Immunol* 28:429–436
47. Senn JJ (2006) Toll-like receptor-2 is essential for the development of palmitate-induced insulin resistance in myotubes. *J Biol Chem* 281:26865–26875
48. Ninomiya-Tsuji J, Kishimoto K, Hiyama A, Inoue J, Cao Z, Matsumoto K (1999) The kinase TAK1 can activate the NIK-I κ B as well as the MAP kinase cascade in the IL-1 signalling pathway. *Nature* 398:252–256
49. Kuo LH, Tsai PJ, Jiang MJ et al (2011) Toll-like receptor 2 deficiency improves insulin sensitivity and hepatic insulin signalling in the mouse. *Diabetologia* 54:168–179



Contents lists available at ScienceDirect

International Journal of Cardiology

journal homepage: www.elsevier.com/locate/ijcard

PPAR β/δ attenuates palmitate-induced endoplasmic reticulum stress and induces autophagic markers in human cardiac cells



Xavier Palomer^a, Eva Capdevila-Busquets^a, Gaia Botteri^a, Laia Salvadó^a, Emma Barroso^a, Mercy M. Davidson^b, Liliane Michalik^c, Walter Wahli^{c,d}, Manuel Vázquez-Carrera^{a,*}

^a Department of Pharmacology and Therapeutic Chemistry, IBUB (Institut de Biomedicina de la Universitat de Barcelona), CIBER de Diabetes y Enfermedades Metabólicas Asociadas (CIBERDEM), Faculty of Pharmacy, University of Barcelona, Diagonal 643, Barcelona E-08028, Spain

^b Department of Radiation Oncology, Columbia University, P&S 11-451, 630 West 168th Street, New York, NY 10032, USA

^c Center for Integrative Genomics, National Research Center Frontiers in Genetics, University of Lausanne, Quartier UNIL-Sorge, Bâtiment Génopode, CH-1015 Lausanne, Switzerland

^d Lee Kong Chian School of Medicine, Nanyang Technological University, School of Nursing Building, SGH, Block C, #01-01, 9 Hospital Drive, Singapore 169612, Singapore

ARTICLE INFO

Article history:

Received 23 December 2013

Received in revised form 24 March 2014

Accepted 29 March 2014

Available online 8 April 2014

Keywords:

Autophagy

Diabetic cardiomyopathy

Endoplasmic reticulum stress

PPAR β/δ

ABSTRACT

Background: Chronic endoplasmic reticulum (ER) stress contributes to the apoptotic cell death in the myocardium, thereby playing a critical role in the development of cardiomyopathy. ER stress has been reported to be induced after high-fat diet feeding in mice and also after saturated fatty acid treatment in vitro. Therefore, since several studies have shown that peroxisome proliferator-activated receptor (PPAR) β/δ inhibits ER stress, the main goal of this study consisted in investigating whether activation of this nuclear receptor was able to prevent lipid-induced ER stress in cardiac cells.

Methods and results: Wild-type and transgenic mice with reduced PPAR β/δ expression were fed a standard diet or a high-fat diet for two months. For in vitro studies, a cardiomyocyte cell line of human origin, AC16, was treated with palmitate and the PPAR β/δ agonist GW501516. Our results demonstrate that palmitate induced ER stress in AC16 cells, a fact which was prevented after PPAR β/δ activation with GW501516. Interestingly, the effect of GW501516 on ER stress occurred in an AMPK-independent manner. The most striking result of this study is that GW501516 treatment also upregulated the protein levels of beclin 1 and LC3II, two well-known markers of autophagy. In accordance with this, feeding mice on a high-fat diet or suppression of PPAR β/δ in knockout mice induced ER stress in the heart. Moreover, PPAR β/δ knockout mice also displayed a reduction in autophagic markers. **Conclusion:** Our data indicate that PPAR β/δ activation might be useful to prevent the harmful effects of ER stress induced by saturated fatty acids in the heart by inducing autophagy.

© 2014 Elsevier Ireland Ltd. All rights reserved.

1. Introduction

If uncorrected, type 2 diabetes and obesity are among the major risk factors for the development of cardiovascular diseases. Plasma free fatty acid levels are often elevated in patients with type 2 diabetes mellitus or obesity, and are responsible for several harmful effects on the heart, such as the activation of endoplasmic reticulum (ER) stress and chronic low-level inflammatory processes. In fact, it has been suggested that saturated fatty acids induce insulin resistance by causing ER stress in pancreatic β -cells [1,2], hepatocytes [3] and muscle cells [4,5] of human and murine origin. ER is the organelle responsible for protein folding and maturation in eukaryotic cells. Any physiological or pathological perturbation that interferes with the folding process will cause the accumulation of unfolded or misfolded proteins, thus leading to

the activation of the unfolded protein response (UPR) by the ER [6]. Initiation of the UPR involves three key signaling proteins: activating transcription factor 6 (ATF6), inositol-requiring enzyme (IRE)-1 α , and PERK-like ER kinase (PERK). In the absence of stress, the N-termini of these trans-membrane proteins are bound to the intra-luminal BiP/GRP78 (binding immunoglobulin protein/glucose-regulated protein 78) protein. On stress exposure, the large excess of unfolded proteins sequesters BiP/GRP78 from trans-membrane ER proteins, thereby inducing the UPR. In particular, ATF6 is transported from the ER to the Golgi complex, where proteolytic cleavage releases a soluble fragment that translocates to the nucleus, in which it acts as a transcription factor for ER chaperones [7]. In addition, the endoribonuclease activity of IRE-1 α cleaves a 26 base-pair segment from the mRNA of the X-box binding protein-1 (XBP1), creating an alternative message that is translated into the spliced and active form of this transcription factor, sXBP1. Finally, PERK phosphorylates and inhibits the eukaryotic initiation factor 2 α (eIF2 α), and by this means inhibits the translation of most mRNAs [8]. However, some mRNAs escape this translational control, for example transcription factor ATF4, a master regulator of the ER stress response

* Corresponding author at: Department of Pharmacology and Therapeutic Chemistry, Faculty of Pharmacy, University of Barcelona, Diagonal 643, E-08028 Barcelona, Spain. Tel.: +34 934024531; fax: +34 934035982.

E-mail address: mvazquezcarrera@ub.edu (M. Vázquez-Carrera).

that is capable of inducing the expression of *ATF3*, *BiP/GRP78*, *CHOP* (CCAAT/enhancer binding protein homologous protein) and genes involved in autophagy, antioxidant responses, and apoptosis [9].

Activation of the UPR initially aims to mitigate adverse effects of ER stress and thus enhance cell survival by halting general mRNA translation, facilitating protein degradation via the ER-associated degradation (ERAD) pathway and enhancing the production of molecular chaperones involved in protein folding. If ER stress is limited, the UPR will potentiate autophagy to protect the cells [10]. This pro-survival pathway has evolved as an alternate mechanism for saving nutrients, recycling intracellular components and eliminating abnormal protein aggregates and misfolded proteins formed during the ER stress that cannot be removed through the ERAD pathway. However, if ER stress is not mitigated within a certain time period or the disturbance is prolonged, then, the UPR will turn on apoptosis for removing cells that threaten the integrity of the organism [11]. Cardiomyocytes rarely proliferate within the adult heart and, as a consequence, their loss due to apoptosis may play an essential pathogenic role during cardiovascular diseases [7]. In consonance with this, ER stress is involved in the pathogenesis of diabetic cardiomyopathy by enhancing cell death in the myocardium of streptozotocin-induced diabetic rats [12]. The myocardium of two rat models of type 2 diabetes mellitus also displays ER stress [13,14]. For this reason, inhibition of ER stress has been suggested as a potential therapeutic target for preventing and treating diabetic cardiomyopathy.

Peroxisome proliferator-activated receptor ($\text{PPAR}\beta/\delta$) is a transcription factor that regulates cardiac metabolism and can limit myocardial inflammation and hypertrophy via inhibition of nuclear factor (NF)- κB [15]. $\text{NF}-\kappa\text{B}$ is a pro-inflammatory transcription factor that is activated in the heart during prolonged ER stress, and is responsible for the induction of apoptosis [16]. Cardiomyocyte-restricted deletion of $\text{PPAR}\beta/\delta$ decreases basal myocardial fatty acid oxidation, thus leading to lipotoxic cardiomyopathy and subsequent cardiac dysfunction, cardiac hypertrophy and congestive heart failure [17,18]. Interestingly, activation of $\text{PPAR}\beta/\delta$ with the GW501516 agonist rescues ER stress induced by palmitate in pancreatic β -cells [19], while another agonist, L165041, attenuates ER stress in the liver [20], although the mechanisms involved remain unknown. Therefore, the present study was designed to gain a better understanding of the mechanisms by which exposure to the saturated fatty acid palmitate results in ER stress in cardiac cells. In addition, since $\text{PPAR}\beta/\delta$ is the most prevalent PPAR isoform in the heart [15], we also aimed to elucidate whether the $\text{PPAR}\beta/\delta$ agonist GW501516 could prevent saturated fatty acid-induced ER stress in cardiac myocytes, as well as the mechanisms involved.

2. Methods

2.1. Cell culture and mice

Human cardiac AC16 cells were maintained and grown as previously described [21]. Palmitate-containing medium was prepared by conjugation with fatty acid-free bovine serum albumin [22]. After incubation, RNA or protein was extracted from cardiac cells as described below.

Male $\text{PPAR}\beta/\delta$ -null mice and their control wild-type littermates with the same genetic background (C57BL/6X129/SV) were used (aged 3–5 months old) [23]. Each strain was randomized into two groups. One group was fed with a standard chow diet, and the other was fed with a Western-type high-fat diet (HFD, 45% kcal from fat, 91.5% saturated fatty acid content) for 8 weeks. Mice were housed under standard light–dark cycle (12-h light/dark cycle) and temperature (21 ± 1 °C) conditions, and food and water were provided ad libitum. At the end of the treatment, mice were anesthetized with 5% isoflurane and, after monitoring the adequacy of anesthesia by testing rear foot reflexes, they were euthanized by cervical dislocation. After this, the heart was excised, rinsed in ice-cold phosphate buffer saline and snap-frozen in liquid nitrogen. All procedures were approved by the University of Barcelona Bioethics Committee, as stated in Law 5/21 July 1995 passed by the Generalitat de Catalunya.

2.2. RNA preparation and quantitative real-time RT-PCR analysis

Relative levels of specific mRNAs were assessed by real-time reverse transcription polymerase chain reaction (RT-PCR), as previously described [24]. The sequences of the

forward and reverse primers are shown in Supplemental Table S1. For measurement of *XBP1* splicing, cDNA was used for PCR amplification using *XBP1* primers spanning the 26-bp intron splicing site (forward: 5'-TGAGAACAGGAGTTAAGAACACGC-3' and reverse: 5'-TTCTGGGTAGACCTCTGGGAGTTC-3'). The PCR cycle consisting of 94 °C for 1 min, 62 °C for 1 min, and 72 °C for 1 min was repeated 30 times. This gave a PCR product of 326 bp for unspliced and 300 bp for spliced *XBP1*. The PCR products were separated by electrophoresis with a 2% agarose gel and visualized by ethidium bromide staining.

2.3. Immunoblot analysis

To obtain total protein extracts, AC16 cardiac cells and the heart tissue were lysed in cold RIPA buffer (Sigma, St Louis, MO, USA) with phosphatase and protease inhibitors (0.2 mmol/L phenylmethylsulfonyl fluoride, 1 mmol/L sodium orthovanadate, 5.4 $\mu\text{g}/\text{mL}$ aprotinin). The homogenate was then centrifuged at 10,000 $\times g$ for 30 min at 4 °C, and protein concentration contained in the supernatant was determined using the Bradford method [25]. Protein extracts were separated by SDS-PAGE on 10% separation gels and transferred to Immobilon polyvinylidene difluoride membranes (Millipore, Bedford, MA, USA) [26]. Proteins were detected using the Western Lightning® Plus-ECL chemiluminescence kit (PerkinElmer, Waltham, MA, USA) and their size was estimated using protein molecular mass standards (Life Technologies, S.A., Spain). All antibodies used throughout the study were purchased from Cell Signaling Technology (Danvers, MA, USA), except actin (Sigma).

2.4. Statistical analysis

Results are expressed as the mean \pm SD of three independent experiments for the in vitro studies, each consisting of three culture plates ($n = 9$), and of four mice for the in vivo experiments. Significant differences were established by one-way ANOVA using the GraphPad Prism (GraphPad Software Inc. V4.03, San Diego, CA, USA) software. When significant variations were found by one-way ANOVA, the Tukey–Kramer multiple comparison post-test was performed. Differences were considered significant at $P < 0.05$.

3. Results

3.1. $\text{PPAR}\beta/\delta$ activation prevents palmitate-induced ER stress in cardiac cells of human origin

As a first approach, we aimed to determine whether palmitate (0.25 mM for 18 h) was capable of inducing the expression of several ER stress markers in human cardiac AC16 cells. Real-time RT-PCR analyses demonstrated that palmitate significantly induced the expression of *sXBP1*, *ATF3* (approximately 2-fold, $P < 0.001$), *BiP/GRP78* (4.5-fold, $P < 0.001$) and *CHOP* (4.5-fold, $P < 0.001$), compared to cells exposed only to BSA (Fig. 1). To investigate whether $\text{PPAR}\beta/\delta$ activation prevented ER stress, human cardiac cells were co-incubated with palmitate and GW501516 (10 μM). As shown in Fig. 2A, the $\text{PPAR}\beta/\delta$ agonist completely abolished the increase in *ATF3* and attenuated the rise in *CHOP* expression caused by the saturated fatty acid, but did not prevent the splicing of *XBP1* or the induction of *BiP/GRP78* expression. In agreement with the above results, *BiP/GRP78* and *CHOP* protein levels were increased in cells exposed to palmitate (Fig. 2B). Since activation of IRE-1 α promotes the splicing of *XBP1*, we also evaluated whether palmitate upregulated IRE-1 α phosphorylation at Ser724 residues, which is indicative of its activity. As expected, palmitate treatment also enhanced the phosphorylation of IRE-1 α with regard to control non-treated cells (2-fold, $P < 0.05$, Fig. 2B). On the contrary, no changes were observed in the phosphorylation levels at the Ser51 residue of eIF2 α (see Supplemental Fig. 1A). Consistent with changes in mRNA levels, GW501516 abrogated the increase in *CHOP* protein levels induced by palmitate, but not those of the *BiP/GRP78* chaperone. Surprisingly, GW501516 prevented IRE-1 α phosphorylation induced by palmitate as well, although *sXBP1* was not downregulated. Incubation with GW501516 alone had no effect on *sXBP1* levels, but prevented IRE-1 α phosphorylation in palmitate-treated cells. On the other hand, co-incubation of cells with palmitate, GW501516 and the $\text{PPAR}\beta/\delta$ antagonist GSK0660 (10 μM) reversed the effects of GW501516 on the expression of *ATF3*, but not on *CHOP* (Fig. 2A), therefore demonstrating that $\text{PPAR}\beta/\delta$ activation was involved, at least in part, in the effects of GW501516 on ER stress.

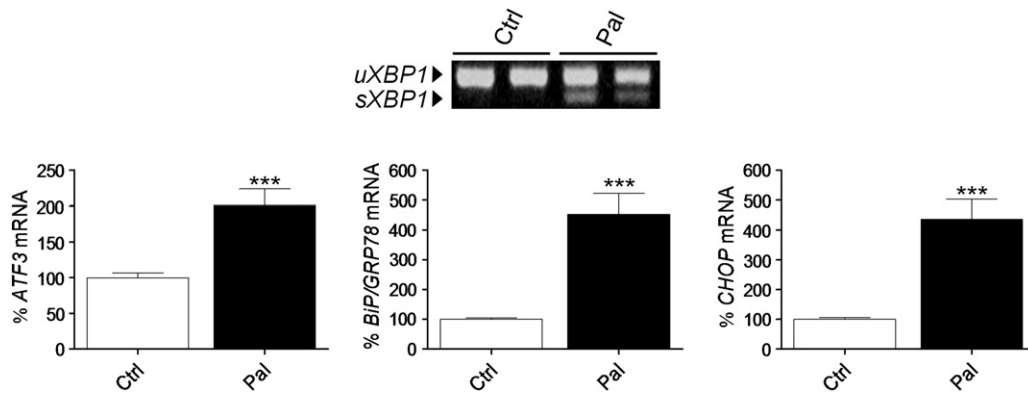


Fig. 1. Palmitate induces endoplasmic reticulum stress markers in human cardiac cells. *sXBP1*, *ATF3*, *BiP/GRP78* and *CHOP* mRNA levels in AC16 cells incubated for 18 h with palmitate (Pal, 0.25 mmol/L). The graphs represent the quantification of the 18S-normalized mRNA levels, expressed as a percentage of control samples \pm SD. *** $P < 0.001$ vs. control (Ctrl).

3.2. The preventive effect of PPAR β/δ activation on palmitate-induced ER stress is AMPK-independent

To investigate the role of 5' AMP-activated protein kinase (AMPK) in palmitate-induced ER stress in human cardiac cells, as well as the preventive effects of GW501516, we took advantage of the AMPK activator AICAR (5-aminoimidazole-4-carboxamide ribonucleotide) and the AMPK inhibitor compound C. As shown in Fig. 3A, the increase in the expression of the ER markers *sXBP1*, *BiP/GRP78* and *CHOP* caused by palmitate was abolished in cells co-incubated with palmitate plus AICAR.

In contrast, AICAR further induced *ATF3* mRNA transcript levels (3.5-fold, $P < 0.001$ vs. control cells). In accordance with these data, AICAR prevented IRE-1 α phosphorylation and the induction of *BiP/GRP78* and *CHOP* protein levels stimulated by the saturated fatty acid (Fig. 3B), but appeared to up-regulate eIF2 α phosphorylation on Ser51 residues (3-fold, $P < 0.01$ vs. control cells, Supplemental Fig. 1B). The outcome observed after co-incubation with compound C demonstrated the involvement of AMPK in ER stress induced by palmitate, since compound C abolished the effects of AMPK activation on *XBP1* splicing, *ATF3* and *CHOP* mRNA expression and protein accumulation, and the

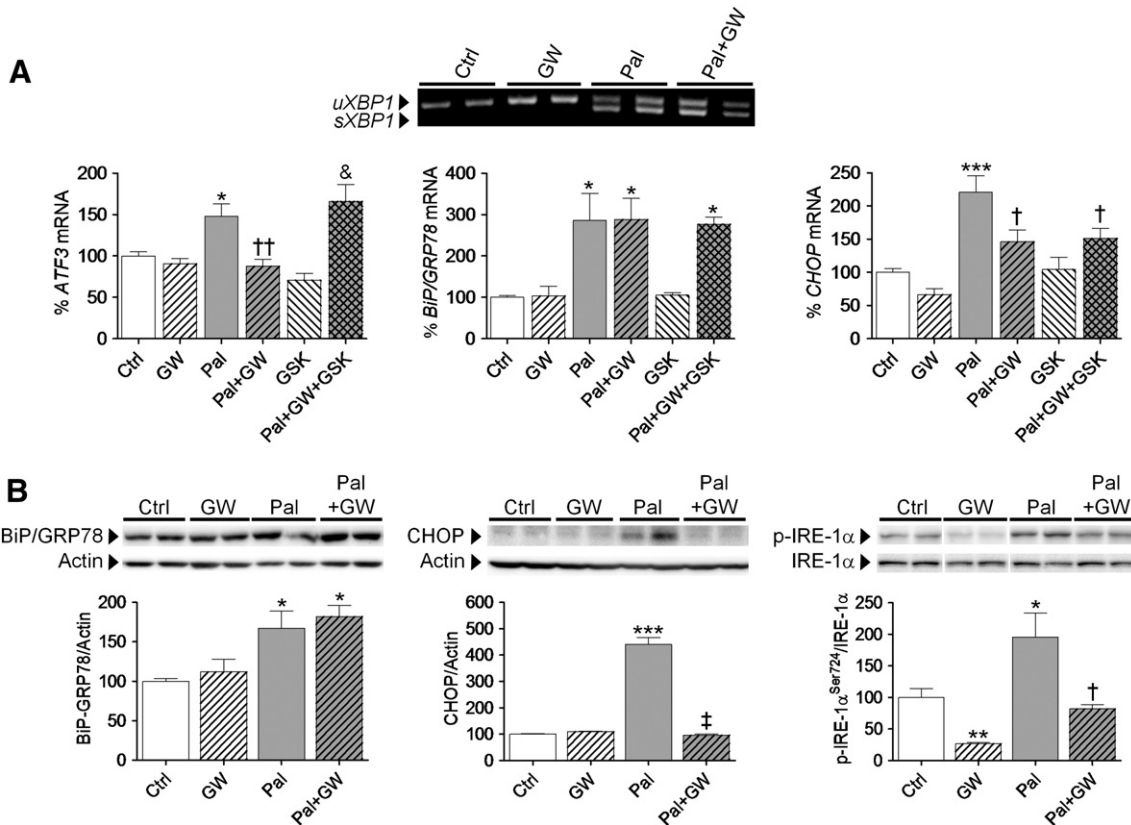


Fig. 2. PPAR β/δ activation prevents palmitate-induced ER stress in human cardiac cells. AC16 cells were incubated for 18 h with palmitate (Pal, 0.25 mmol/L) in the presence or absence of GW501516 (GW, 10 μ mol/L) or GSK0660 (GSK, 10 μ mol/L). (A) *sXBP1*, *ATF3*, *BiP/GRP78* and *CHOP* mRNA levels. The graphs represent the quantification of the 18S-normalized mRNA levels, expressed as a percentage of control samples \pm SD. (B) Western-blot analysis showing protein levels of *BiP/GRP78*, *CHOP* and the ratio phosphorylated IRE-1 α ^{Ser724}/IRE-1 α in total protein extracts. To show equal loading of protein, the actin signal is included from the same blot. The graphs represent the quantification of the normalized protein levels expressed as a percentage of control samples \pm SD. All autoradiograph data are representative of two separate experiments. * $P < 0.05$, ** $P < 0.01$ and *** $P < 0.001$ vs. Ctrl; † $P < 0.05$, †† $P < 0.01$ and ††† $P < 0.001$ vs. Pal; &#P < 0.05 vs. Pal + GW.

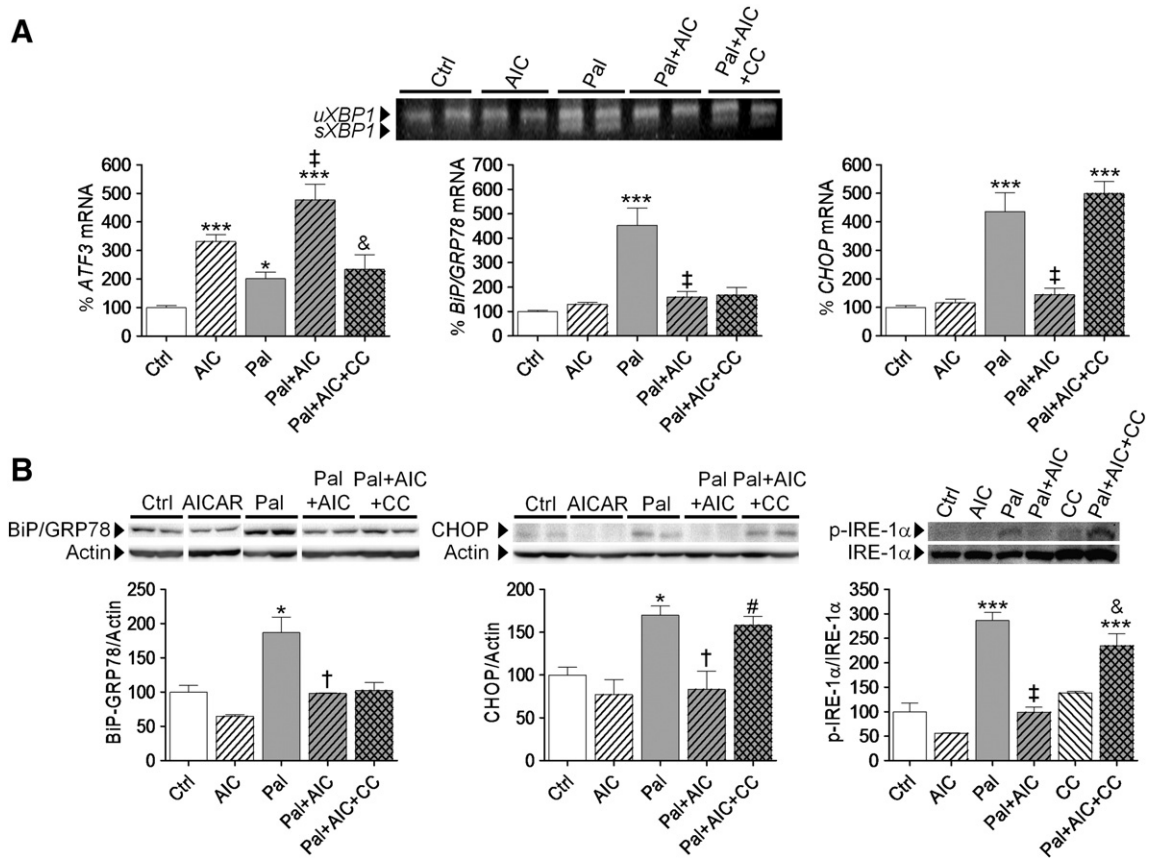


Fig. 3. AMPK activation avoids palmitate-induced ER stress in human cardiac cells. AC16 cells were incubated for 18 h with palmitate (Pal, 0.25 mmol/L) in the presence or absence of AICAR (AIC, 2 mmol/L) or compound C (CC, 30 μmol/L). (A) *sXBP1*, *ATF3*, *BIP/GRP78* and *CHOP* mRNA levels. The graphs represent the quantification of the 18S-normalized mRNA levels, expressed as a percentage of control samples ± SD. (B) Western-blot analysis showing protein levels of *BIP/GRP78*, *CHOP* and the ratio phosphorylated IRE-1α^{Ser724}/IRE-1α in total protein extracts. To show equal loading of protein, the actin signal is included from the same blot. The graphs represent the quantification of the normalized protein levels expressed as a percentage of control samples ± SD. All autoradiograph data are representative of two separate experiments. **P* < 0.05, ***P* < 0.01 and ****P* < 0.001 vs. Ctrl; †*P* < 0.05, ††*P* < 0.01 and †††*P* < 0.001 vs. Pal; #*P* < 0.05 and &*P* < 0.01 vs. Pal + AIC.

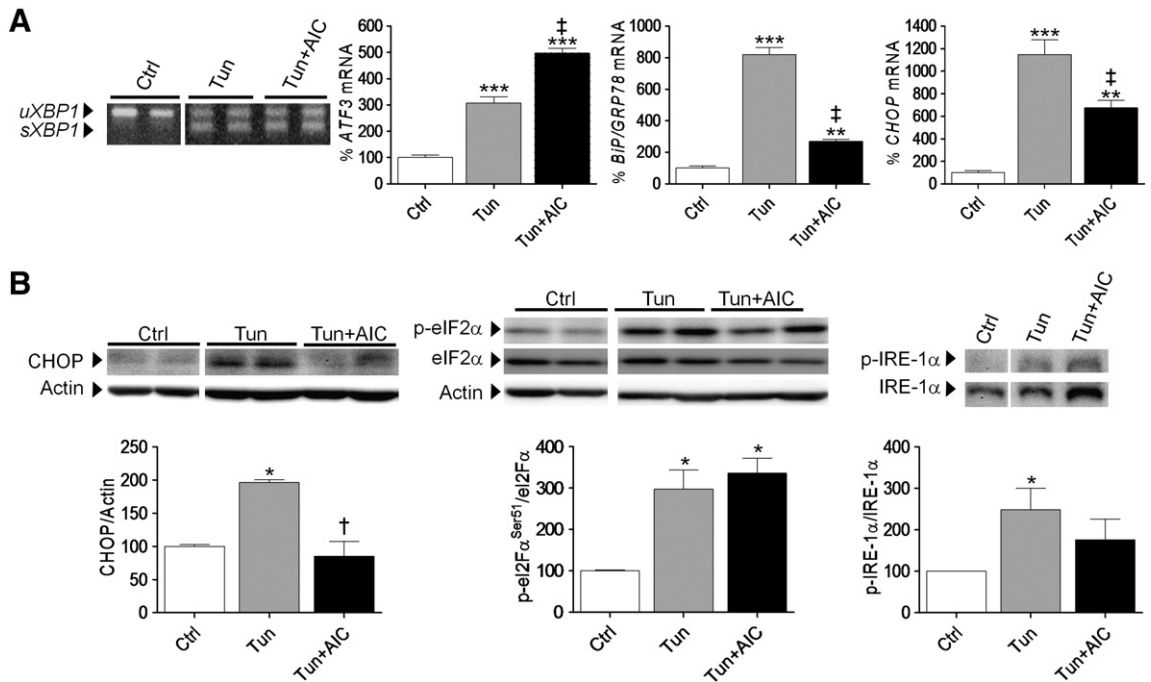


Fig. 4. Tunicamycin elicits ER stress in human cardiac cells. AC16 cells were incubated for 4 h with tunicamycin (Tun, 5 μg/mL) and AICAR (AIC, 2 mmol/L). (A) *sXBP1*, *ATF3*, *BIP/GRP78* and *CHOP* mRNA levels. The graphs represent the quantification of the 18S-normalized mRNA levels, expressed as a percentage of control samples ± SD. (B) Western-blot analysis showing protein levels of *CHOP*, phosphorylated eIF2α^{Ser51}/eIF2α and phosphorylated IRE-1α^{Ser724}/IRE-1α in total protein extracts. To show equal loading of protein, the actin signal is included from the same blot. The graphs represent the quantification of the normalized protein levels expressed as a percentage of control samples ± SD. All autoradiograph data are representative of two separate experiments. **P* < 0.05, ***P* < 0.01 and ****P* < 0.001 vs. Ctrl; †*P* < 0.05, ††*P* < 0.01 and †††*P* < 0.001 vs. Tun.

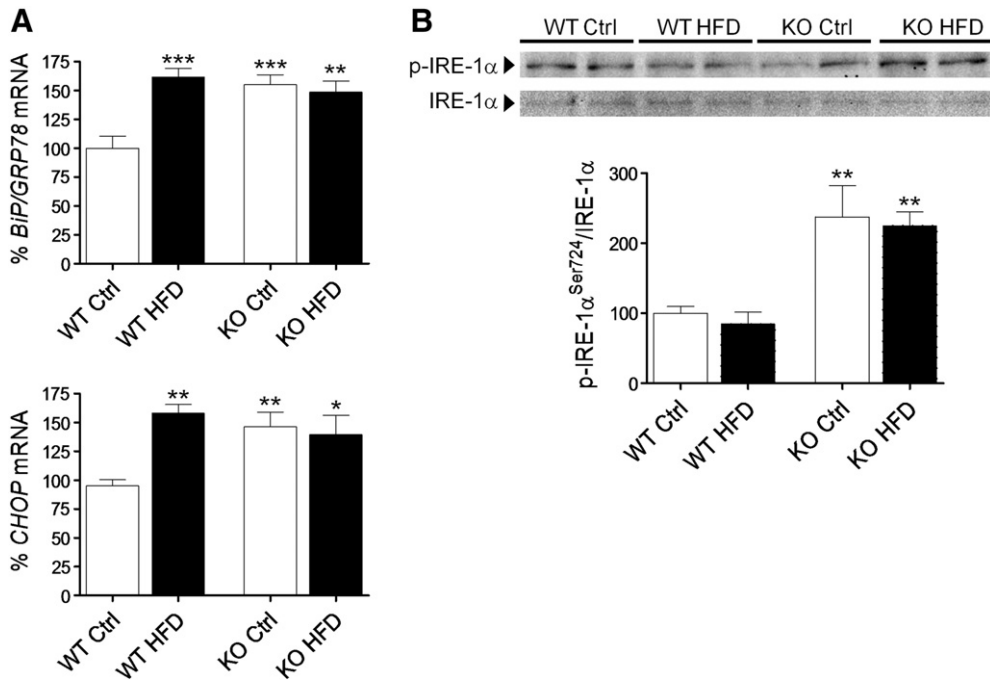


Fig. 5. ER stress induced by an HFD in the heart of mice is exacerbated in PPAR β/δ knockout mice. (A) Relative quantification of *BiP/GRP78* and *CHOP* mRNA levels assessed by real-time RT-PCR of samples obtained from the heart of wild-type (WT) or knockout PPAR β/δ (KO) mice fed a standard chow diet (Ctrl) or a saturated fatty acid-rich diet (HFD) for two months. The graphs represent the quantification of the *APPT*-normalized mRNA levels, expressed as a percentage of control samples \pm SD. (B) Western-blot analysis showing the levels of phosphorylated IRE-1 α ^{Ser724}/IRE-1 α in total protein extracts obtained from the samples depicted in panel A. The graphs represent the quantification of the normalized protein levels expressed as a percentage of control samples \pm SD. All autoradiograph data are representative of two separate experiments. * $P < 0.05$, ** $P < 0.01$ and *** $P < 0.001$ vs. WT Ctrl.

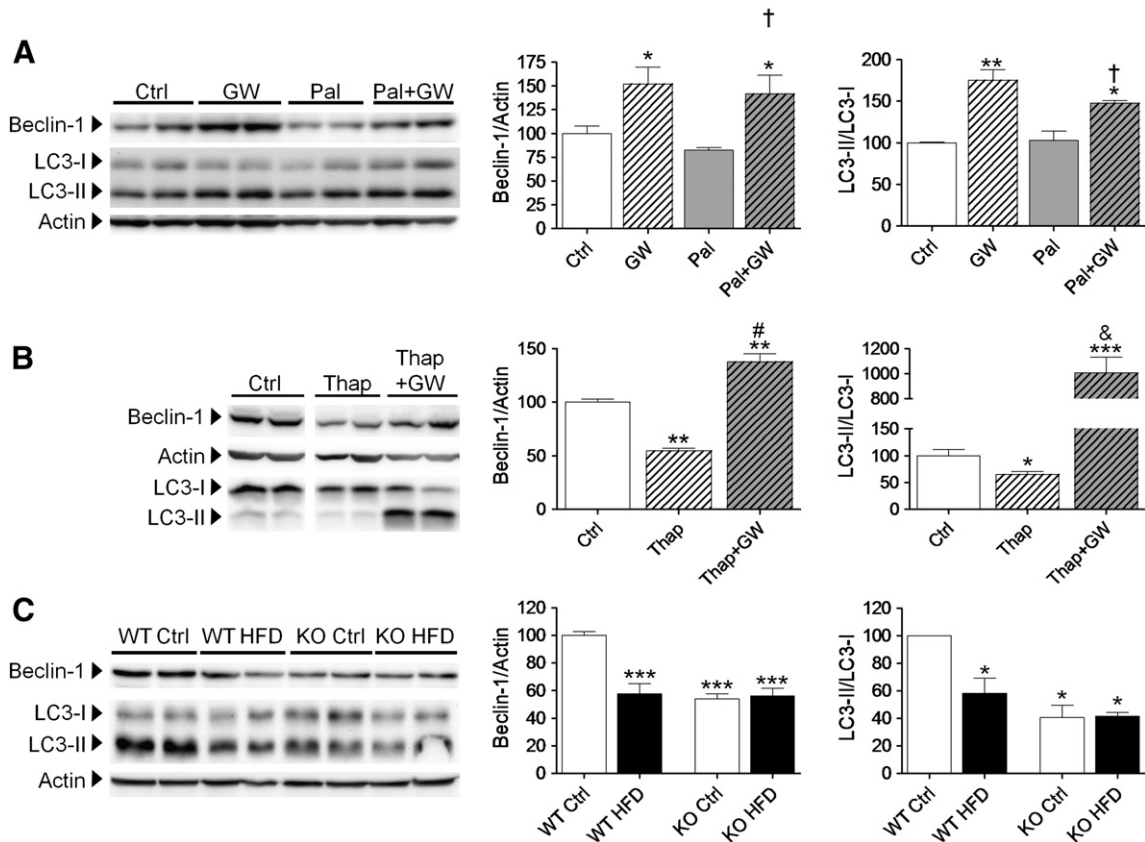


Fig. 6. PPAR β/δ activity regulates autophagy in cardiac cells. Western-blot analysis showing protein levels of beclin-1 and the LC3-II/LC3-I ratio in total protein extracts obtained from human cardiac AC16 cells incubated for (A) 18 h with palmitate (Pal, 0.25 mmol/L) or (B) 18 h with thapsigargin (Thap, 1 μ mol/L), both in the presence or absence of GW501516 (GW, 10 μ mol/L). (C) Western-blot analysis showing protein levels of beclin-1 and the LC3-II/LC3-I ratio in total protein extracts isolated from the heart of wild-type (WT) or knockout PPAR β/δ (KO) mice fed a standard chow diet (Ctrl) or a saturated fatty acid-rich diet (HFD) for two months. The graphs represent the quantification of the normalized protein levels expressed as a percentage of control samples \pm SD. All autoradiograph data are representative of two separate experiments. (A) and (B) * $P < 0.05$, ** $P < 0.01$ and *** $P < 0.001$ vs. Ctrl; † $P < 0.05$ vs. Pal; & $P < 0.01$, # $P < 0.001$ vs. Thap. (C) * $P < 0.05$, ** $P < 0.01$ and *** $P < 0.001$ vs. WT Ctrl.

phosphorylation of eIF2 α and IRE-1 α (Fig. 3 and Supplemental Fig. 1B). To further confirm the role of AMPK in regulating ER stress in our cells, we monitored AMPK phosphorylation at Thr172, which is essential for its activity. As expected, compound C reduced AMPK phosphorylation (~90% reduction, $P < 0.05$ vs. control cells) in human AC16 cardiac cells but, strikingly, both AICAR (2-fold, $P < 0.05$ vs. control cells) and palmitate (3.5-fold, $P < 0.001$) enhanced this phosphorylation (Supplemental Fig. 2A). We also explored the phosphorylation of the cardiac-specific acetyl-CoA carboxylase (ACC) isoform, ACC2, a substrate for AMPK that serves as a surrogate for determining its activity. In contrast to AMPK phosphorylation, phospho-ACC2 levels were slightly reduced in cells exposed to palmitate or compound C, whereas in the presence of AICAR, they were significantly raised (2-fold, $P < 0.05$, Supplemental Fig. 2A).

ER stress inhibition after AMPK activation was also demonstrated after cardiac AC16 cells had been induced with tunicamycin, a mixture of homologous nucleoside antibiotics that acts as a potent pharmacologic ER-stress inducer. Tunicamycin elicited a huge increase in *sXBP1*, *ATF3* (3-fold, $P < 0.001$), *BiP/GRP78* (8-fold, $P < 0.001$) and *CHOP* (11-fold, $P < 0.001$) expression, as well as IRE-1 α phosphorylation (2.5-fold, $P < 0.05$) (Fig. 4A). Co-incubation of tunicamycin-treated cells with AICAR prevented the rise of some of these ER stress markers, such as *BiP/GRP78* and *CHOP* expression, but not all (*sXBP1* and *ATF3*). Western-blot analyses revealed that AICAR also abolished the increase in *CHOP* protein induced by tunicamycin, as observed by mRNA levels, but not eIF2 α or IRE-1 α phosphorylation (Fig. 4B). Activation of AMPK by AICAR was again monitored by determination of ACC2 phosphorylation (Supplemental Fig. 2B).

Therefore, given that GW501516 can induce AMPK phosphorylation at Thr172 independently of PPAR β/δ activation, and we had observed that AMPK activation prevented palmitate-induced ER stress, we next examined whether this kinase was involved in the effects of GW501516. However, we found that compound C did not prevent GW501516-mediated effects on any of the ER stress markers examined (*ATF3*, *BiP/GRP78* and *CHOP* expression, Supplemental Fig. 3A). This indicates that AMPK did not mediate the beneficial effects of GW501516 on ER stress, and may be explained by the fact that, in contrast to previously reported data [27], GW501516 did not enhance AMPK and ACC2 phosphorylation in AC16 cells (Supplemental Fig. 3B). Likewise, GW501516 did not prevent either the effects of tunicamycin on the expression of *sXBP1*, *BiP/GRP78* and *CHOP*, or the phosphorylation of IRE-1 α (Supplemental Fig. 4). Overall, this reinforces the notion that the effects of GW501516 are not dependant on AMPK activation.

3.3. ER stress induced by an HFD in the heart of mice is exacerbated in PPAR β/δ knockout mice

To corroborate the results obtained with cultured human cardiac cells, we also conducted in vivo studies with mice fed an HFD rich in saturated fatty acids. Consistent with the in vitro studies, an HFD significantly induced *BiP/GRP78* and *CHOP* expression in the heart of male wild type mice (1.5-fold, $P < 0.001$, and 1.5-fold, $P < 0.01$, respectively, vs. wild type control diet) (Fig. 5A). To further confirm the protective role of PPAR β/δ , we took advantage of PPAR β/δ knockout mice. Interestingly, *BiP/GRP78* (1.5-fold, $P < 0.01$ vs. wild type mice) and *CHOP* (1.5-fold, $P < 0.05$) expression was also higher in PPAR β/δ knockout mice than in wild type mice (Fig. 5A). This indicates that PPAR β/δ somehow prevented ER stress in the heart of these mice. Western-blot analysis revealed that PPAR β/δ suppression also enhanced IRE-1 α phosphorylation (2.5-fold, $P < 0.01$) (Fig. 5B), although no splicing of *XBP1* was detected (Supplemental Fig. 5A). All these changes coincided with diminished AMPK and ACC2 activity, as revealed by western-blot (Supplemental Fig. 5B). This suggests that there was reduced fatty acid β -oxidation in mice fed an HFD and in PPAR β/δ knockout mice.

3.4. PPAR β/δ activity regulates autophagy in cardiac cells

As reported above, when ER stress becomes chronically activated, apoptosis is induced to remove affected cells. Therefore, the next goal of this study was to evaluate the presence of apoptosis in human cardiac cells treated with palmitate. This was attained by determining different apoptotic markers that are essential for the elimination of irreversibly damaged cells under chronic ER stress, such as α -spectrin breakdown and Bcl-2 protein levels, by means of western-blot analysis, or *Bax*, *Bim* and *Puma* mRNA levels by real-time RT-PCR. As observed in Supplemental Fig. 6, 0.25 mM palmitate treatment for 18 h did not induce apoptosis in human cardiac AC16 cells. GW501516 did not display any effect on apoptosis, except for a slight but interesting decrease of *Bim* expression after co-incubation with palmitate (40% reduction, $P < 0.01$ vs. palmitate-treated cells).

After that, we examined the occurrence of autophagy in human cardiac cells by checking two well-established autophagic markers in eukaryotes, the LC3-II/LC3-I ratio and the protein levels of beclin-1, which are both required for the formation of the autophagosome during autophagy. LC3 is considered a marker for autophagy when it is proteolytically processed to form LC3-II. In spite of beclin-1 and LC3 expression (Supplemental Fig. 7A) and the fact that protein levels (Fig. 6A) were not modified in palmitate-treated cells, we found that GW501516, alone or in combination with palmitate, significantly enhanced both markers of autophagy, beclin-1 (1.5-fold, $P < 0.05$) and the LC3-II/LC3-I ratio (1.75-fold, $P < 0.01$, Fig. 6A). GW501516 also induced autophagy in the presence of tunicamycin, which indicates that its effect was not dependent on the type of ER stress inducer (Supplemental Fig. 7B). On the contrary, autophagy was not observed after treatment with AICAR (Supplemental Fig. 7C). These results suggest that GW501516 induces autophagy by post-transcriptional mechanisms, and in an AMPK-independent manner. To further corroborate the effect of GW501516 on autophagy, we next incubated human cardiac cells with thapsigargin. Thapsigargin is a sesquiterpene lactone that is experimentally used to specifically inhibit the last step in the autophagic process, which also raises cytosolic calcium concentration, thereby inducing ER-stress. As shown in Fig. 6B, thapsigargin down-regulated the protein levels of beclin-1 (45% reduction, $P < 0.01$ vs. control cells) and the LC3-II/LC3-I ratio (35% reduction, $P < 0.05$), a fact which was not only prevented, but also further increased, after GW501516 co-incubation. Besides inhibiting autophagy, thapsigargin triggers expression of *CHOP*, a transcription factor involved in ER stress-induced apoptosis [10,28]. In accordance with this, we found that thapsigargin up-regulated *BiP/GRP78* (3.5-fold, $P < 0.01$) and *CHOP* protein levels (7.5-fold, $P < 0.001$). The PPAR β/δ agonist GW501516 did not prevent the increase in *BiP/GRP78* protein levels, but did attenuate those of *CHOP* (Supplemental Fig. 8), which suggests that this drug also down-regulated the ER stress induced by thapsigargin. Last, but not least, we demonstrated that HFD feeding or PPAR β/δ suppression clearly down-regulated beclin-1 and the LC3-II/LC3-I ratio in the heart of mice (Fig. 6C), which indicates that this nuclear receptor plays a key role in the control of the autophagic process in cardiac cells.

4. Discussion

In recent years, activation of the UPR during ER stress has evolved as a new mechanism involved in the association between saturated free fatty acid-induced inflammation and chronic metabolic diseases, such as obesity, insulin resistance, and type 2 diabetes [6,29]. Studies performed in muscle [4,30] and pancreatic β -cells [28] have demonstrated that palmitate induces the splicing of *XBP1* and enhances the expression of ER stress markers such as *ATF3*, *BiP/GRP78* and *CHOP*, as well as the phosphorylation of IRE-1 α [4,30]. In agreement with this, we report that palmitate induces *XBP1* splicing and IRE-1 α phosphorylation, as well as *ATF3*, *BiP/GRP78* and *CHOP* gene expression and protein accumulation in human cardiac cells. However, and in contrast to muscle

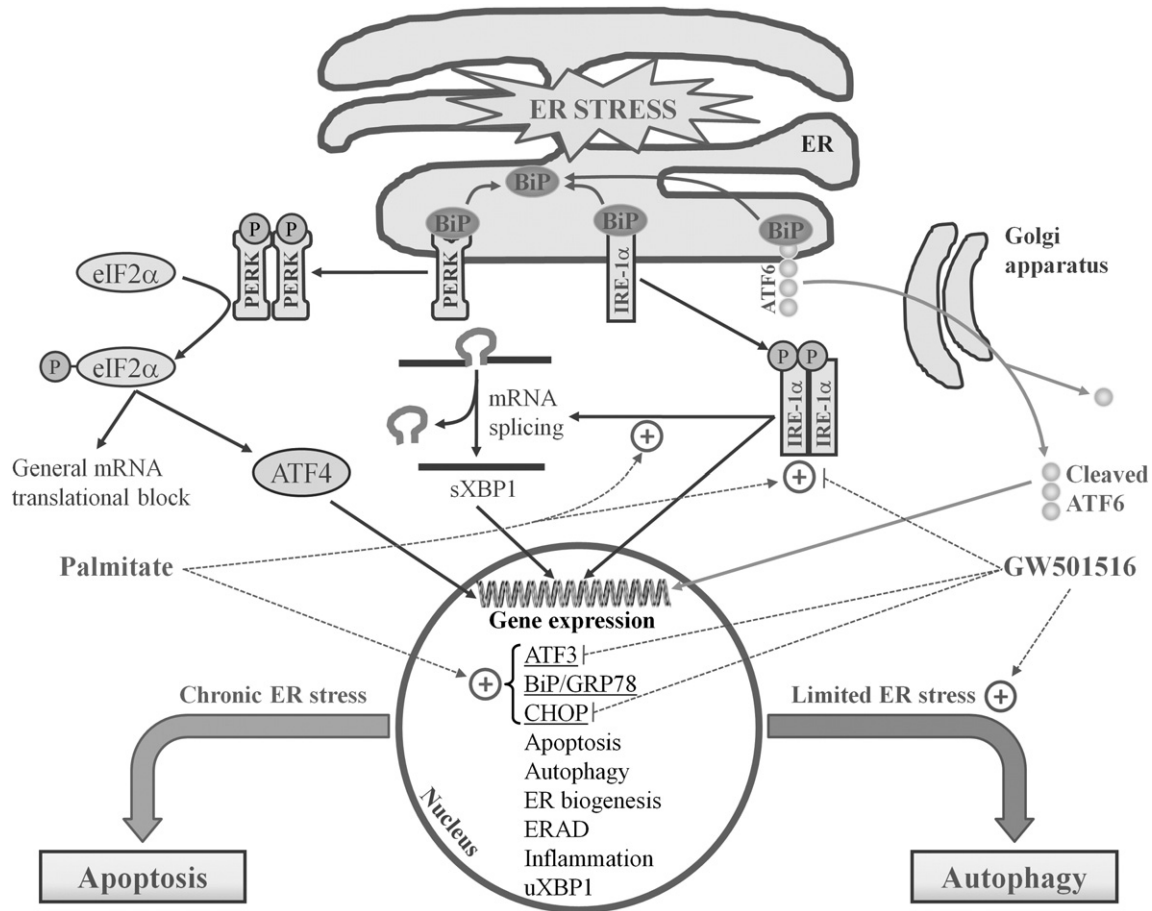


Fig. 7. PPAR β/δ attenuates palmitate-induced endoplasmic reticulum stress and induces autophagy. Initiation of the UPR involves the activation of ATF6, IRE-1 α and PERK pathways. In the absence of stress, these trans-membrane proteins are bound to the intra-luminal BiP/GRP78 protein. On stress exposure, the large excess of unfolded proteins sequesters BiP/GRP78 from trans-membrane ER proteins, thereby inducing the UPR. After proteolytically processing at the Golgi complex, ATF6 translocates to the nucleus, in which it acts as a transcription factor for ER chaperones and ERAD-related genes. On the other hand, the endoribonuclease activity of IRE-1 α cleaves the mRNA of *XBP1*, creating an alternative message that is translated into the spliced and active form of this transcription factor (sXBP1). Active IRE-1 α also regulates responses mediated by mitogen-activated protein kinases (MAPKs) and NF- κ B, which are relevant factors for the induction of apoptosis and inflammatory processes by ER stress. Finally, PERK phosphorylates and inhibits eIF2 α , and by this means inhibits the translation of most mRNAs. However, some mRNAs escape this translational control, for example transcription factor *ATF4* (and its target genes *ATF3*, *BiP/GRP78* and *CHOP*) and genes involved in autophagy and apoptosis. If ER stress is limited, the UPR will potentiate autophagy to protect the cells. However, if ER stress is prolonged, the UPR will turn on apoptosis for removing cells that threaten the integrity of the organism. Palmitate induces *XBP1* splicing and IRE-1 α phosphorylation, as well as ATF3, BiP/GRP78 and CHOP gene expression and protein accumulation in human cardiac cells. PPAR β/δ activation with GW501516 prevents saturated fatty acid-induced ER stress, since it abolishes the rise in ATF3 and CHOP levels and prevents IRE-1 α phosphorylation in palmitate-treated cells. ATF, activating transcription factor; BiP/GRP78, binding immunoglobulin protein/glucose-regulated protein 78; CHOP, CCAAT/enhancer binding protein homologous protein; eIF2 α , eukaryotic initiation factor 2 α ; ERAD, ER-associated degradation; IRE-1 α , inositol-requiring enzyme; PERK, PKR-like ER kinase.

cells [4,5,31], the PERK/eIF2 α branch of the UPR pathway was not activated in human cardiac cells, since eIF2 α phosphorylation at Ser51 remained unaltered after palmitate treatment. In addition, we demonstrate here for the first time in cardiac cells that PPAR β/δ activation with GW501516 prevents saturated fatty acid-induced ER stress, since it abolishes the rise in ATF3 and CHOP levels. Strikingly, GW501516 prevented IRE-1 α phosphorylation, but this was not accompanied by *sXBP1* downregulation. This suggests that in human cardiac cells *XBP1* splicing depends on the action of a yet to uncover endoribonuclease or that the time chosen for analyses was too short. *sXBP1* up-regulates many essential UPR genes involved in folding, organelle biogenesis, ERAD, autophagy, and protein quality control, but its specific target genes may vary depending on the cell type and the nature of the stressor stimulus [8]. Although *BiP/GRP78* expression may be transcriptionally controlled by the three UPR branches, and given that the effects of GW501516 on *XBP1* splicing fairly correlated with those of *BiP/GRP78* expression, our results suggest that, at least in human cardiac cells, *BiP/GRP78* might be transcriptionally controlled by *sXBP1*.

Owing to its high fat content, the Western-type diet is known to cause insulin resistance and type 2 diabetes mellitus, besides inducing ER stress and inflammation [30,32]. Our studies conducted in vivo

with mice also demonstrate that saturated fatty acid-rich HFD feeding induces *BiP/GRP78* and *CHOP* expression in the heart. More importantly, the expression of these ER stress markers was also enhanced in PPAR β/δ knockout mice, thus indicating that PPAR β/δ somehow prevented ER stress in the heart of mice. In agreement to what happened in vitro, PPAR β/δ suppression enhanced IRE-1 α phosphorylation, but not *XBP1* splicing. Unlike human cardiac cells in vitro, we found that eIF2 α phosphorylation was enhanced in the heart of mice fed an HFD and also in PPAR β/δ knockout mice (Supplemental Fig. 9).

AMPK activation brings about multiple protective effects, including inhibition of inflammation, oxidative stress and insulin resistance, which result in a diminution of the risk for developing obesity and type 2 diabetes [33]. Recently, it has been reported that AMPK protects against cardiomyocyte hypoxic injury [34] and atherosclerosis [35] by reducing ER stress. When we examined the potential mechanisms responsible for the increase in ER stress following palmitate exposure, we observed that this saturated fatty acid reduced AMPK activity. In consonance with this, AICAR prevented the rise of most palmitate-induced ER stress markers. Similar results were obtained after induction of ER stress with tunicamycin. In contrast, our results clearly indicate that the preventive effects of GW501516 on palmitate- and

tunicamycin-induced ER stress are AMPK-independent. On the contrary, results obtained in both mice fed an HFD and in PPAR β/δ knockout mice suggest that reduced fatty acid β -oxidation occurs in the heart. Nevertheless, our *in vivo* results match with those obtained in the liver and muscle of rodents after HFD feeding, in which saturated fatty acids appear to contribute to AMPK inhibition [36].

Prolonged or severe ER stress during diabetic cardiomyopathy leads to apoptotic cell death of cardiomyocytes [14] and, because myocytes rarely proliferate in the adult heart, the loss of cardiomyocytes will compromise cardiac function. The initiation of the caspase cascade during intrinsic apoptosis is mediated by BH3-only domain proteins such as Bim (B-cell lymphoma-2 [Bcl-2]-like 11) and Puma (Bcl-2 binding component 3), which are responsible for transmitting death signals by either inhibiting the Bcl-2 anti-apoptotic members (Bcl-2; Bcl-xL, B-cell lymphoma-extra large) or activating the pro-apoptotic Bcl-2 multi-domain proteins (Bax, Bcl-2-associated \times protein; Bak, Bcl-2 homologous antagonist/killer) at the mitochondria. The UPR promotes the expression of CHOP, a pro-apoptotic transcription factor that has a critical role in cardiac cell death caused by chronic ER stress during heart failure [11] and cardiac hypertrophy [37]. The UPR, possibly through CHOP, down-regulates the anti-apoptotic Bcl-2 family of proteins, but transcriptionally up-regulates Bim and Puma. Overall, this contributes to apoptosis in cells undergoing irreversible ER stress [8]. However, although we had found a significant increase in CHOP protein levels after palmitate treatment, no changes in any of the apoptotic markers examined were detected in human cardiac cells. In accordance with this, Quentin et al. [38] demonstrated that CHOP is not necessarily a mediator of apoptosis in rat cardiomyocytes. Nevertheless, our results contrast with those obtained in diverse hepatoma cell lines [39,40], in which palmitic acid was found to induce ER stress and subsequent apoptosis. Although GW501516 prevented the rise in CHOP protein levels after palmitate treatment in human cardiac cells, it did not reduce apoptosis. The relatively short duration of palmitate treatment might account for the lack of apoptotic activation in human cardiac cells, since several authors have speculated that the transition between adaptive UPR and apoptosis depends, at least in part, on the duration of ER stress stimulation [8].

It is widely accepted that, when ER stress is limited, the UPR potentiates autophagy as a short-term strategy to protect cells. Thus, suppression of autophagy favors the development of heart failure during diabetes [41], whereas its induction may reduce myocardial ischemia/reperfusion-induced lethal injury [10]. The most striking result of our study is the enhancement of two well-known markers of autophagy in cardiac cells after GW501516 treatment and in the heart of mice fed an HFD. More importantly, we also report here that PPAR β/δ suppression down-regulates autophagic markers in the heart of mice, hence suggesting that this nuclear receptor is crucial in regulating the autophagic process in cardiac cells. However, and unlike a previous study performed with rat heart [10], we did not find any correlation between eIF2 α phosphorylation and the conversion of LC3-II from LC3-I. This suggests that the PERK/eIF2 α pathway is not essential for autophagy in our model. In fact, our results better fit with those obtained by Ogata et al. [42] in mouse embryonic fibroblasts, which demonstrated that activation of autophagy by ER stress depends on the kinase domain of IRE-1 α , but not on its endoribonuclease activity on XBP1 nor on the PERK/eIF2 α pathway. A recent study demonstrated that activation of AMPK restores cardiac autophagy and protects against cardiac cell apoptosis, which ultimately improves cardiac function in diabetic mice [41]. In contrast, our results indicate that GW501516 induces autophagy by post-transcriptional mechanisms in an AMPK-independent manner. This discrepancy might be explained by the fact that He and collaborators investigated autophagy in the context of high glucose conditions, and AMPK is a well-recognized regulator of glucose homeostasis. However, recent studies performed in mice fed an HFD reported that

autophagy is down-regulated in adipose tissue [43] and in the heart [44]. The former study also demonstrates that autophagy suppression induces inflammatory responses via ER stress activation, while the opposite, that is activation of autophagy with rapamycin, decreases inflammatory gene expression [43]. Overall, and taking into account our previous data demonstrating that PPAR β/δ can limit myocardial inflammation by NF- κ B inhibition [15], we hypothesize that GW501516 might prevent ER stress in human cardiac cells by means of autophagy activation. This is supported by our results demonstrating that the NF- κ B inhibitor parthenolide prevented the up-regulation of *ATF3* and *CHOP* expression induced by palmitate in human cardiac cells (Supplemental Fig. 10).

Given its causative role in cardiovascular diseases associated with metabolic disorders such as obesity and diabetes, ER stress has been suggested as a useful therapeutic target. With this aim, several chemical chaperones have been examined in a number of disease models as potential tools for preventing ER stress and the activation of the UPR, since they play a similar role to endogenous chaperones, stabilizing proteins and assisting in their proper folding [45]. For instance, 4-phenylbutyric acid (PBA) and tauroursodeoxycholic acid (TUDCA) have had beneficial effects on insulin resistance, obesity and diabetes in several *in vitro* [4,5] and *in vivo* [46] models. However, chemical chaperones have major drawbacks: their null specificity and a high-dose are required to obtain effective protein folding properties. Therefore, the research and development of new drugs that target ER stress during metabolic diseases without the undesired effects of chemical chaperones are of great interest.

5. Study limitations

A major drawback of the study might be the origin of the AC16 cell line itself, since it consists of a fusion of primary ventricular cells with SV-40-transformed fibroblasts. However, this cell line develops many of the biochemical and morphological properties characteristic of cardiac muscle cells, even though it does not form completely differentiated cardiomyocytes [47]. Furthermore, the more relevant findings obtained in this study with AC16 human cardiac cells have been further corroborated later in the heart of mice.

6. Conclusions

Results herein reported demonstrate that PPAR β/δ activation with GW501516 attenuates palmitate-induced ER stress and induces autophagy in human cardiac cells (Fig. 7), thereby adding a new beneficial mechanism for this drug. In this context, activation of autophagy has already been suggested as a useful therapeutic approach for diabetes, owing to its ability to reduce ER stress in pancreatic β -cells [48]. PPAR β/δ has many valuable physiological functions ranging from enhanced fatty acid catabolism and improved insulin sensitivity, to inflammation inhibition, thus displaying a potential therapeutic role for the prevention and treatment of diseases including diabetes, dyslipidemias or metabolic syndrome. Since chronic low-grade inflammation and ER stress play a significant role in cardiac hypertrophy and heart failure, and GW501516 has been shown to ameliorate metabolic disturbances in heart caused by high-fat diets [15], it is tempting to speculate that PPAR β/δ might serve as a therapeutic target to prevent cardiac hypertrophy and heart failure induced by ER stress during metabolic disorders.

Supplementary data to this article can be found online at <http://dx.doi.org/10.1016/j.ijcard.2014.03.176>.

Acknowledgments

This study was supported by funds from the *Ministerio de Economía y Competitividad* of the Spanish Government (SAF2009-06939 and SAF2012-30708). *CIBER de Diabetes y Enfermedades Metabólicas Asociadas* (CIBERDEM) is an initiative of the *Instituto de*

Salud Carlos III (ISCIII) – Ministerio de Economía y Competitividad. We thank the University of Barcelona's Language Advisory Service for their assistance.

The authors of this manuscript have certified that they comply with the Principles of Ethical Publishing in the International Journal of Cardiology.

References

- Diakogiannaki E, Welters HJ, Morgan NG. Differential regulation of the endoplasmic reticulum stress response in pancreatic beta-cells exposed to long-chain saturated and monounsaturated fatty acids. *J Endocrinol* 2008;197:553–63.
- Karaskov E, Scott C, Zhang L, Teodoro T, Ravazzola M, Volchuk A. Chronic palmitate but not oleate exposure induces endoplasmic reticulum stress, which may contribute to INS-1 pancreatic beta-cell apoptosis. *Endocrinology* 2006;147:3398–407.
- Jung TW, Lee KT, Lee MW, Ka KH. SIRT1 attenuates palmitate-induced endoplasmic reticulum stress and insulin resistance in HepG2 cells via induction of oxygen-regulated protein 150. *Biochem Biophys Res Commun* 2012;422:229–32.
- Salvadó L, Coll T, Gomez-Foix AM, et al. Oleate prevents saturated-fatty-acid-induced ER stress, inflammation and insulin resistance in skeletal muscle cells through an AMPK-dependent mechanism. *Diabetologia* 2013;56:1372–82.
- Peng G, Li L, Liu Y, et al. Oleate blocks palmitate-induced abnormal lipid distribution, endoplasmic reticulum expansion and stress, and insulin resistance in skeletal muscle. *Endocrinology* 2011;152:2206–18.
- Hotamisligil GS. Endoplasmic reticulum stress and the inflammatory basis of metabolic disease. *Cell* 2010;140:900–17.
- Xu J, Zhou Q, Xu W, Cai L. Endoplasmic reticulum stress and diabetic cardiomyopathy. *Exp Diabetes Res* 2012;2012:827971.
- Hetz C, Martinon F, Rodriguez D, Glimcher LH. The unfolded protein response: integrating stress signals through the stress sensor IRE1 α . *Physiol Rev* 2011;91:1219–43.
- Ma Y, Brewer JW, Diehl JA, Hendershot LM. Two distinct stress signaling pathways converge upon the CHOP promoter during the mammalian unfolded protein response. *J Mol Biol* 2002;318:1351–65.
- Petrovski G, Das S, Juhasz B, Kertesz A, Tosaki A, Das DK. Cardioprotection by endoplasmic reticulum stress-induced autophagy. *Antioxid Redox Signal* 2011;14:2191–200.
- Zhao H, Liao Y, Minamino T, et al. Inhibition of cardiac remodeling by pravastatin is associated with amelioration of endoplasmic reticulum stress. *Hypertens Res* 2008;31:1977–87.
- Li Z, Zhang T, Dai H, et al. Involvement of endoplasmic reticulum stress in myocardial apoptosis of streptozocin-induced diabetic rats. *J Clin Biochem Nutr* 2007;41:58–67.
- Lakshmanan AP, Meilei H, Suzuki K, et al. The hyperglycemia stimulated myocardial endoplasmic reticulum (ER) stress contributes to diabetic cardiomyopathy in the transgenic non-obese type 2 diabetic rats: a differential role of unfolded protein response (UPR) signaling proteins. *Int J Biochem Cell Biol* 2012;45:438–47.
- Takada A, Miki T, Kuno A, et al. Role of ER stress in ventricular contractile dysfunction in type 2 diabetes. *PLoS ONE* 2012;7:e39893.
- Álvarez-Guardia D, Palomer X, Coll T, et al. PPARbeta/delta activation blocks lipid-induced inflammatory pathways in mouse heart and human cardiac cells. *Biochim Biophys Acta* 1811;2011:59–67.
- Hamid T, Guo SZ, Kingery JR, Xiang X, Dawn B, Prabhu SD. Cardiomyocyte NF-kappaB p65 promotes adverse remodeling, apoptosis, and endoplasmic reticulum stress in heart failure. *Cardiovasc Res* 2011;89:129–38.
- Cheng L, Ding G, Qin Q, et al. Cardiomyocyte-restricted peroxisome proliferator-activated receptor-delta deletion perturbs myocardial fatty acid oxidation and leads to cardiomyopathy. *Nat Med* 2004;10:1245–50.
- Wang P, Liu J, Li Y, et al. Peroxisome proliferator-activated receptor delta is an essential transcriptional regulator for mitochondrial protection and biogenesis in adult heart. *Circ Res* 2010;106:911–9.
- Cao M, Tong Y, Lv Q, et al. PPARdelta activation rescues pancreatic beta-cell line INS-1E from palmitate-induced endoplasmic reticulum stress through enhanced fatty acid oxidation. *PPAR Res* 2012;2012:680684.
- Ramirez T, Tong M, Chen WC, Nguyen QG, Wands JR, de la Monte SM. Chronic alcohol-induced hepatic insulin resistance and ER stress ameliorated by PPAR-delta agonist treatment. *J Gastroenterol Hepatol* 2013;28:179–87.
- Palomer X, Álvarez-Guardia D, Rodríguez-Calvo R, et al. TNF-alpha reduces PGC-1alpha expression through NF-kappaB and p38 MAPK leading to increased glucose oxidation in a human cardiac cell model. *Cardiovasc Res* 2009;81:703–12.
- Coll T, Palomer X, Blanco-Vaca F, et al. Cyclooxygenase 2 inhibition exacerbates palmitate-induced inflammation and insulin resistance in skeletal muscle cells. *Endocrinology* 2010;151:537–48.
- Nadra K, Anghel SI, Joye E, et al. Differentiation of trophoblast giant cells and their metabolic functions are dependent on peroxisome proliferator-activated receptor beta/delta. *Mol Cell Biol* 2006;26:3266–81.
- Palomer X, Capdevila-Busquets E, Álvarez-Guardia D, et al. Resveratrol induces nuclear factor-kappaB activity in human cardiac cells. *Int J Cardiol* 2013;167:2507–16.
- Bradford MM. A rapid and sensitive method for the quantitation of microgram quantities of protein utilizing the principle of protein-dye binding. *Anal Biochem* 1976;72:248–54.
- Álvarez-Guardia D, Palomer X, Coll T, et al. The p65 subunit of NF-kappaB binds to PGC-1alpha, linking inflammation and metabolic disturbances in cardiac cells. *Cardiovasc Res* 2010;87:449–58.
- Kramer DK, Al Khalili L, Guigas B, Leng Y, Garcia-Roves PM, Krook A. Role of AMP kinase and PPARdelta in the regulation of lipid and glucose metabolism in human skeletal muscle. *J Biol Chem* 2007;282:19313–20.
- Kharroubi I, Ladrèere L, Cardozo AK, Dogusan Z, Chop M, Eizirik DL. Free fatty acids and cytokines induce pancreatic beta-cell apoptosis by different mechanisms: role of nuclear factor-kappaB and endoplasmic reticulum stress. *Endocrinology* 2004;145:5087–96.
- Zhang K, Kaufman RJ. From endoplasmic-reticulum stress to the inflammatory response. *Nature* 2008;454:455–62.
- Rieusset J, Chauvin MA, Durand A, et al. Reduction of endoplasmic reticulum stress using chemical chaperones or Grp78 overexpression does not protect muscle cells from palmitate-induced insulin resistance. *Biochem Biophys Res Commun* 2011;417:439–45.
- Hage Hassan R, Hainault I, Vilquin JT, et al. Endoplasmic reticulum stress does not mediate palmitate-induced insulin resistance in mouse and human muscle cells. *Diabetologia* 2012;55:204–14.
- Panzhinskiy E, Hua Y, Culver B, Ren J, Nair S. Endoplasmic reticulum stress upregulates protein tyrosine phosphatase 1B and impairs glucose uptake in cultured myotubes. *Diabetologia* 2012;56:598–607.
- Shaw RJ, Lamia KA, Vasquez D, et al. The kinase LKB1 mediates glucose homeostasis in liver and therapeutic effects of metformin. *Science* 2005;310:1642–6.
- Yeh CH, Chen TP, Wang YC, Lin YM, Fang SW. AMP-activated protein kinase activation during cardioplegia-induced hypoxia/reoxygenation injury attenuates cardiomyocyte apoptosis via reduction of endoplasmic reticulum stress. *Mediators Inflamm* 2010;2010:130636.
- Dong Y, Zhang M, Liang B, et al. Reduction of AMP-activated protein kinase alpha2 increases endoplasmic reticulum stress and atherosclerosis in vivo. *Circulation* 2010;121:792–803.
- Muse ED, Obici S, Bhanot S, et al. Role of resistin in diet-induced hepatic insulin resistance. *J Clin Invest* 2004;114:232–9.
- Ni L, Zhou C, Duan Q, et al. Beta-AR blockers suppresses ER stress in cardiac hypertrophy and heart failure. *PLoS ONE* 2011;6:e27294.
- Quentin T, Steinmetz M, Poppe A, Thoms S. Metformin differentially activates ER stress signaling pathways without inducing apoptosis. *Dis Model Mech* 2011;5:259–69.
- Zhang Y, Xue R, Zhang Z, Yang X, Shi H. Palmitic and linoleic acids induce ER stress and apoptosis in hepatoma cells. *Lipids Health Dis* 2012;11:1.
- Cao J, Dai DL, Yao L, et al. Saturated fatty acid induction of endoplasmic reticulum stress and apoptosis in human liver cells via the PERK/ATF4/CHOP signaling pathway. *Mol Cell Biochem* 2012;364:115–29.
- He C, Zhu H, Li H, Zou MH, Xie Z. Dissociation of Bcl-2–Beclin1 complex by activated AMPK enhances cardiac autophagy and protects against cardiomyocyte apoptosis in diabetes. *Diabetes* 2012;62:1270–81.
- Ogata M, Hino S, Saito A, et al. Autophagy is activated for cell survival after endoplasmic reticulum stress. *Mol Cell Biol* 2006;26:9220–31.
- Yoshizaki T, Kusunoki C, Kondo M, et al. Autophagy regulates inflammation in adipocytes. *Biochem Biophys Res Commun* 2012;417:352–7.
- Guo R, Zhang Y, Turdi S, Ren J. Adiponectin knockout accentuates high fat diet-induced obesity and cardiac dysfunction: role of autophagy. *Biochim Biophys Acta* 1832;2013:1136–48.
- Basseri S, Austin RC. Endoplasmic reticulum stress and lipid metabolism: mechanisms and therapeutic potential. *Biochem Res Int* 2012;2012:841362.
- Ozcan U, Yilmaz E, Ozcan L, et al. Chemical chaperones reduce ER stress and restore glucose homeostasis in a mouse model of type 2 diabetes. *Science* 2006;313:1137–40.
- Davidson MM, Nesti C, Palenzuela L, et al. Novel cell lines derived from adult human ventricular cardiomyocytes. *J Mol Cell Cardiol* 2005;39:133–47.
- Bachar-Wikstrom E, Wikstrom JD, Ariav Y, et al. Stimulation of autophagy improves endoplasmic reticulum stress-induced diabetes. *Diabetes* 2012;62:1227–37.

Glossary

ACC: acetyl-CoA carboxylase
 ACO: acyl-CoA oxidase
 AICAR: 5-aminoimidazole-4-carboxamide ribonucleotide
 AMPK: 5' AMP-activated protein kinase
 ATF: activating transcription factor
 Bax: Bcl-2-associated X protein
 Bcl-2: B-cell lymphoma 2
 Bim: Bcl-2-like 11
 BiP/GRP78: binding immunoglobulin protein/glucose-regulated protein
 CHOP: CCAAT/enhancer binding protein (C/EBP) homologous protein
 CPT-1b: carnitine palmitoyltransferase 1b
 ER: endoplasmic reticulum
 ERAD: ER-associated degradation
 HFD: high-fat diet
 IRE-1 α : inositol-requiring enzyme-1 α
 LC3: microtubule-associated protein 1A/1B-light chain 3
 NF- κ B: nuclear factor- κ B
 PERK: PKR-like ER kinase
 PPAR β/δ : peroxisome proliferator-activated receptor β/δ
 Puma: Bcl-2 binding component 3
 UPR: unfolded protein response
 XBP1: X-box binding protein 1

RESEARCH ARTICLE

miR-146a targets *Fos* expression in human cardiac cells

Xavier Palomer¹, Eva Capdevila-Busquets¹, Gaia Botteri¹, Mercy M. Davidson², Cristina Rodríguez³, José Martínez-González³, Francisco Vidal⁴, Emma Barroso¹, Tung O. Chan⁵, Arthur M. Feldman⁶ and Manuel Vázquez-Carrera^{1,*}

ABSTRACT

miR-146a is a microRNA whose transcript levels are induced in the heart upon activation of NF- κ B, a transcription factor induced by pro-inflammatory molecules (such as TNF- α) that is strongly related to the pathogenesis of cardiac disorders. The main goal of this study consisted of studying new roles of miR-146a in cardiac pathological processes caused by the pro-inflammatory cytokine TNF- α . Our results demonstrate that miR-146a transcript levels were sharply increased in cardiac ventricular tissue of transgenic mice with specific overexpression of TNF- α in the heart, and also in a cardiomyocyte cell line of human origin (AC16) exposed to TNF- α . Among all the *in silico* predicted miR-146a target genes, *Fos* mRNA and protein levels notably decreased after TNF- α treatment or miR-146a overexpression. These changes correlated with a diminution in the DNA-binding activity of AP-1, the *Fos*-containing transcription factor complex. Interestingly, AP-1 inhibition was accompanied by a reduction in matrix metalloproteinase (MMP)-9 mRNA levels in human cardiac cells. The specific regulation of this MMP by miR-146a was further confirmed at the secretion and enzymatic activity levels, as well as after anti-miR-mediated miR-146a inhibition. The results reported here demonstrate that *Fos* is a direct target of miR-146a activity and that downregulation of the *Fos*-AP-1 pathway by miR-146a has the capacity to inhibit MMP-9 activity. Given that MMP-9 is an AP-1 target gene involved in cardiac remodeling, myocardial dysfunction and progression of heart failure, these findings suggest that miR-146a might be a new and promising therapeutic tool for treating cardiac disorders associated with enhanced inflammation in the heart.

KEY WORDS: *Fos*, Cardiac remodeling, Inflammation, miR-146a, Matrix metalloproteinase-9

INTRODUCTION

The myocardium responds to various pathological stimuli by expressing and secreting several pro-inflammatory cytokines and

chemokines such as interleukin-6 (IL-6), monocyte chemoattractant protein-1 (MCP-1) and tumor necrosis factor- α (TNF- α) (Palomer et al., 2013a,b). These pro-inflammatory mediators, which are transcriptionally regulated by the ubiquitous and inducible nuclear factor- κ B (NF- κ B), exert their pleiotropic autocrine effects via downstream activation of activator protein-1 (AP-1) and NF- κ B itself, thereby contributing to myocardial inflammation, dilated cardiomyopathy, cardiac hypertrophy and heart failure (Gupta et al., 2008; Palomer et al., 2013a,b). Myocardial injury caused by these pathologies leads to myocyte function failure, fibrosis and ensuing ventricular remodeling, which can eventually trigger heart failure. In this regard, TNF- α production is enhanced in the heart of spontaneously hypertensive rats and in the failing human heart; this then contributes to cardiac remodeling and malfunction, thereby speeding up heart failure progression (Bergman et al., 1999). Likewise, continual intra-cardiac expression of TNF- α promotes the development of cardiac allograft hypertrophy (Stetson et al., 2001). Therefore, it is not surprising that pharmacological inhibition of TNF- α activity improves myocardial function during heart failure (Isic et al., 2008).

A recent study performed in rats has revealed an essential role for NF- κ B and AP-1 in the pathogenesis of cardiac hypertrophy (Wang et al., 2009). AP-1 is a heterodimeric transcription factor composed of members belonging to the Jun, Fos, activating transcription factors (ATFs) and Jun-dimerization partner families. AP-1 regulates a number of cellular processes, including differentiation, proliferation and apoptosis. In the heart, AP-1 causes changes in the extracellular matrix and decreases contractility and cell permeability, inducing hypertrophy of cardiomyocytes and fibrosis of the interstitial substance, which eventually lead to heart failure (Wang et al., 2009).

The last decade has seen a plethora of studies reporting a critical role of microRNAs (miRNAs) as regulators of cardiac development, function and performance, as well as in the development of cardiac disease. miRNAs are endogenous non-coding small RNAs that modulate gene expression by targeting mRNAs for post-transcriptional repression through imperfect base-pairing, thereby participating in many essential biological processes. To date, more than 900 mature miRNAs have been identified in the human genome, which alter the translation of up to 50% of all genes (van de Vrie et al., 2011). Furthermore, a single miRNA could target multiple mRNAs, and most mRNAs can be regulated by different miRNAs, hence bringing enormous complexity to the regulation of gene expression. Chronic immune activation and anomalous miRNA expression have been regarded as important players in the pathological molecular mechanisms underlying cardiac disease. As an example, microarray studies have shed some light on the specific miRNAs that are aberrantly downregulated (miR-1, -29, -30, -133 and -150) or upregulated (miR-21, -23a, -125, -146, -195, -199 and -214) in heart failure patients (van de Vrie et al., 2011). However, little is known at present about the function of specific miRNAs

¹Department of Pharmacology and Therapeutic Chemistry, IBUB (Institut de Biomedicina de la Universitat de Barcelona) and CIBER de Diabetes y Enfermedades Metabólicas Asociadas (CIBERDEM), Faculty of Pharmacy, University of Barcelona, Diagonal 643, Barcelona E-08028, Spain. ²Department of Radiation Oncology, Columbia University, P&S 11-451, 630 West 168th Street, New York, NY 10032, USA. ³Centro de Investigación Cardiovascular, CSIC-ICCC, IIB-Sant Pau, Avda. Sant Antoni Maria Claret 167, Barcelona 08025, Spain. ⁴Unitat de Diagnòstic i Teràpia Molecular, Banc de Sang i Teixits, Passeig Vall d'Hebron 119-129, Barcelona 08035, Spain. ⁵Department of Medicine, The Center for Translational Medicine, Jefferson Medical College, 1025 Walnut Street, Philadelphia, PA 19107, USA. ⁶Departments of Medicine and Physiology, Cardiovascular Research Center, Temple University School of Medicine, 3500 N. Broad Street, Philadelphia, PA 19140, USA.

*Author for correspondence (mvazquezcarrera@ub.edu)

This is an Open Access article distributed under the terms of the Creative Commons Attribution License (<http://creativecommons.org/licenses/by/3.0>), which permits unrestricted use, distribution and reproduction in any medium provided that the original work is properly attributed.

TRANSLATIONAL IMPACT**Clinical issue**

Heart disease is the leading cause of death in diabetic patients. Diabetic cardiomyopathy is characterized by concentric left ventricular hypertrophy, dilated cardiomyopathy, myocardial fibrosis and subsequent ventricular remodeling, eventually leading to heart failure. However, despite the added burden that diabetes poses on the heart, current therapeutic strategies do not specifically address diabetic cardiomyopathy. An increasing body of evidence suggests a potential link between chronic low-grade inflammation and metabolic disorders such as insulin resistance and type 2 diabetes. Chronic immune activation and aberrant microRNA (miRNA) expression have been regarded as important players in the pathological molecular mechanisms underlying cardiac disease, although little is known at present about the function of specific miRNAs during inflammatory responses in the heart.

Results

In this study, the authors investigate the role of miR-146a in the pathological processes induced by the pro-inflammatory cytokine TNF- α in the heart. They find a huge increase in miR-146a levels in the heart of transgenic mice with cardiac-specific overexpression of TNF- α and in human cardiac AC16 cells exposed to TNF- α . The authors demonstrate that *Fos* is a direct target of miR-146a activity: overexpression of the latter results in a notable decrease in both *Fos* mRNA and protein levels, which correlated with a diminution in the DNA-binding activity of AP-1, the Fos-containing transcription factor complex. The authors also report that AP-1 inhibition is accompanied by a reduction in matrix metalloproteinase (MMP)-9 secretion and enzymatic activity in human cardiac cells.

Implications and future directions

In the heart, AP-1 causes changes in the extracellular matrix and decreases contractility, inducing hypertrophy of cardiomyocytes and fibrosis of the interstitial substance, which ultimately lead to heart failure. The results reported here demonstrate that *Fos* is a direct target of miR-146a activity and that downregulation of the Fos-AP-1 pathway by miR-146a has the capacity to inhibit MMP-9 activity. These results are very appealing because upregulation of MMP-9 expression correlates fairly well with heart failure, whereas its downregulation suppresses ventricular remodeling, myocardial dysfunction and progression of heart failure. The recently developed antisense-oligonucleotide-mediated knockdown and miRNA overexpression techniques have become very attractive pharmacological strategies in the treatment of cardiovascular disease. In this respect, miR-146a emerges as a new and promising therapeutic tool for preventing cardiac disorders associated with inflammatory states in the heart.

during inflammatory responses in the heart. For this reason, the main goal of the present study was to investigate the potential role of miRNAs in the pathological processes induced by TNF- α in cardiac cells.

RESULTS**TNF- α induces miR-146a expression and reduces Fos in cardiac cells**

As a first approach, we assessed the effects of TNF- α on the expression of a panel of miRNAs previously related to heart disease, obesity, type 2 diabetes and inflammation. Of these, only miR-146a expression was significantly induced by TNF- α [approximately sixfold, $P < 0.01$ vs control (Ctrl), Fig. 1A] in human cardiac AC16 cells, whereas the remaining miRNAs were not modified or simply not detected (see supplementary material Fig. S1). To further confirm these results, neonatal rat cardiomyocytes were cultured *in vitro* and treated with TNF- α ; as shown in Fig. 1B, miR-146a was also significantly upregulated by this pro-inflammatory cytokine (1.5-fold, $P < 0.05$ vs Ctrl). Consistent with this finding, miR-146a

was also hugely stimulated in left ventricular tissue of TNF1.6 transgenic mice with cardiac-specific TNF- α overexpression [tenfold, $P < 0.01$ vs wild type (WT), Fig. 1C].

The miRgator analysis tool (available at <http://genome.ezra.ac.kr/miRgator/miRNAexpression.html>), an online interface that uses multiple target prediction algorithms, was then used to identify unknown downstream targets of miR-146a. Of all the predicted genes, *Fos* (FBJ murine osteosarcoma viral oncogene homolog; also known as *c-Fos*) displayed a notable decrease in its mRNA levels in human cardiac AC16 cells after TNF- α treatment, which was sustained over time and with different TNF- α concentrations (Fig. 1D,E). Interestingly, there was a time-dependent significant negative correlation between *Fos* mRNA levels and miR-146a expression in human cardiac AC16 cells (Fig. 1D, Spearman rank correlation $r = -0.8929$, $P < 0.05$).

After that, we examined the effects of TNF- α on neonatal rat cardiomyocytes cultured *in vitro* and, in agreement with the enhanced miR-146a levels, TNF- α partially inhibited *Fos* expression (~50% reduction, $P < 0.05$ vs Ctrl, Fig. 1F). *Fos* is a leucine zipper protein that forms the transcription factor AP-1 and, for this reason, we next carried out an electrophoretic mobility shift assay (EMSA) to assess the transcriptional activity of AP-1. AP-1 formed one specific DNA-binding complex (I) with nuclear proteins in human cardiac cells (Fig. 1G). The competitor lane demonstrated that this complex was specific for the AP-1 probe, whereas addition of a Fos-specific antibody to the binding reaction disrupted the protein:DNA interaction, hence suggesting that complex I contained the Fos subunit. More importantly, treatment of AC16 cells with TNF- α inhibited AP-1 DNA-binding activity compared with control cells.

miR-146a is directly responsible for Fos downregulation in cardiac cells

To determine whether *Fos* was a direct target of miR-146a activity, human AC16 cardiac cells were transfected with a plasmid carrying pre-miR-146a in the absence of TNF- α , which yielded an important increase in miR-146a expression (15-fold, $P < 0.05$ vs *lacZ*, Fig. 2A). Compatible with our hypothesis, real-time RT-PCR analysis revealed that this miRNA was inhibiting *Fos* expression (~45% reduction, $P < 0.01$, Fig. 2B). Such inhibition resulted in a significant downregulation of Fos protein levels at both the cytoplasm (CP fraction, ~50% reduction, $P < 0.05$) and the nucleus (NE fraction, ~50% reduction, $P < 0.05$) of miR-146a-transfected cells (Fig. 2C), and caused a significant decrease in the DNA-binding activity of the AP-1 transcription factor (Fig. 2D). In agreement with this, downregulation of miR-146a levels (~98% reduction, Fig. 3A) by transfecting AC16 cells with a human anti-miR-146a inhibitor coincided with a significant increase in *Fos* expression (1.9-fold, $P < 0.001$ vs Ctrl anti-miR, Fig. 3B). In addition, the anti-miR-146a inhibitor partially reversed the effects of TNF- α on *Fos* expression (1.7-fold, $P < 0.001$ vs anti-miR+TNF- α). In agreement with gene expression data, Fos protein levels were enhanced by 1.4-fold ($P < 0.05$ vs Ctrl anti-miR+TNF- α) in the nucleus of AC16 cells transfected with anti-miR-146a (NE fraction, Fig. 3C). In order to demonstrate the specificity of Fos regulation by miR-146a, the protein levels of Jun and the p65 subunit of NF- κ B were also determined in cytoplasmic and nuclear extracts of cells overexpressing miR-146a (Fig. 2C) and after downregulation of miR-146a with an anti-miR-146a inhibitor (Fig. 3C). It is worth mentioning that p65 and Jun were not altered after modulation of miR-146a levels. As expected, p65 protein levels were increased in the nucleus after TNF- α treatment, owing to NF- κ B activation. In

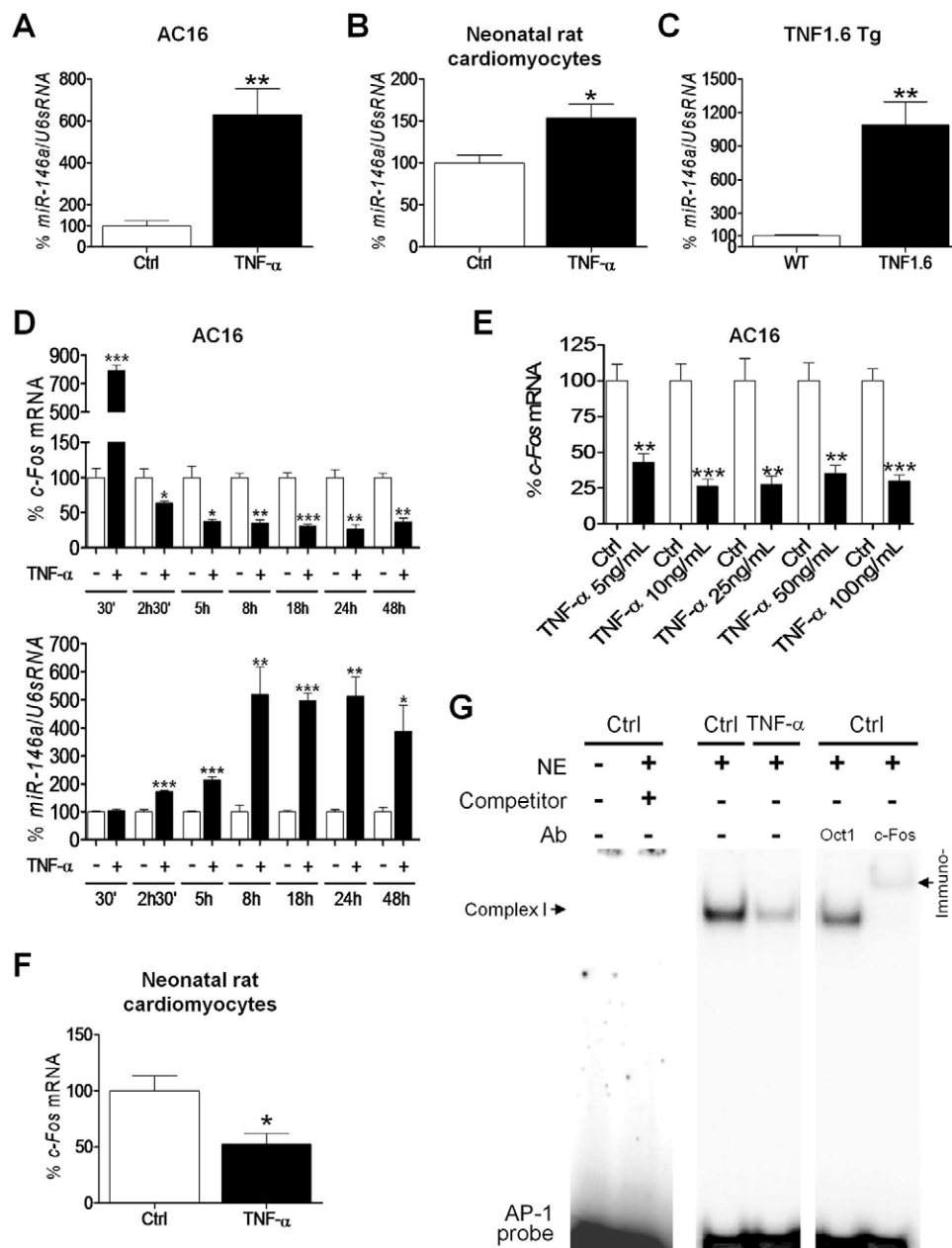


Fig. 1. TNF- α upregulates miR-146a and reduces Fos expression in cardiac cells. Relative quantification of miR-146a levels in samples obtained from: (A) non-differentiated AC16 cells treated with TNF- α (100 ng/ml, 24 h); (B) neonatal rat cardiomyocytes treated with TNF- α (10 ng/ml, 6 h); and (C) left ventricle tissue of transgenic TNF1.6 or control wild-type (WT) mice. Relative quantification of Fos and miR-146a expression in: (D) non-differentiated AC16 cells treated with 100 ng/ml TNF- α for 30 min to 48 h; (E) non-differentiated AC16 cells treated with 5, 10, 25, 50 and 100 ng/ml TNF- α for 24 h; and (F) neonatal rat cardiomyocytes treated with TNF- α (10 ng/ml, 6 h). Graphs represent the quantification of (A-C) U6sRNA-, (D,E) 18S- or (F) APRT-normalized mRNA levels, expressed as a percentage of control (Ctrl) or wild-type (WT) samples \pm s.d. * P <0.05, ** P <0.01 and *** P <0.001 vs Ctrl. (G) EMSA assay showing AP-1 DNA-binding activity in non-differentiated AC16 cells treated with TNF- α . Ab, antibody; NE, nuclear extracts.

non-stimulated cells, NF- κ B remains inactive in the cytoplasm owing to its heterodimerization with the inhibitor protein I κ B. In the presence of a stimulus (e.g. TNF- α), the I κ B kinase (IKK) complex phosphorylates I κ B, which induces ubiquitylation and ensuing proteasome-mediated degradation of the latter. The subsequent release of the NF- κ B heterodimer makes possible its translocation to the nucleus, where it can begin the transcription of its target genes.

miR-146a modulates inflammation in human cardiac cells

After dimerization with Jun family members and by binding to the so-called TPA-responsive elements (TREs; TGAC/GTCA) in the promoter region of target genes, Fos regulates the expression of genes involved in multiple processes, including inflammation, endoplasmic reticulum stress, metabolism, fibrosis, proliferation and survival (Chinenov and Kerppola, 2001; Durchdewald et al., 2009). Dysregulation of Fos has been linked with a variety of pathological conditions. In the heart, for instance, AP-1 stimulates

the expression of inflammatory genes, endothelin, fibronectin, matrix metalloproteinases (MMPs), transforming growth factor (TGF)- β and collagen, thereby displaying potent effects on matrix remodeling and favoring cardiac fibroblast proliferation (Wang et al., 2009; Takimoto and Kass, 2007; Pan et al., 2012). Therefore, in order to determine the pathophysiological relevance of AP-1 down-modulation in human cardiac cells, we next analyzed the expression of various genes that had been reportedly demonstrated to be targeted by the AP-1 transcription factor and also be involved in cardiac disease. As shown in supplementary material Fig. S2, no significant variation was observed in the expression of genes such as *ATF4* (activating transcription factor 4), *BiP/GRP78* (binding immunoglobulin protein/glucose-regulated protein 78), endothelin 1 (*ET-1*), fibronectin 1 (*FNI*), lipin 1, lipoprotein lipase (*LPL*), *TGF- β 1*, type I collagen or type IV collagen.

On the other hand, miR-146a has been shown to modulate NF- κ B activity through the direct targeting of well-established mediators of

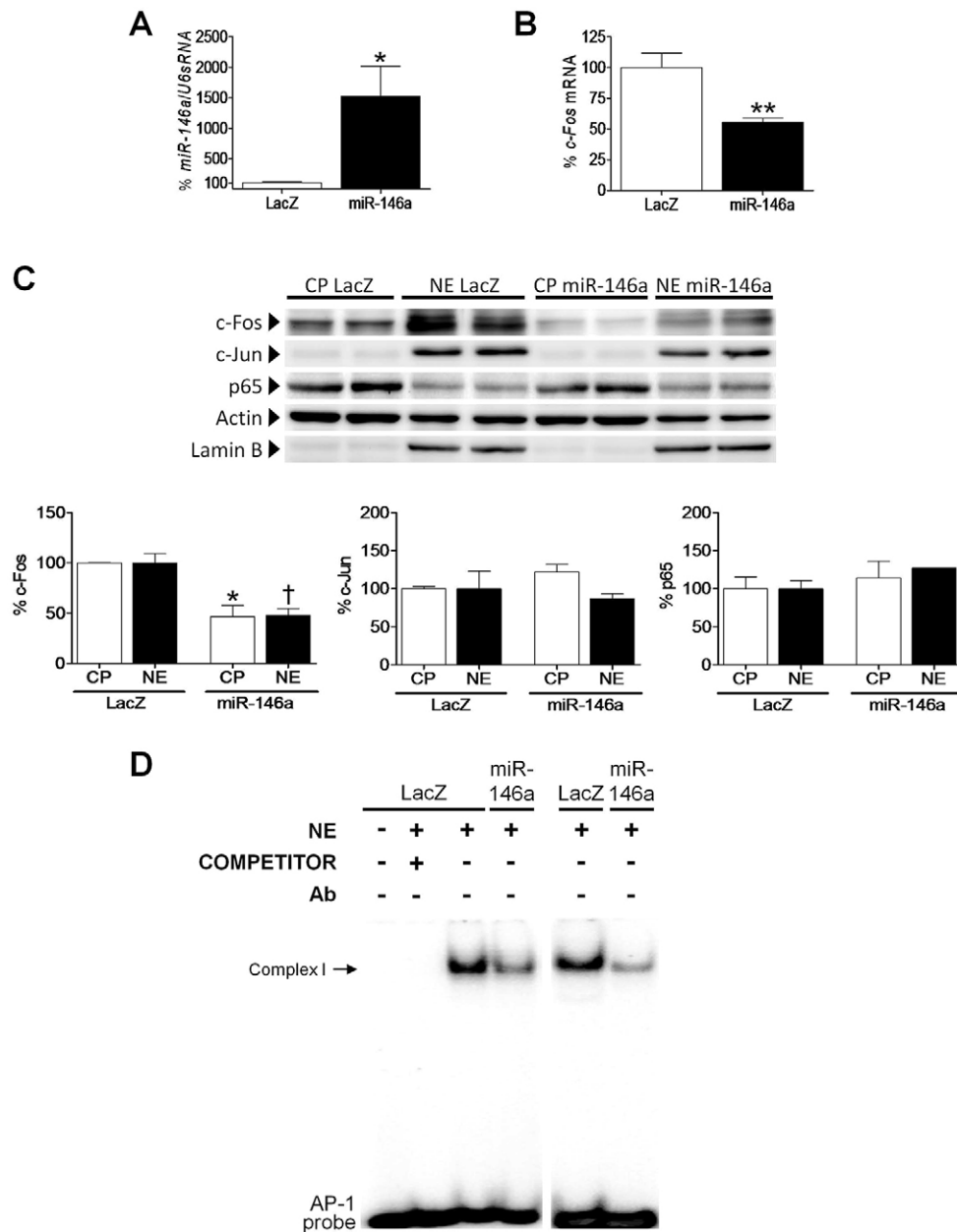


Fig. 2. miR-146a overexpression inhibits Fos in human cardiac cells. Relative quantification of miR-146a (A) and Fos (B) mRNA levels in human cardiac AC16 cells transfected with *lacZ*- or miR-146a-carrying plasmids. The graph represents the quantification of (A) U6sRNA- or (B) 18S-normalized mRNA levels, expressed as a percentage of control samples \pm s.d. * P <0.05 and ** P <0.01 vs *lacZ*. (C) Western-blot analysis showing the protein levels of Fos, Jun and p65 in cytosolic (CP) and nuclear (NE) protein fractions obtained from human cardiac AC16 cells as described in panel A. To show equal loading of protein, the actin and lamin B signals from the same blot are included. The graphs at the bottom of panel C represent the quantification of protein levels normalized to actin (CP) or lamin B (NE), expressed as a percentage of CP or NE control samples \pm s.d. The blot data are representative of two separate experiments. * P <0.05 vs *lacZ* CP; † P <0.05 vs *lacZ* NE. (D) EMSA assay showing AP-1 DNA-binding activity after transfection of AC16 cells as described in panel A. Ab, antibody; NE, nuclear extracts.

its activation, including interleukin-1 receptor-associated kinase (IRAK)1, IRAK2, TNF receptor-associated factor (TRAF)2 and TRAF6 (Wang et al., 2013; Tanic et al., 2012). However, none of the transcript levels for these genes was found to be modified after miR-146a overexpression or inhibition, thus indicating that they were not regulated by this miRNA in human cardiac AC16 cells (see supplementary material Fig. S3). However, miR-146a overexpression inhibited *IL-6* (~40% reduction, P <0.05 vs *lacZ*) and *MCP-1* (~50% reduction, P <0.01) transcript levels, although *TNF- α* levels remained unaltered (Fig. 4A). In consonance with this, transfection of AC16 cells with the anti-miR-146a inhibitor upregulated the expression of *IL-6* (1.3-fold, P <0.05 vs anti-miR+ *TNF- α*), although only when the pro-inflammatory stimulus *TNF- α* was added to the medium (Fig. 4B). As previously reported (Palomer et al., 2009), treatment of AC16 cells with *TNF- α* (100 ng/ml for 24 h) significantly induced the expression of *IL-6*, *MCP-1* and *TNF- α* , regardless of miR-146a levels. After that, an EMSA was carried out to verify whether modulation of miR-146a

levels in AC16 cells led to changes in NF- κ B activity. As shown in Fig. 4C, NF- κ B formed four specific DNA-binding complexes (I to IV) with nuclear proteins. The competitor lane confirmed that all four complexes were specific for the NF- κ B probe, and supershift analyses provided evidence that only complexes I and II contained the p65 subunit of NF- κ B. Interestingly, complexes I, II and III were increased in *TNF- α* -treated cells, but no variations were detected after miR-146a modulation. These results suggest that *IL-6* and *MCP-1* gene expression might be regulated by transcription factors other than NF- κ B.

Inhibition of AP-1 activity by miR-146a coincides with a reduction in MMP-9 activity

Examination of *MMP-9* expression in human cardiac cells transfected with miR-146a revealed that, unlike *MMP-2*, its transcript levels were downregulated (~40% reduction, P <0.05, Fig. 5A). According to these results, anti-miR-146a stimulated *MMP-9* expression regardless of the presence (1.5-fold, P <0.001) or

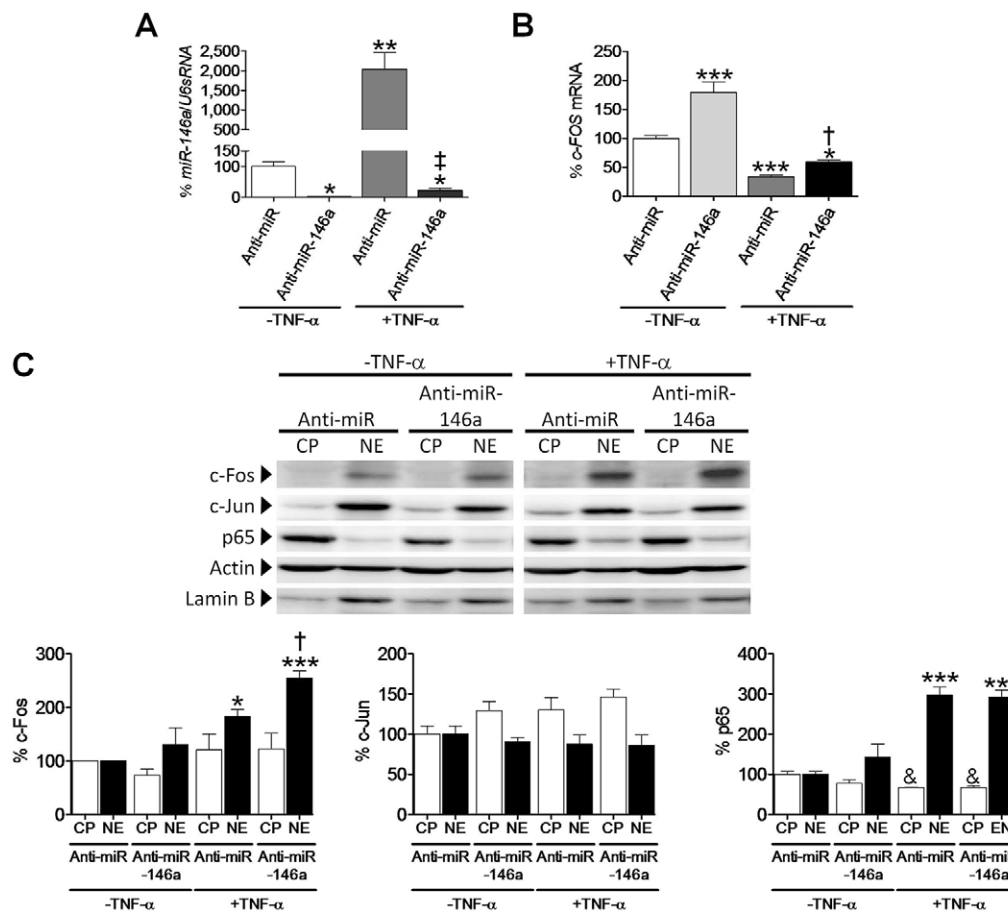


Fig. 3. miR-146a inhibition induces Fos in human cardiac cells. Relative quantification of miR-146a (A) and Fos (B) mRNA levels in human cardiac AC16 cells after transfection with a human anti-miR-146a inhibitor or an anti-miR negative control (Anti-miR). The graph represents the quantification of (A) U6sRNA- or (B) 18S-normalized mRNA levels, expressed as a percentage of control samples \pm s.d. * P <0.05, ** P <0.01 and *** P <0.001 vs Anti-miR-TNF- α ; † P <0.05 and ‡ P <0.001 vs Anti-miR +TNF- α . (C) Western-blot analysis showing the protein levels of Fos, Jun and p65 in cytosolic (CP) and nuclear (NE) protein fractions obtained from human cardiac AC16 cells as described in panel A. To show equal loading of protein, the actin and lamin B signals from the same blot are included. The graphs at the bottom of panel C represent the quantification of protein levels normalized to actin (CP) or lamin B (NE), expressed as a percentage of CP or NE control samples \pm s.d. The blot data are representative of two separate experiments. * P <0.05 and *** P <0.001 vs NE Anti-miR-TNF- α ; † P <0.05 vs NE Anti-miR+TNF- α ; ‡ P <0.05 vs CP Anti-miR-TNF- α .

absence (1.5-fold, P <0.001) of TNF- α (Fig. 5B). We next examined this issue in left ventricular tissue obtained from patients undergoing heart transplantation. The relative expression of miR-146a positively correlated with that of TNF- α (Fig. 5C, top panel, Spearman rank correlation $r=0.5480$), a finding that, despite being only marginally significant ($P=0.08$), matched the previous results obtained in AC16 cells fairly closely. Of note, miR-146a levels negatively correlated with the expression of Fos (Fig. 5C, middle panel, Spearman rank correlation $r=-0.6208$, P <0.05) and MMP-9 (Fig. 5C, bottom panel, $r=-0.5659$, P <0.05) in these patients. Finally, we aimed to examine the effects of MMP-9 downregulation by miR-146a on its enzymatic activity. As expected, miR-146a overexpression elicited a reduction in MMP-9 secretion to the media (~25% reduction, P <0.001, Fig. 5D) and MMP-9 activity (~35% reduction, P <0.05, Fig. 5E). The zymogram also yielded a stronger gelatinolytic activity band, which was concentrated in the area corresponding to the molecular mass of MMP-2 (62 kDa), which was not modified under our conditions.

DISCUSSION

The molecular mechanisms that lie behind the development of heart failure induced by cytokines remain, at least in part, elusive, but there are consistent observations indicating that chronic immune activation and anomalous miRNA expression come together in the failing heart (van de Vrie et al., 2011). Our results demonstrate that miR-146a is strongly induced in human cardiac cells and neonatal rat cardiomyocytes exposed to TNF- α *in vitro*, as well as in the heart of transgenic mice with cardiac-specific overexpression of TNF- α . This is not surprising, given that this miRNA has already been

shown to be transcriptionally upregulated after NF- κ B activation by TNF- α and IL-1 β in other cell types (Taganov et al., 2006; Perry et al., 2008; Schroen and Heymans, 2012; Li et al., 2012). This regulatory mechanism is fundamental because continuous NF- κ B activation aggravates cardiac remodeling, worsens cardiac function, and hastens progression to heart failure and cardiac hypertrophy (Bergman et al., 1999; Stetson et al., 2001). In agreement with this, miR-146a, which is abundantly expressed in the heart (van de Vrie et al., 2011), protects the myocardium from ischemia-reperfusion injury in a process that involves attenuation of NF- κ B activation (Wang et al., 2013).

Owing to the crucial function of miRNAs in controlling mRNA expression, the discovery of currently unknown targets of specific miRNAs is paramount, but the fact that most miRNAs are only partially complementary to their target genes hinders this identification. Therefore, the chief finding of this study is the identification of a new miR-146a target, Fos, an AP-1 subunit that is rapidly activated upon cardiac stress to mediate changes in gene expression (Shieh et al., 2011). Validation of new miRNA targets is often complicated because many putative targets display little or indeed no detectable modification when tested *in vitro* (Small et al., 2010), and this might account for the relatively modest effect of miR-146a on Fos mRNA levels, despite the huge miR-146a changes observed in transfected cells. The lack of any change in Jun protein levels indicated the specificity of miR-146a over the Fos subunit of the AP-1 transcription factor.

The next logical step in this study consisted of finding out which genes were regulated by Fos-AP-1 under our conditions. AP-1 protein typically binds to TREs in target promoter regions often

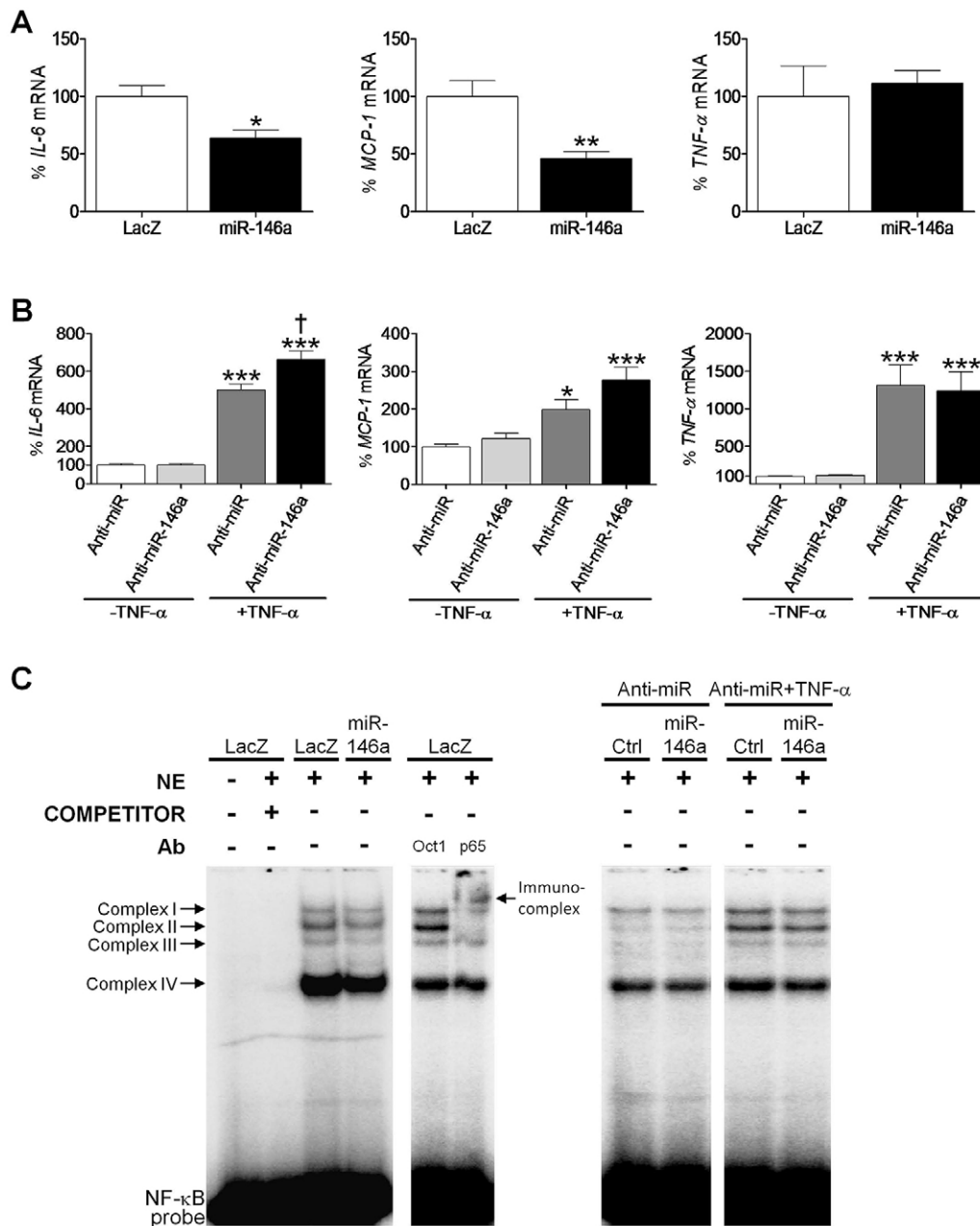


Fig. 4. miR-146a regulates IL-6 and MCP-1 expression in human cardiac cells. Relative quantification of *IL-6*, *MCP-1* and *TNF-α* mRNA levels in non-differentiated human cardiac AC16 cells transfected with: (A) *lacZ*- or miR-146a-carrying plasmids, or (B) a human anti-miR-146a inhibitor or an anti-miR negative control (Anti-miR). The graphs represent the quantification of 18S-normalized mRNA levels, expressed as a percentage of control samples \pm s.d. (A) * P <0.05 and ** P <0.01 vs *lacZ*; (B) * P <0.05 and *** P <0.001 vs Anti-miR-TNF- α ; † P <0.05 vs Anti-miR+TNF- α . (C) EMSA assay showing NF- κ B DNA-binding activity after transfection of AC16 cells as described in panels A and B. Ab, antibody; Ctrl, control; NE, nuclear extracts.

adjacent to NF- κ B or nuclear factor of activated T-cells (NFAT) to coordinately regulate transcription in response to immune and inflammatory stimuli (Chinenov and Kerppola, 2001). Gene expression assessment revealed that miR-146a was modulating mRNA levels of *IL-6* and *MCP-1* in AC16 cells. Taking into account that this was not accompanied by changes in the DNA-binding activity of NF- κ B, and bearing in mind that *in silico* data indicate that these pro-inflammatory genes are not direct targets of miR-146a, our results suggest that AP-1 might be regulating their expression. In support of this, we can cite our previous data demonstrating that, besides NF- κ B, other transcription factors are controlling *IL-6* and *MCP-1* mRNA levels in human cardiac cells

(Palomer et al., 2014; Álvarez-Guardia et al., 2011). In fact, other studies have demonstrated the involvement of AP-1 but not NF- κ B in the transcriptional control of *IL-6* in other cell types (Lu et al., 2010). In contrast, the expression of other genes such as *ATF4*, *BiP/GRP78*, *IRAK1*, *IRAK2*, *TRAF2*, *TRAF6*, *ET-1*, *FNI*, lipin 1, *LPL*, *TGF- β 1*, type I collagen or type IV collagen did not seem to be regulated by miR-146a. In fact, the expression of AP-1 target genes depends on the cell type and is also influenced by the particular signals that trigger their expression (Chinenov and Kerppola, 2001). Besides regulation at the transcriptional level, additional mechanisms might contribute to the target gene specificity of AP-1, including mRNA translation and turnover, post-translational

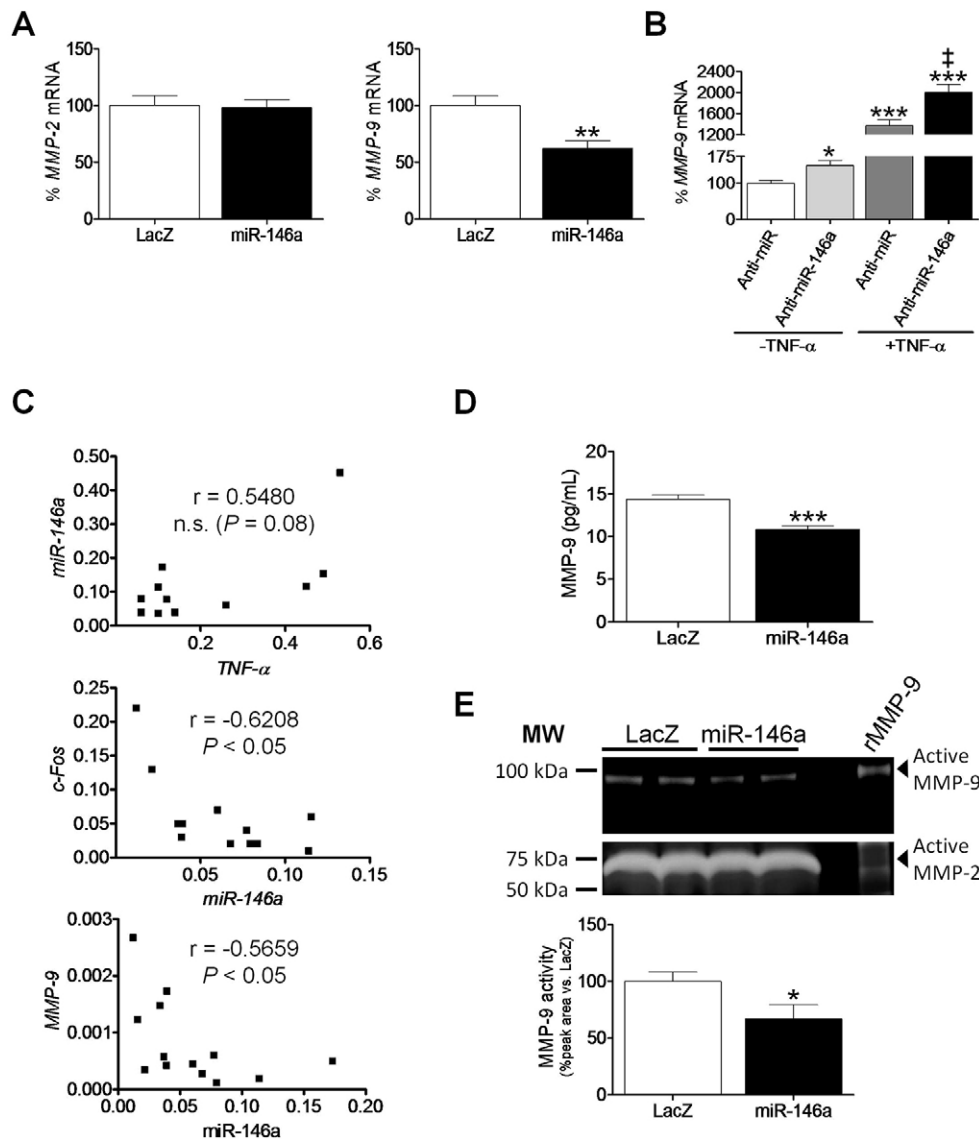


Fig. 5. miR-146a downregulates MMP-9 expression, secretion and activity in human cardiac cells. Relative quantification of *MMP-2* and *MMP-9* mRNA levels in non-differentiated human cardiac AC16 cells transfected with: (A) *lacZ*- or miR-146a-carrying plasmids, or (B) a human anti-miR-146a inhibitor or an anti-miR negative control (Anti-miR). The graphs represent the quantification of 18S-normalized mRNA levels, expressed as a percentage of control samples \pm s.d. (C) Spearman rank correlation between *TNF- α* and miR-146a, miR-146a and *Fos*, and miR-146a and *MMP-9* gene expression in left ventricular tissue obtained from patients undergoing heart transplantation. The relative transcript levels of the target genes, in arbitrary units, were used to calculate the Spearman correlation coefficients (n.s., non-significant). (D) Determination by ELISA of *MMP-9* secretion into the culture media in AC16 cells transfected with *lacZ*- or miR-146a-carrying plasmids. (E) Representative gel zymography and corresponding densitometric analysis of *MMP-9* gelatinolytic activity in culture media of cells transfected with *lacZ*- or miR-146a-carrying plasmids. MW, molecular weight; rMMP-9, human recombinant MMP-9. (A,D,E) * P <0.05, ** P <0.01 and *** P <0.001 vs *lacZ*; (B) * P <0.05 and *** P <0.001 vs Anti-miR-TNF- α ; † P <0.05 vs Anti-miR+TNF- α .

modifications, selective dimerization, protein stability, and interactions with other regulatory proteins and transcription factors (Chinenov and Kerppola, 2001; Schonhaler et al., 2011).

Interstitial fibrosis is a characteristic pathological alteration of myocardial remodeling that occurs in several cardiomyopathies and is considered as a primary determinant of deteriorated performance of the heart. Fibrosis occurs as a result of excess deposition of extracellular matrix proteins in the myocardium (Pan et al., 2012). A complex interplay of transcription factors is implicated in the regulation of extracellular matrix protein homeostasis, including NF- κ B and AP-1. In particular, the Fos-AP-1 pathway transcriptionally stimulates the synthesis of ET-1 and the deposition of collagen (type I, type IV collagens), fibronectin and TGF- β , thereby causing changes in the extracellular matrix that alter cardiac cell proliferation and function, ultimately leading to cardiomyocyte hypertrophy and heart failure (Pan et al., 2012; Wang et al., 2009; Avouac et al., 2012). Even so, miR-146a overexpression did not inhibit the expression of most cardiac-fibrosis-related genes examined in human cardiac cells, except for *MMP-9*. MMPs are under the transcriptional control of AP-1 (Takimoto and Kass, 2007) and NF- κ B (Meiners et al., 2004),

which are in turn induced by growth factors and inflammatory cytokines in cardiac cells, although MMP activity is also dependent on post-translational modifications. MMPs are the enzymes responsible for controlling extracellular matrix remodeling in the heart and, interestingly, inhibition of these enzymes is associated with reduced collagen deposition and lower cardiac fibrosis (Meiners et al., 2004). This astonishing paradox is due to the fact that total collagen amount in the heart depends on both the synthesis and degradation. The results reported here demonstrate that miR-146a can inhibit MMP-9 expression and activity in human cardiac cells. Infiltrating cells (i.e. neutrophils, macrophages and fibroblasts) together with cardiomyocytes are the major source of MMPs in the myocardium (Li et al., 2001). Macrophages are an important source of MMP-9 during acute myocardial infarction and, for instance, MMP-9-knockout mice show a reduced rupture rate and attenuated ventricular dilation during myocardial infarction (Fang et al., 2010). A recent study has also reported that miR-146a might be a potential inhibitor of MMP-9 secretion in macrophages, although regulation in these cells was achieved through attenuation of the inflammatory response by blocking the TRAF6-IRAK1 pathway (Yang et al., 2011). Likewise, cardiac fibroblasts express

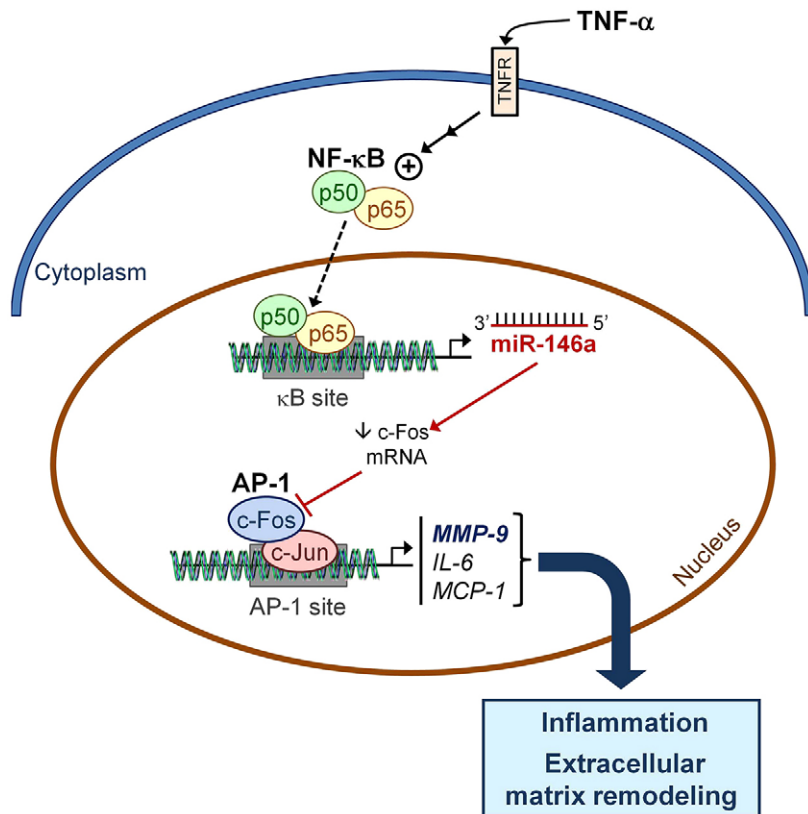


Fig. 6. Schematic model depicting the potential role of miR-146a in TNF- α -induced effects in the heart. Exposure of cardiac cells to TNF- α strongly induces miR-146a, probably in a process dependent on NF- κ B transcriptional activity (dashed arrow). Enhanced miR-146a levels are directly responsible for *Fos* expression downregulation. The subsequent reduction in AP-1 DNA-binding activity results in the modulation of inflammation by attenuating *IL-6* and *MCP-1* expression, together with a reduction in MMP-9 expression and activity. AP-1, activator protein-1; Fos, FBJ murine osteosarcoma viral oncogene homolog; IL-6, interleukin 6; MCP-1, monocyte chemoattractant protein 1; MMP-9, matrix metalloproteinase 9; NF- κ B, nuclear factor- κ B; TNF- α , tumor necrosis factor α .

MMP-9 after treatment with TNF- α , a fact that is concomitant with a decrease in collagen synthesis (Brown et al., 2007). Therefore, all these results indicate that the miR-146a-mediated inhibition of MMP-9 might occur in both infiltrating cells and cardiomyocytes in the heart, by this means magnifying its beneficial effects.

A major drawback of this study is the origin of the AC16 cells, which were derived from the fusion of primary ventricular cells and SV-40-transformed fibroblasts. The heart consists of various cell types, including cardiomyocytes and cardiac fibroblasts, which play a pivotal role in cardiac development and function (Palomer et al., 2009). Both cell types are capable of secreting TNF- α and are responsive to the action of this cytokine (Turner et al., 2007) but, in diseased states, quiescent cardiac fibroblasts are transformed into myofibroblasts, becoming a major source of pro-inflammatory molecules (Brown et al., 2005), in addition to the main source of extracellular matrix production (Pan et al., 2012). As stated above, excess extracellular matrix production by activated cardiac fibroblasts during cardiac hypertrophy, heart failure and myocardial infarction promotes interstitial fibrosis. The consequent cardiac remodeling might eventually lead to functional decompensation and development of heart failure due to apoptosis of cardiac myofibroblasts (Camelliti et al., 2005).

Conclusions

In summary, the results reported here demonstrate that *Fos* is a direct target of miR-146a activity and that downregulation of the Fos–AP-1 pathway by miR-146a can inhibit MMP-9 activity (Fig. 6). Fos is one of the immediate early genes whose expression is boosted during ischemic injury, heart failure and cardiomyopathy. Likewise, it has been reported that *Fos* gene expression is stimulated as a result of insulin insufficiency in the diabetic myocardium (Wang et al., 1999) and also in the adipose tissue of streptozotocin-induced

diabetic rats (Olson and Pessin, 1994). In fact, the transcriptional activity of AP-1 is among the most robustly enhanced of 54 transcription factors examined in the failing heart (Freire et al., 2007). In order to prevent the pathological effects caused by its dysfunction, regulation of AP-1 is complex and occurs at multiple interwoven transcriptional and post-transcriptional levels. This includes transcription of its subunits, mRNA translation and turnover, protein stability and activity, subcellular localization, and interaction with other transcription factors and cofactors (Schonthaler et al., 2011). Here, we demonstrate that miR-146a might post-transcriptionally regulate Fos levels and, consequently, AP-1 activity as well. Furthermore, the results presented here are very appealing because numerous studies have shown that upregulation of *MMP-2* and *MMP-9* expression correlates fairly well with heart failure, whereas their inhibition suppresses ventricular remodeling, myocardial dysfunction and development of heart failure (Meiners et al., 2004). In recent years, the development of antisense-oligonucleotide-mediated (anti-miR) knockdown and miRNA overexpression techniques has become a very attractive pharmacological target in the treatment of cardiovascular disease. In this respect, miR-146a emerges as a new and promising therapeutic tool for preventing cardiac disorders associated with inflammatory states in the heart.

MATERIALS AND METHODS

Cell culture and transfection

The human AC16 cell line, which develops many of the biochemical and morphological properties characteristic of cardiac muscle cells, even though it does not form completely differentiated cardiomyocytes, was grown as previously described (Davidson et al., 2005). Briefly, non-differentiated AC16 cells were maintained in medium composed of Dulbecco's modified Eagle's medium (DMEM):F12 (Life Technologies, Spain) supplemented with 12.5% fetal bovine serum (FBS), 1% penicillin-streptomycin and 1%

Fungizone (Life Technologies), and grown at 37°C in a humid atmosphere of 5% CO₂/95% air until they reached 70-80% confluence. For *in vitro* overexpression studies, AC16 cells were transfected with pcDNA3/pre-miR-146a (Addgene plasmid #15092) (Taganov et al., 2006) and the corresponding *lacZ*-carrying plasmid (Life Technologies) as a control. Cells were transfected for 48 h with Lipofectamine 2000 in OPTI-MEM reduced serum medium following the manufacturer's recommendations (Life Technologies). Transfection time and the DNA to Lipofectamine ratio were set after optimization with the corresponding *lacZ*-carrying plasmid and using a β -galactosidase reporter gene staining kit (Sigma-Aldrich Co. LLC., St Louis, MO, USA). Downregulation of miR-146a activity was carried out by transfecting AC16 cells with 50 nmol/l human anti-miR-146a inhibitor, using a random sequence anti-miR molecule as negative control (Life Technologies).

To obtain neonatal rat cardiomyocytes, 1- to 2-day-old Sprague-Dawley rats were decapitated and their hearts removed. Hearts were digested with a collagenase solution (Collagenase Type I, Life Technologies) followed by differential plating. Cells were plated at a density of 2.5×10^4 cells/well in six-well plates coated with 1% gelatin, and cultured overnight in plating medium [DMEM supplemented with 10% horse serum, 5% newborn calf serum, 50 mg/l gentamicin and 10 mM cytosine b-D-arabino furanoside (Ara C)]. Ara C was added to suppress the growth of the remaining fibroblasts. Sixteen hours after isolating cells, neonatal rat cardiomyocytes were incubated in serum-free medium consisting of DMEM and gentamicin (50 mg/l) as the sole substrate for 24 h. Thereafter, the medium was replaced with experimental medium consisting of serum-free medium enriched with 0.25 mM L-carnitine, 0.25 mU/ml insulin and 1% bovine serum albumin. All procedures were approved by the University of Barcelona Bioethics Committee, as stated in Law 5/21 July 1995 passed by the Generalitat de Catalunya.

After treatment, RNA and protein were extracted from cardiac cells as described below. Culture supernatants were collected, and secretion of MMP-9 was assessed by enzyme-linked immunosorbent assay (Life Technologies).

TNF- α transgenic mouse cardiac sample preparation

We used transgenic TNF1.6 male mice (8- to 12-weeks old) with cardiac-specific overexpression of TNF- α , which has been established as a suitable model of cytokine-induced cardiomyopathy and congestive heart failure (Kubota et al., 1997). These transgenic mice develop myocardial inflammation with premature death from heart failure in association with extracellular matrix remodeling (Kubota et al., 1997; Li et al., 2000). Left ventricular end-diastolic diameter and left ventricular end-diastolic pressure are significantly greater, and fractional shortening is significantly less in TNF1.6 than in wild-type mice (Matsusaka et al., 2005). Myocyte cross-sectional area and collagen volume fraction are also enhanced in the transgenic TNF1.6 mice compared with littermate controls (Matsusaka et al., 2005).

Mice were housed under standard light-dark cycle (12-h light/dark cycle) and temperature ($21 \pm 1^\circ\text{C}$) conditions, and food and water were provided *ad libitum*. Ventricular sample tissues were obtained from mice euthanized using deep isoflurane (5%) anesthesia, rinsed in ice-cold phosphate buffer saline and snap-frozen in liquid nitrogen, as described previously (Álvarez-Guardia et al., 2010). The study was approved by the Institutional Animal Care and Use Committee of Thomas Jefferson University and conformed to the *Guide for the Care and Use of Laboratory Animals* published by the US National Institutes of Health (NIH Publication No. 85-23, revised 1996).

Tissue collection

Left ventricular tissue was obtained from patients undergoing heart transplantation at the Hospital de la Santa Creu i Sant Pau, Barcelona. All participants provided informed consent. Transmural tissue samples (near the apex) were collected from patients (eight male and five female) with both dilated (DCM; $n=10$) and ischemic (ICM; $n=3$) cardiomyopathy. Samples were quickly frozen in liquid nitrogen in the operating room and stored at -80°C until processing for gene expression analysis. All the procedures

were approved by the Reviewer Institutional Committee on Human Research of the Hospital de la Santa Creu i Sant Pau and conformed to the Declaration of Helsinki.

RNA preparation and analysis

Total RNA was isolated using Ultraspec reagent (Biotex, Houston, TX, USA). RNA samples were cleaned (NucleoSpin RNA II; Macherey-Nagel, Düren, Germany) and checked for integrity by agarose gel electrophoresis. The total RNA isolated by this method was undegraded and free of protein and DNA contamination. Relative levels of specific mRNAs were assessed by real-time reverse transcription-polymerase chain reaction (RT-PCR), as previously described (Palomer et al., 2014). Reverse transcription was performed from 0.5 μg total RNA using Oligo(dT)₂₃ and M-MLV Reverse Transcriptase (Life Technologies). The PCR reaction contained 10 ng of reverse-transcribed RNA, 2X IQTM SYBRGreen Supermix (Bio-Rad, Barcelona, Spain) and 900 nM of each primer. PCR assays were performed on a MiniOpticonTM Real-Time PCR system (Bio-Rad). Thermal cycling conditions were as follows: activation of Taq DNA polymerase at 95°C for 10 min, followed by 40 cycles of amplification at 95°C for 15 s and at 60°C for 1 min. The sequences of the forward and reverse primers used for amplification are shown in supplementary material Table S1. Optimal primer amplification efficiency for each primer set was assessed and a dissociation protocol was carried out to ensure a single PCR product. The results for the expression of specific mRNAs are always presented relative to the expression of the control gene.

To quantify the abundance of selected mature miRNAs, total miRNAs were reverse-transcribed using the Megaplex Primer Pools (Human Pool A v2.1 and Rodent Pool A) and the Taqman MicroRNA Reverse Transcription according to the manufacturer's instructions (Life Technologies). The RT reaction product was combined with 1 μl Taqman miRNA assay and 10 μl Taqman Universal PCR Master Mix No AmpErase UNG (Life Technologies) to a final volume of 20 μl . The quantitative real-time RT-PCR reaction was carried out on a MiniOpticonTM Real-Time PCR system at 95°C for 10 min, followed by 40 cycles at 95°C for 15 s and 60°C for 1 min. All samples were run in duplicates. *U6sRNA* expression was used for normalization purposes.

Immunoblot analysis

To obtain total protein extracts, AC16 cardiac cells or frozen tissue slides were lysed in cold RIPA buffer with phosphatase and protease inhibitors (0.2 mmol/l phenylmethylsulfonyl fluoride, 1 mmol/l sodium orthovanadate, 5.4 $\mu\text{g}/\text{ml}$ aprotinin). The homogenate was then centrifuged at 10,000 g for 30 min at 4°C, and the supernatant protein concentration was determined using the Bradford method (Bradford, 1976). Isolation of cytosolic and nuclear fractions was adapted from a previously described method (Ba et al., 2010). Briefly, AC16 cells were incubated on ice for 30 min in buffer A (10 mmol/l HEPES, pH 7.9, 10 mmol/l KCl, 0.2 mmol/l EDTA, 1 mmol/l dithiothreitol, plus phosphatase and protease inhibitors) containing 0.625% (v:v) Nonidet P-40. Cell lysates were centrifuged at 4°C, 10,000 g for 1 min, and supernatants were stored as cytosolic fraction. Pellets were suspended in buffer B (20 mmol/l HEPES, pH 7.9, 0.42 mol/l NaCl, 2 mmol/l EDTA and 1 mmol/l dithiothreitol, with phosphatase and protease inhibitors), centrifuged at 4°C, 13,000 g for 5 min, and the resultant supernatant (nuclear extract) stored at -80°C .

Proteins from whole-cell lysates and cytosolic/nuclear extracts were separated by sodium dodecyl sulfate-polyacrylamide gel electrophoresis (SDS-PAGE) on 10% separation gels and transferred to Immobilon polyvinylidene difluoride membranes (Millipore, Bedford, MA, USA). Proteins were detected using the Western Lightning[®] Plus-ECL chemiluminescence kit (PerkinElmer, Waltham, MA, USA) and their size was estimated using protein molecular mass standards (Life Technologies). All antibodies were purchased from Santa Cruz Biotechnology (Inc., Heidelberg, Germany), except Actin (Sigma-Aldrich Co. LLC.).

Electrophoretic mobility shift assay

The EMSA was performed using double-stranded oligonucleotides for the consensus binding sites of AP-1 and NF- κB (Santa Cruz Biotechnology).

Nuclear extracts (NEs) from AC16 cells were isolated as previously reported (Palomer et al., 2011). Oligonucleotides were labeled by incubating the following reaction at 37°C for 2 h: 2 µl oligonucleotide (1.75 pmol/µl), 2 µl of 5× kinase buffer, 1 µl of T4 polynucleotide kinase (10 U/µl) and 2.5 µl [γ -³²P] ATP (3000 Ci/mmol at 10 mCi/ml, PerkinElmer, Waltham, MA, USA). The reaction was stopped by adding 90 µl of TE buffer (10 mmol/l Tris-HCl, pH 7.4, and 1 mmol/l EDTA). To separate the labeled probe from the unbound ATP, the reaction mixture was eluted in a Nick column (GE Healthcare Life Sciences, Barcelona, Spain) according to the manufacturer's instructions. Five micrograms of crude nuclear protein was incubated for 10 min on ice in binding buffer [10 mmol/l Tris-HCl, pH 8.0, 25 mmol/l KCl, 0.5 mmol/l dithiothreitol, 0.1 mmol/l EDTA, pH 8.0, 5% (v:v) glycerol, 5 mg/ml BSA and 50 µg/ml poly(di-dC)] in a final volume of 15 µl. Then, specific competitor oligonucleotide or antibody for supershift assays were added and incubated for 15 min on ice. Subsequently, the labeled probe (100,000 cpm) was added and the reaction was incubated for an additional 15 min on ice. Finally, protein-DNA complexes were resolved by electrophoresis at 4°C on 5% (w:v) polyacrylamide gels in 0.5× Tris-borate-EDTA buffer and subjected to autoradiography.

Gelatinase activity assay

MMP-9 activity was examined by gelatin zymography as previously reported in AC16 cell cultures after protein concentration using 3000 MW Amicon Ultra centrifugal filters (Millipore) (Casals et al., 2013). 150 µg of protein per lane were subjected to 10% SDS-PAGE electrophoresis (125 V for 90 min) using 0.2% gelatin-containing gels. After electrophoresis, gels were washed and incubated for 30 min at room temperature in Renaturing Buffer (Novex, Life Technologies) to remove the SDS. After this, gels were incubated with gentle agitation for 30 min with Developing Buffer (Life Technologies), rinsed three times with deionized water and stained by adding SimplyBlue Safe Stain (Life Technologies) for 1 h. 50 µg recombinant human MMP-9 (Life Technologies) were also run in parallel as a positive control for enzymatic activity. Proteolytic bands of 92 kDa, which correspond to the active form of MMP-9, were scanned and the intensity of the bands analyzed.

Statistical analysis

Results are expressed as the mean±s.d. of three independent experiments for the *in vitro* studies, each consisting of three culture plates ($n=9$), and of five mice for the *in vivo* experiments. Significant differences were established by either the Student's *t*-test or one-way ANOVA, according to the number of groups compared, using GraphPad Prism software (GraphPad Software Inc. V4.03, San Diego, CA, USA). When significant variations were found by one-way ANOVA, the Tukey-Kramer multiple comparison post-test was performed. The non-parametric Spearman rank correlation coefficient was used to calculate the correlation between *Fos*, *miR-146a* and *TNF-α* expression. Differences were considered significant at $P<0.05$.

Acknowledgements

We thank Dr D. Baltimore (California Institute of Technology, Pasadena, CA, USA) for providing the pcDNA3/miR-146a plasmid. We thank the University of Barcelona's Language Advisory Service for their assistance.

Competing interests

The authors declare no competing or financial interests.

Author contributions

All authors contributed substantially to the work presented in this paper. X.P. and M.V.-C. designed the study. X.P., E.C.-B. and G.B. performed all *in vitro* and *in vivo* experiments. M.M.D. developed and provided the human cardiac cell line. C.R., J.M.-G. and F.V. collected and provided the left ventricular tissue from patients. T.O.C. and A.M.F. provided the heart samples from transgenic mice. E.B. analyzed the quantitative data and contributed to data interpretation. X.P. wrote the paper with input from all authors.

Funding

This study was supported by funds from the Ministerio de Economía y Competitividad of the Spanish Government [SAF2009-06939, SAF2012-30708 and SAF2012-40127]. CIBER de Diabetes y Enfermedades Metabólicas Asociadas

(CIBERDEM) is an initiative of the Instituto de Salud Carlos III (ISCIII) - Ministerio de Economía y Competitividad.

Supplementary material

Supplementary material available online at <http://dmm.biologists.org/lookup/suppl/doi:10.1242/dmm.020768/-DC1>

References

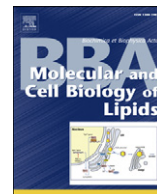
- Álvarez-Guardia, D., Palomer, X., Coll, T., Davidson, M. M., Chan, T. O., Feldman, A. M., Laguna, J. C. and Vazquez-Carrera, M. (2010). The p65 subunit of NF-κappaB binds to PGC-1alpha, linking inflammation and metabolic disturbances in cardiac cells. *Cardiovasc. Res.* **87**, 449-458.
- Álvarez-Guardia, D., Palomer, X., Coll, T., Serrano, L., Rodríguez-Calvo, R., Davidson, M. M., Merlos, M., El Kochairi, I., Michalik, L., Wahli, W. et al. (2011). PPARbeta/delta activation blocks lipid-induced inflammatory pathways in mouse heart and human cardiac cells. *Biochim. Biophys. Acta* **1811**, 59-67.
- Avouac, J., Palumbo, K., Tomcik, M., Zerr, P., Dees, C., Horn, A., Maurer, B., Akhmetshina, A., Beyer, C., Sadowski, A. et al. (2012). Inhibition of activator protein 1 signaling abrogates transforming growth factor beta-mediated activation of fibroblasts and prevents experimental fibrosis. *Arthritis Rheum.* **64**, 1642-1652.
- Ba, X., Gupta, S., Davidson, M. and Garg, N. J. (2010). Trypanosoma cruzi induces the reactive oxygen species-PARP-1-RelA pathway for up-regulation of cytokine expression in cardiomyocytes. *J. Biol. Chem.* **285**, 11596-11606.
- Bergman, M. R., Kao, R. H., McCune, S. A. and Holycross, B. J. (1999). Myocardial tumor necrosis factor-alpha secretion in hypertensive and heart failure-prone rats. *Am. J. Physiol.* **277**, H543-H550.
- Bradford, M. M. (1976). A rapid and sensitive method for the quantitation of microgram quantities of protein utilizing the principle of protein-dye binding. *Anal. Biochem.* **72**, 248-254.
- Brown, R. D., Ambler, S. K., Mitchell, M. D. and Long, C. S. (2005). The cardiac fibroblast: therapeutic target in myocardial remodeling and failure. *Annu. Rev. Pharmacol. Toxicol.* **45**, 657-687.
- Brown, R. D., Jones, G. M., Laird, R. E., Hudson, P. and Long, C. S. (2007). Cytokines regulate matrix metalloproteinases and migration in cardiac fibroblasts. *Biochem. Biophys. Res. Commun.* **362**, 200-205.
- Camelliti, P., Borg, T. K. and Kohl, P. (2005). Structural and functional characterisation of cardiac fibroblasts. *Cardiovasc. Res.* **65**, 40-51.
- Casals, G., Fernández-Varo, G., Melgar-Lesmes, P., Marfà, S., Reichenbach, V., Morales-Ruiz, M. and Jiménez, W. (2013). Factors involved in extracellular matrix turnover in human derived cardiomyocytes. *Cell Physiol. Biochem.* **32**, 1125-1136.
- Chinenov, Y. and Kerppola, T. K. (2001). Close encounters of many kinds: Fos-Jun interactions that mediate transcription regulatory specificity. *Oncogene* **20**, 2438-2452.
- Davidson, M. M., Nesti, C., Palenzuela, L., Walker, W. F., Hernandez, E., Protas, L., Hirano, M. and Isaac, N. D. (2005). Novel cell lines derived from adult human ventricular cardiomyocytes. *J. Mol. Cell. Cardiol.* **39**, 133-147.
- Durchwald, M., Angel, P. and Hess, J. (2009). The transcription factor Fos: a Janus-type regulator in health and disease. *Histol. Histopathol.* **24**, 1451-1461.
- Fang, L., Du, X.-J., Gao, X.-M. and Dart, A. M. (2010). Activation of peripheral blood mononuclear cells and extracellular matrix and inflammatory gene profile in acute myocardial infarction. *Clin. Sci.* **119**, 175-183.
- Freire, G., Ocampo, C., Ilbawi, N., Griffin, A. J. and Gupta, M. (2007). Overt expression of AP-1 reduces alpha myosin heavy chain expression and contributes to heart failure from chronic volume overload. *J. Mol. Cell. Cardiol.* **43**, 465-478.
- Gupta, S., Young, D., Maitra, R. K., Gupta, A., Popovic, Z. B., Yong, S. L., Mahajan, A., Wang, Q. and Sen, S. (2008). Prevention of cardiac hypertrophy and heart failure by silencing of NF-κappaB. *J. Mol. Biol.* **375**, 637-649.
- Isic, A., Scharin Täng, M., Haugen, E. and Fu, M. (2008). TNFAlpha-antagonist neither improve cardiac remodeling or cardiac function at early stage of heart failure in diabetic rats. *Autoimmunity* **41**, 473-477.
- Kubota, T., McTiernan, C. F., Frye, C. S., Slawson, S. E., Lemster, B. H., Koretsky, A. P., Demetris, A. J. and Feldman, A. M. (1997). Dilated cardiomyopathy in transgenic mice with cardiac-specific overexpression of tumor necrosis factor-alpha. *Circ. Res.* **81**, 627-635.
- Li, Y. Y., Feng, Y. Q., Kadokami, T., McTiernan, C. F., Draviam, R., Watkins, S. C. and Feldman, A. M. (2000). Myocardial extracellular matrix remodeling in transgenic mice overexpressing tumor necrosis factor alpha can be modulated by anti-tumor necrosis factor alpha therapy. *Proc. Natl. Acad. Sci. USA* **97**, 12746-12751.
- Li, Y. Y., Feng, Y., McTiernan, C. F., Pei, W., Moravec, C. S., Wang, P., Rosenblum, W., Kormos, R. L. and Feldman, A. M. (2001). Downregulation of matrix metalloproteinases and reduction in collagen damage in the failing human heart after support with left ventricular assist devices. *Circulation* **104**, 1147-1152.
- Li, N., Xu, X., Xiao, B., Zhu, E.-D., Li, B.-S., Liu, Z., Tang, B., Zou, Q.-M., Liang, H.-P. and Mao, X.-H. (2012). H. pylori related proinflammatory cytokines contribute to the induction of miR-146a in human gastric epithelial cells. *Mol. Biol. Rep.* **39**, 4655-4661.

- Lu, X., Ma, L., Ruan, L., Kong, Y., Mou, H., Zhang, Z., Wang, Z., Wang, J. and Le, Y. (2010). Resveratrol differentially modulates inflammatory responses of microglia and astrocytes. *J. Neuroinflammation* **7**, 46.
- Matsusaka, H., Ikeuchi, M., Matsushima, S., Ide, T., Kubota, T., Feldman, A. M., Takeshita, A., Sunagawa, K. and Tsutsui, H. (2005). Selective disruption of MMP-2 gene exacerbates myocardial inflammation and dysfunction in mice with cytokine-induced cardiomyopathy. *Am. J. Physiol. Heart Circ. Physiol.* **289**, H1858-H1864.
- Meiners, S., Hoher, B., Weller, A., Laule, M., Stangl, V., Guenther, C., Godes, M., Mrozikiewicz, A., Baumann, G. and Stangl, K. (2004). Downregulation of matrix metalloproteinases and collagens and suppression of cardiac fibrosis by inhibition of the proteasome. *Hypertension* **44**, 471-477.
- Olson, A. L. and Pessin, J. E. (1994). Regulation of c-fos expression in adipose and muscle tissue of diabetic rats. *Endocrinology* **134**, 271-276.
- Palomer, X., Álvarez-Guardia, D., Rodríguez-Calvo, R., Coll, T., Laguna, J. C., Davidson, M. M., Chan, T. O., Feldman, A. M. and Vázquez-Carrera, M. (2009). TNF-alpha reduces PGC-1alpha expression through NF-kappaB and p38 MAPK leading to increased glucose oxidation in a human cardiac cell model. *Cardiovasc. Res.* **81**, 703-712.
- Palomer, X., Álvarez-Guardia, D., Davidson, M. M., Chan, T. O., Feldman, A. M. and Vázquez-Carrera, M. (2011). The interplay between NF-kappaB and E2F1 coordinately regulates inflammation and metabolism in human cardiac cells. *PLoS ONE* **6**, e19724.
- Palomer, X., Capdevila-Busquets, E., Álvarez-Guardia, D., Barroso, E., Pallàs, M., Camins, A., Davidson, M. M., Planavila, A., Villarroya, F. and Vázquez-Carrera, M. (2013a). Resveratrol induces nuclear factor-kappaB activity in human cardiac cells. *Int. J. Cardiol.* **167**, 2507-2516.
- Palomer, X., Salvadó, L., Barroso, E. and Vázquez-Carrera, M. (2013b). An overview of the crosstalk between inflammatory processes and metabolic dysregulation during diabetic cardiomyopathy. *Int. J. Cardiol.* **168**, 3160-3172.
- Palomer, X., Capdevila-Busquets, E., Botteri, G., Salvadó, L., Barroso, E., Davidson, M. M., Michalik, L., Wahli, W. and Vázquez-Carrera, M. (2014). PPARbeta/delta attenuates palmitate-induced endoplasmic reticulum stress and induces autophagic markers in human cardiac cells. *Int. J. Cardiol.* **174**, 110-118.
- Pan, Z., Sun, X., Shan, H., Wang, N., Wang, J., Ren, J., Feng, S., Xie, L., Lu, C., Yuan, Y. et al. (2012). MicroRNA-101 inhibited postinfarct cardiac fibrosis and improved left ventricular compliance via the FBJ osteosarcoma oncogene/transforming growth factor-beta1 pathway. *Circulation* **126**, 840-850.
- Perry, M. M., Moschos, S. A., Williams, A. E., Shepherd, N. J., Lerner-Svensson, H. M. and Lindsay, M. A. (2008). Rapid changes in microRNA-146a expression negatively regulate the IL-1beta-induced inflammatory response in human lung alveolar epithelial cells. *J. Immunol.* **180**, 5689-5698.
- Schonhaler, H. B., Guinea-Viniegra, J. and Wagner, E. F. (2011). Targeting inflammation by modulating the Jun/AP-1 pathway. *Ann. Rheum. Dis.* **70** Suppl. 1, i109-i112.
- Schroen, B. and Heymans, S. (2012). Small but smart-microRNAs in the centre of inflammatory processes during cardiovascular diseases, the metabolic syndrome, and ageing. *Cardiovasc. Res.* **93**, 605-613.
- Shieh, J. T. C., Huang, Y., Gilmore, J. and Srivastava, D. (2011). Elevated miR-499 levels blunt the cardiac stress response. *PLoS ONE* **6**, e19481.
- Small, E. M., Frost, R. J. A. and Olson, E. N. (2010). MicroRNAs add a new dimension to cardiovascular disease. *Circulation* **121**, 1022-1032.
- Stetson, S. J., Perez-Verdia, A., Mazur, W., Farmer, J. A., Koerner, M. M., Weilbaecher, D. G., Entman, M. L., Quinones, M. A., Noon, G. P. and Torre-Amione, G. (2001). Cardiac hypertrophy after transplantation is associated with persistent expression of tumor necrosis factor-alpha. *Circulation* **104**, 676-681.
- Taganov, K. D., Boldin, M. P., Chang, K.-J. and Baltimore, D. (2006). NF-kappaB-dependent induction of microRNA miR-146, an inhibitor targeted to signaling proteins of innate immune responses. *Proc. Natl. Acad. Sci. USA* **103**, 12481-12486.
- Takimoto, E. and Kass, D. A. (2007). Role of oxidative stress in cardiac hypertrophy and remodeling. *Hypertension* **49**, 241-248.
- Tanic, M., Zajac, M., Gómez-López, G., Benítez, J. and Martínez-Delgado, B. (2012). Integration of BRCA1-mediated miRNA and mRNA profiles reveals microRNA regulation of TRAF2 and NFkappaB pathway. *Breast Cancer Res. Treat.* **134**, 41-51.
- Turner, N. A., Mughal, R. S., Warburton, P., O'regan, D. J., Ball, S. G. and Porter, K. E. (2007). Mechanism of TNFalpha-induced IL-1alpha, IL-1beta and IL-6 expression in human cardiac fibroblasts: effects of statins and thiazolidinediones. *Cardiovasc. Res.* **76**, 81-90.
- van de Vrie, M., Heymans, S. and Schroen, B. (2011). MicroRNA involvement in immune activation during heart failure. *Cardiovasc. Drugs Ther.* **25**, 161-170.
- Wang, P. H., Almahfouz, A., Giorgino, F., McCowen, K. C. and Smith, R. J. (1999). In vivo insulin signaling in the myocardium of streptozotocin-diabetic rats: opposite effects of diabetes on insulin stimulation of glycogen synthase and c-Fos. *Endocrinology* **140**, 1141-1150.
- Wang, M., Zhang, W.-B., Zhu, J.-H., Fu, G.-S. and Zhou, B.-Q. (2009). Breviscapine ameliorates hypertrophy of cardiomyocytes induced by high glucose in diabetic rats via the PKC signaling pathway. *Acta Pharmacol. Sin.* **30**, 1081-1091.
- Wang, X., Ha, T., Liu, L., Zou, J., Zhang, X., Kalbfleisch, J., Gao, X., Williams, D. and Li, C. (2013). Increased expression of microRNA-146a decreases myocardial ischaemia/reperfusion injury. *Cardiovasc. Res.* **97**, 432-442.
- Yang, K., He, Y. S., Wang, X. Q., Lu, L., Chen, Q. J., Liu, J., Sun, Z. and Shen, W. F. (2011). MiR-146a inhibits oxidized low-density lipoprotein-induced lipid accumulation and inflammatory response via targeting toll-like receptor 4. *FEBS Lett.* **585**, 854-860.



Contents lists available at ScienceDirect

Biochimica et Biophysica Acta

journal homepage: www.elsevier.com/locate/bbalip

Review

PPAR β/δ and lipid metabolism in the heart[☆]Xavier Palomer, Emma Barroso, Mohammad Zarei, Gaia Botteri, Manuel Vázquez-Carrera^{*}

Pharmacology Unit, Department of Pharmacology and Therapeutic Chemistry, Institut de Biomedicina de la UB (IBUB), Faculty of Pharmacy, University of Barcelona, Barcelona, Spain
 Institut de Recerca Pediàtrica, Hospital Sant Joan de Déu, Barcelona, Spain
 CIBER de Diabetes y Enfermedades Metabólicas Asociadas (CIBERDEM), Instituto de Salud Carlos III, Barcelona, Spain

ARTICLE INFO

Article history:

Received 3 November 2015

Received in revised form 23 December 2015

Accepted 22 January 2016

Available online 26 January 2016

Keywords:

PPAR β/δ

Cardiomyocyte

Fatty acid

Inflammation

Lipid metabolism

ABSTRACT

Cardiac lipid metabolism is the focus of attention due to its involvement in the development of cardiac disorders. Both a reduction and an increase in fatty acid utilization make the heart more prone to the development of lipotoxic cardiac dysfunction. The ligand-activated transcription factor peroxisome proliferator-activated receptor (PPAR) β/δ modulates different aspects of cardiac fatty acid metabolism, and targeting this nuclear receptor can improve heart diseases caused by altered fatty acid metabolism. In addition, PPAR β/δ regulates glucose metabolism, the cardiac levels of endogenous antioxidants, mitochondrial biogenesis, cardiomyocyte apoptosis, the insulin signaling pathway and lipid-induced myocardial inflammatory responses. As a result, PPAR β/δ ligands can improve cardiac function and ameliorate the pathological progression of cardiac hypertrophy, heart failure, cardiac oxidative damage, ischemia–reperfusion injury, lipotoxic cardiac dysfunction and lipid-induced cardiac inflammation. Most of these findings have been observed in preclinical studies and it remains to be established to what extent these intriguing observations can be translated into clinical practice. This article is part of a Special Issue entitled: Heart Lipid Metabolism edited by G.D. Lopaschuk.

© 2016 Elsevier B.V. All rights reserved.

1. Introduction

Constant pump function of the heart requires a high-energy demand in the form of adenosine triphosphate (ATP), which is mainly satisfied by fatty acids (FAs) and glucose. Thus, in the adult heart, about 70% of cardiac energy metabolism relies on the oxidation of FAs, whereas glucose (20%), lactate and ketone bodies are additional fuel sources [1]. The heart, unlike other tissues such as the brain, adapts its metabolism to substrate availability for ATP generation [2]. Due to low oxygen pressure, the fetal heart mainly depends on anaerobic glucose and lactate for ATP generation. In contrast, the adult heart primarily relies on mitochondrial fatty acid oxidation (FAO) to ensure ATP generation, but conserves the metabolic flexibility to switch to other substrates, mainly glucose. This switch in substrate preference from FAO towards increased glucose utilization in the heart for ATP generation is observed in myocardial ischemia, cardiac hypertrophy and heart failure [1]. This metabolic shift has long been interpreted as an oxygen-sparing mechanism of the heart. Consequently, several animal studies have demonstrated that inhibition of FAO might be useful for protecting the heart from the consequences of ischemia and ischemia–reperfusion injury

[1,3]. However, the reduction in FAO has a major impact on the availability of ATP [4], since long-chain FAO produces 3–4 times more ATP per molecule compared with glucose oxidation, and this decrease in ATP synthesis can limit energy supply, contributing to cardiac remodeling. Further, the reduction in FAO can promote an imbalance between FA uptake and its oxidation, leading to accumulation of FA derivatives, including triglycerides, but also more toxic lipids, such as diacylglycerol (DAG) and ceramide that can alter cellular structures and activate downstream pathways leading to inflammation and toxicity. On the other hand, excessive FAO is also harmful [5]. Thus, in hearts of obese and/or diabetic patients, myocardial insulin resistance and increased rates of systemic lipolysis force the heart to rely almost exclusively on FAO as an energy source, indicating the presence of a loss of substrate flexibility [5,6]. When sustained over long term, increased myocardial FA utilization makes the heart more prone to the development of lipotoxic cardiac dysfunction characterized by lipid accumulation, mitochondrial dysfunction and the generation of reactive oxygen species (ROS) [5,6].

Since the discovery of the first peroxisome proliferator-activated receptor (PPAR), the PPAR α isoform, by Isseman and Green [7], the biological roles of these receptors in the heart have received widespread attention due to their key role in controlling cardiac lipid metabolism. The pioneering work by Cheng et al. [8] demonstrated that the nuclear receptor PPAR β/δ plays a major role in cardiac lipid metabolism, since mice with cardiac-specific deletion of this receptor developed myocardial lipid accumulation and cardiomyopathy. This review discusses

[☆] This article is part of a Special Issue entitled: Heart Lipid Metabolism edited by G.D. Lopaschuk.

^{*} Corresponding author at: Unitat de Farmacologia, Facultat de Farmàcia, Diagonal 643, E-08028 Barcelona, Spain.

E-mail address: mvazquezcarrera@ub.edu (M. Vázquez-Carrera).

new insights on the role of PPAR β/δ in cardiac lipid metabolism and how targeting this nuclear receptor can ameliorate cardiac disorders caused by altered FA metabolism.

2. Peroxisome proliferator-activated receptors (PPARs)

PPARs belong to a subfamily of the nuclear receptor superfamily that allows the cell to respond to extracellular stimuli by regulating transcriptional gene expression. The PPAR family comprises three isoforms; PPAR α (NR1C1, according to the unified nomenclature system for the nuclear receptor superfamily), PPAR β/δ (NR1C2) and PPAR γ (NR1C3) [9]. When PPAR β/δ was initially cloned in *Xenopus laevis* it was named PPAR β . However, when cloned in other species it was not clearly identified as being homologous to the *Xenopus* PPAR β and it was alternatively called NUC-1 in humans [10] and PPAR δ in mice [11,12]. Currently, it is accepted that *Xenopus* PPAR β is homologous to murine PPAR δ and this explains the terminology PPAR β/δ .

Like most members of the nuclear-receptor superfamily, PPARs have a common domain structure consisting of four major functional domains: the N-terminal ligand-independent transactivation domain (A/B domain) often known as activation function 1 (AF-1), the DNA binding domain (DBD or C domain), hinge region (D domain) and the carboxy-terminal E domain or AF-2, including the ligand-binding domain and the ligand-dependent transactivation domain [13] (Fig. 1A).

The physiological role of PPARs depends on tissue distribution, ligand binding and the recruitment of co-activators and co-repressors. PPAR α is the molecular target of the fibrate hypolipidemic class of drugs and is expressed primarily in tissues with a high level of fatty

acid catabolism such as liver, brown fat, kidney, heart and skeletal muscle [14]. The γ isoform is the molecular target for the anti-diabetic drugs thiazolidinediones or glitazones and is expressed as two splice variants, PPAR γ 1 and γ 2. PPAR γ 1 is mainly expressed in white and brown adipose tissues, colon, retina, spleen and hematopoietic cells. PPAR γ 2 is exclusively expressed in white and brown adipose tissues [15] and differs from PPAR γ 1 in the presence of 28 (mouse) or 30 (human) additional amino acids at its N-terminal end. PPAR β/δ is almost ubiquitously expressed, although it is most abundant in metabolically active tissues such as skeletal and cardiac muscles [16]. The predominant isoforms in the heart are PPAR α and PPAR β/δ , more specifically in cardiac muscle cells and fibroblasts [17,18], while the abundance of PPAR γ is very low.

To be transcriptionally active, PPARs need to heterodimerize with the 9-cis retinoic acid receptor (RXR or NR2B). PPAR–RXR heterodimers bind to peroxisome proliferator response elements (PPREs) located in the promoter regions of their target genes, thereby increasing gene transcription in a ligand-dependent manner (transactivation) [16,19] (Fig. 1B). In the absence of ligand, high-affinity complexes are formed between PPAR–RXR heterodimers and nuclear co-repressor proteins, such as the nuclear receptor co-repressor (N-CoR) and the silencing mediator of retinoid and thyroid signaling (SMRT), which block transcriptional activation by sequestering the heterodimer from the promoter. Binding of the ligand to PPAR induces a conformational change resulting in dissociation of co-repressor proteins, so that the PPAR–RXR heterodimer can then bind to PPREs. Moreover, once activated by the ligand, the heterodimer recruits co-activator proteins that promote the initiation of transcription [20], such as PPAR γ co-activator 1 α (PGC-1 α) or steroid receptor co-activator 1 (SRC-1) with intrinsic histone acetylase (HAT)

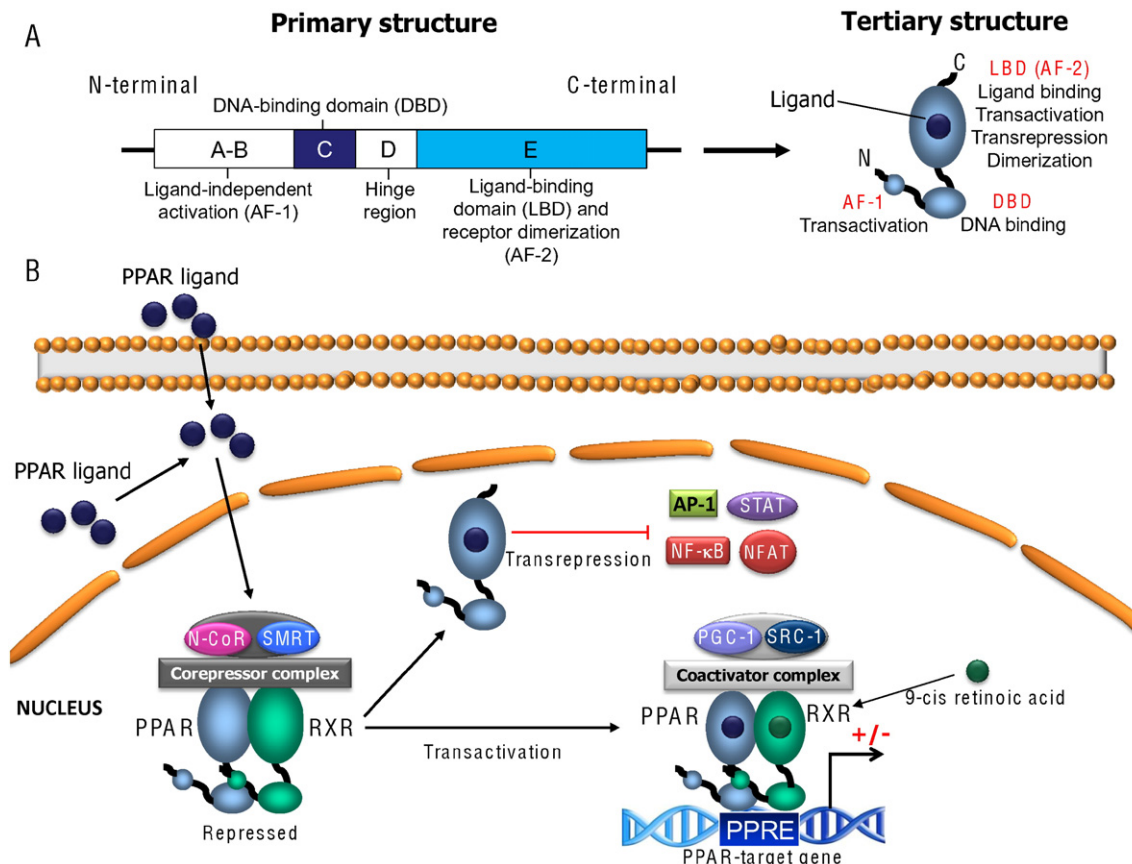


Fig. 1. Structure and transcriptional activation of PPARs. A, Primary and tertiary PPAR domain structures. N and C represent the amino and carboxyl termini, respectively. Activation function 1 (AF-1) is a variable amino-terminal transactivation domain. The ligand-binding domain (LBD) also mediates dimerization, transcriptional activation, and transcriptional repression functions. B, PPAR mechanisms of action. PPAR activation leads to heterodimerization with RXR. Binding of the ligand to PPAR results in a conformational change that allows its dissociation from a repressed binding protein complex which may contain the nuclear receptor co-repressor (N-CoR) and the silencing mediator of retinoid and thyroid signaling (SMRT) and the subsequent recruitment of a transcriptional complex that may contain the steroid receptor co-activator-1 (SRC-1) or the PPAR γ co-activator 1 α (PGC-1 α), among others. DBD, DNA-binding domain. PPRE, Peroxisome proliferator response element.

activity, or recruit proteins with HAT activity to initiate transcription [21]. In a specific cellular context, the activity of PPARs in terms of regulating the transcription of their target genes depends on many factors (relative expression of the PPARs, the promoter context of the target gene, the presence of co-activator and co-repressor proteins, etc.).

The regulation of gene transcription by PPARs extends beyond their ability to transactivate specific target genes in an agonist-dependent manner. PPARs also regulate gene expression independently of binding to PPREs (Fig. 1B). They cross-talk with other types of transcription factors and influence their function without binding to DNA, through a mechanism termed receptor-dependent transrepression [22]. Most of the anti-inflammatory effects of PPARs are probably explained by this mechanism [23,24]. Thus, through this DNA-binding independent mechanism, PPARs suppress the activities of several transcription factors, including nuclear factor κ B (NF- κ B), activator protein 1 (AP-1), signal transducers and activators of transcription (STATs) and nuclear factor of activated T cells (NFAT). There are three main transrepression mechanisms by which ligand-activated PPAR-RXR complexes negatively regulate the activities of other transcription factors (Fig. 2). First, transrepression may result from competition for limiting amounts of shared co-activators. Under conditions in which the levels of specific co-activators are rate-limiting, activation of PPAR may suppress the activity of other transcription factors that use the same co-activators [25, 26]. In the second mechanism, activated PPAR-RXR heterodimers are believed to act through physical interaction with other transcription factors (for example AP-1, NF- κ B, NFAT or STATs). This association prevents the transcription factor from binding to its response element and thereby inhibits its ability to induce gene transcription [27]. The third transrepression mechanism relies on the ability of activated PPAR-RXR heterodimers to inhibit the phosphorylation and activation of certain members of the mitogen-activated protein kinase (MAPK) cascade [28], preventing activation of downstream transcription factors.

The crystal structure of the ligand-binding domain of the PPAR β/δ isoform revealed an exceptionally large pocket of approximately 1300 Å³. This pocket is similar to that of PPAR γ , but much larger than the pockets of other nuclear receptors [29,30], which may explain, at least in part, the great variety of natural and synthetic ligands that bind to and activate this nuclear receptor. Saturated (14 to 18 carbons) and polyunsaturated (20 carbons in length) fatty acids in the low micromolar range have affinity for PPAR β/δ , but also for the other PPAR isoforms [30–33], showing little affinity towards the different isoforms. In addition, all-trans-retinoic acid (vitamin A) [34] and fatty acids

derived from VLDL [35] can activate PPAR β/δ . Finally, the availability of three synthetic ligands (GW501516, GW0742 and L-165041) that activate PPAR β/δ at very low concentrations both in vivo and in vitro with high selectivity over other PPAR isoforms [36] led to a huge increase in experimental studies on the role of PPAR β/δ in cellular processes. The EC₅₀ for these compounds assessed with recombinant human PPAR β/δ was 1.0 nM for GW0742, 1.1 nM for GW501516 and 50 nM for L-165041 [37,38]. There are no clinically available drugs targeting PPAR β/δ , but two PPAR β/δ agonists are in clinical trials: MBX-8025 (Metabolex) [39] and KD-3010 (Kalypsos) [40]. PPAR β/δ antagonists have also been used to study the functions of this receptor, especially GSK0660 [38], although its poor bioavailability has reduced its use in in vivo studies. GSK3787 is another potent PPAR β/δ antagonist with good bioavailability that allows its use in animal studies [41,42].

In addition to pharmacological approaches, the development of genetically-modified mouse models has allowed the study of the biological functions of PPAR β/δ . For more detailed information on these animal models, the reader is referred to the excellent review by Giordano et al. [43].

3. PPAR β/δ effects in cardiac lipid metabolism

The heart obtains lipids from de novo synthesis or it acquires them from the exogenous supply provided by albumin-bound non-esterified or free fatty acids (FFA) or esterified FAs bound to triglyceride-rich lipoproteins [44]. Although it is thought that the heart has a limited capacity for de novo FA synthesis from glucose, this pathway seems to be important for maintaining cardiac function in aortic constriction and aging [45].

Lipoprotein-derived FAs are acquired by the heart following triglyceride hydrolysis by endothelial-bound lipoprotein-lipase (LpL). FAs can be imported into the cardiomyocytes through passive diffusion, but this is a very slow process, and the uptake is facilitated by the presence of several FA transporters, including fatty acid translocase (FAT)/CD36, FA transport protein (FATP), and plasma membrane FA-binding protein (FABP_{pm}) (Fig. 2). Of these FA transporters, CD36 is the best characterized due to its key role in FA translocation. Thus, studies using CD36-null mice have demonstrated that this transporter is responsible for up to 70% of FA uptake in contracting cardiomyocytes [46]. Once within the cytosol, approximately 75% of FAs are transferred into the mitochondria and oxidized for ATP generation, while the remainder is converted to triglycerides for storage. Long-chain FAs cannot freely enter

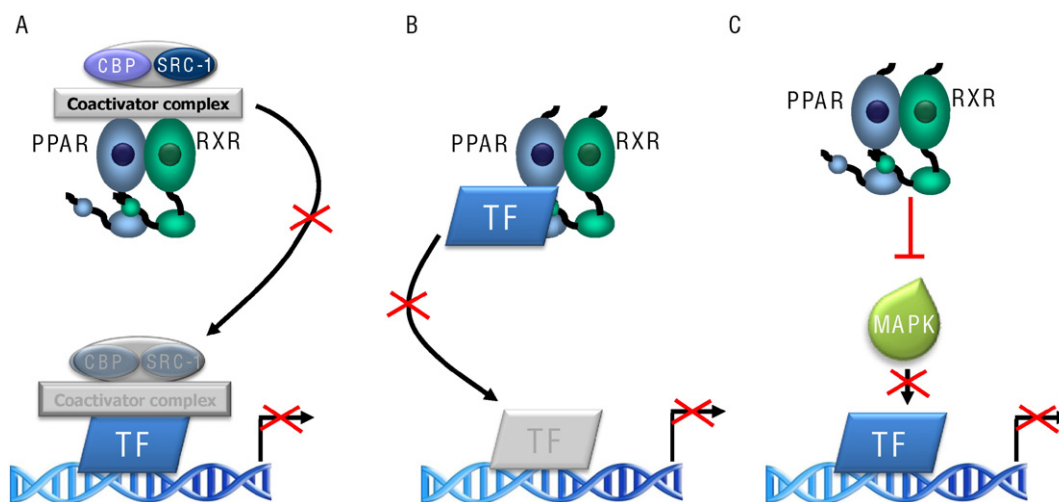


Fig. 2. PPAR-dependent transrepression mechanism. Most of the anti-inflammatory effects of PPARs are likely mediated through this DNA-independent mechanism. Three main transrepression mechanisms have been described for PPARs. A, PPARs compete for limiting amounts of co-activator proteins – such as cAMP response element binding (CREB)-binding protein (CBP) and steroid receptor co-activator (SRC1) – reducing the availability of these co-activators to other transcription factors (TF). B, PPARs associate physically with other TF, preventing the binding of this TF to its response elements and thereby inhibits its ability to induce gene transcription. C, PPARs inhibit the activation of a mitogen-activated protein kinase (MAPK), resulting in the attenuation of the activity of the MAPK for phosphorylating and activating TF.

the mitochondria and need to be esterified into fatty acyl-coenzyme A (CoA) by cytosolic fatty acyl-CoA synthetase (ACS). The acyl group of fatty acyl-CoA can be transferred to carnitine via carnitine palmitoyltransferase 1 (CPT-1) and the acylcarnitine is then shuttled into the mitochondria by carnitine translocase to undergo β -oxidation, producing acetyl-CoA, which can be used in the tricarboxylic acid (TCA) cycle to produce ATP. The rate of FA uptake by the heart is largely determined by plasma FFA levels, and patients with diabetes and metabolic syndrome have elevated circulating plasma FFA [47,48], promoting greater FFA uptake by the heart. If FA uptake exceeds the requirements for energy production, these FA accumulate as lipid metabolites leading to accumulation of triglycerides and other more harmful lipids, such as diacylglycerol (a toxic lipid intermediate generated in triglyceride synthesis) and ceramide (whose de novo synthesis is initiated by the action of serine palmitoyl transferase on the saturated fatty acid palmitate) (Fig. 3). For instance, cardiac-specific overexpression of human LpL promotes increased FA uptake and utilization from circulating VLDL, causing cardiac lipid accumulation and dilated cardiomyopathy [49].

3.1. PPAR β/δ effects in FA transport and oxidation

Proteins involved in FA transport and oxidation are under the transcriptional control of PPAR β/δ . In fact, specific *knockout* of PPAR β/δ in cardiomyocytes decreased the basal expression of genes involved in FAO, including mitochondrial FA uptake (CPT-1), malonyl-CoA metabolism (malonyl-CoA decarboxylase), mitochondrial FA β -oxidation

(very-long-chain acyl-CoA dehydrogenase, long-chain acyl-CoA dehydrogenase), peroxisomal oxidation (acyl-CoA oxidase) and glucose oxidation (pyruvate dehydrogenase kinase 4) [8]. As a result of these changes, basal myocardial fatty acid oxidation was reduced and subsequent lipid accumulation was observed. In addition, these mice displayed cardiac dysfunction, cardiac hypertrophy and congestive heart failure with reduced survival. In another mouse model, short-term PPAR β/δ specific deletion in the adult heart confirmed the role of this nuclear receptor in transcriptional regulation of FAO as well as in glucose oxidation, showing a reduction in both cardiac fatty acid and glucose oxidation rates [50]. It is worth noting that this study also demonstrated that PPAR β/δ has an important role in regulating endogenous antioxidants (Cu/Zn superoxide dismutase and manganese superoxide dismutase) and that the attenuation in the expression of these genes leads to increased oxidative damage to the heart. Moreover, expression of PGC-1 α , a transcriptional co-activator involved in FAO and a key mitochondrial biogenesis determinant, was decreased in the heart of these mice, concomitant with a reduction in mitochondrial DNA copy number. As a result of PPAR β/δ deficiency in the adult heart, depressed cardiac performance and cardiac hypertrophy were observed in this model. On the other hand, constitutive cardiomyocyte-specific expression of PPAR β/δ (driven by the myosin heavy chain promoter, MHC-PPAR β/δ mice) induced the expression of FAO-associated genes and did not lead to lipid accumulation and cardiac dysfunction, in contrast to that observed in MHC-PPAR α mice [51]. Besides the role of elevated FAO in the prevention of fatty acid accumulation

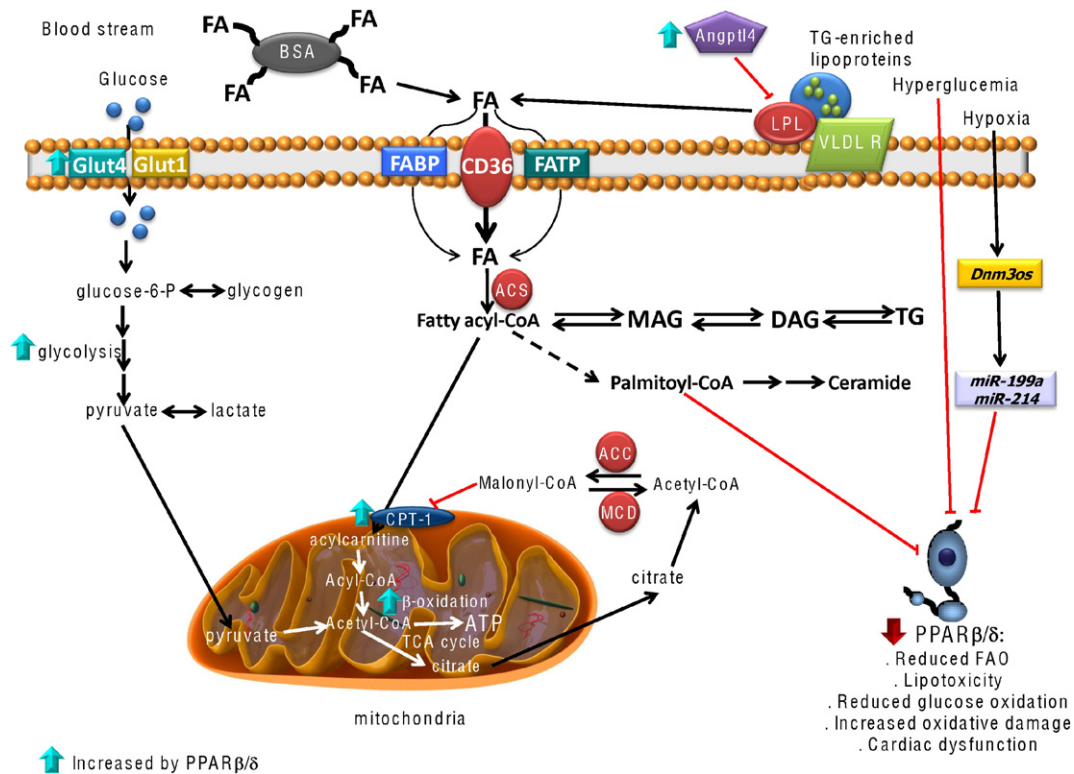


Fig. 3. Effects of PPAR β/δ activation on cardiac and glucose metabolic pathways. Fatty acids (FA) derived from triglyceride-rich lipoproteins, chylomicrons, and VLDL are hydrolyzed by lipoprotein lipase (LpL). This lipase is inhibited by angiopoietin-like 4 (Angptl4). Lipoprotein-derived FA or albumin-bound free FA are internalized by the cells via membrane receptors such as CD36 or other transporters (FA transport protein, FATP; FA-binding protein, FABP). Internalization of whole lipoproteins is also possible through the VLDL receptor (VLDL-R). Once inside the cardiomyocyte, FA are converted to fatty acyl-CoAs by acyl-CoA synthetase (ACS), which can either be stored as triglycerides or imported into mitochondria for β -oxidation. Triglyceride synthesis is achieved in several steps by incorporating them into a glycerol backbone forming mono- (monoacylglycerol, MAG), di- (diacylglycerol, DAG) and triacylglycerol or triglycerides (TG). The stored TG can be made available for oxidation by its hydrolysis into DAG and MAG, releasing fatty acyl-CoA that can be oxidized into the mitochondria. The de novo synthesis of ceramide is initiated by palmitoyl-CoA. Carnitine palmitoyltransferase 1 (CPT-1) converts acyl-CoA into acylcarnitine, which then crosses the outer mitochondrial membrane. This is the first step in mitochondrial fatty acid β -oxidation. CPT-1 activity is inhibited by malonyl-CoA, which is formed via carboxylation of acetyl-CoA by acetyl-CoA carboxylase (ACC). The effect of PPAR β/δ -mediated upregulation is shown by blue arrows. Palmitate, hyperglycemia, and hypoxia have been reported to reduce PPAR β/δ levels in cardiomyocytes, causing deleterious effects that can result in cardiac dysfunction. MCD: malonyl-CoA decarboxylase. TCA, tricarboxylic acid.

and heart dysfunction in the MHC-PPAR β/δ mouse, the increased expression of the LpL inhibitor angiopoietin-like 4 may also contribute by attenuating FA uptake [52] (Fig. 3). It is worth pointing out that the expression of genes involved in cellular FA transport (CD36 and FATP1) was activated in hearts of MHC-PPAR α , but not in MHC-PPAR β/δ mice. In contrast, cardiac glucose transport and glycolytic genes were activated in MHC-PPAR β/δ mice, but repressed in MHC-PPAR α mice. This increased capacity for myocardial glucose utilization in MHC-PPAR β/δ mice may explain the reduction in myocardial injury due to ischemia/reperfusion in these mice compared to the MHC-PPAR α mice. More recently, PPAR β/δ activation in the adult heart by generating a transgenic mouse model expressing a constitutively active form of PPAR β/δ upon tamoxifen administration in a tissue-specific manner [53] resulted in enhanced expression of genes involved in FAO and endogenous antioxidants, increased mitochondrial DNA copy number and elevated cardiac performance. Moreover, PPAR β/δ activation improved cardiac function and attenuated progression to cardiac hypertrophy induced by pressure-overload stimuli. Consistent with genetic approaches, PPAR β/δ ligands (L-165,041, GW501516 and GW0742) increased the expression of genes involved in FAO and FA oxidation rates in both neonatal and adult cardiomyocytes as well as in embryonic rat heart-derived H9c2 cells [17,54].

Given the important role of PPAR β/δ in regulating FAO, the reduction of its expression or activity might lead to activation of pathological processes causing cardiac dysfunction. By regulating the stability and translation of messenger RNAs by base-pairing with the 3' UTRs, small noncoding RNAs (~18–24 nucleotides), such as microRNAs (miRNAs, miRs), have emerged as important regulators of gene expression in cardiac disease [55]. Interestingly, PPAR β/δ levels are strongly repressed by the miRNA cluster *miR-199a~214*, embedded in chromosome 1 in a large noncoding RNA, *Dnm3os* [56] (Fig. 2). Moreover, myocardial hypoxia, a characteristic of heart failure, provokes activation of *Dnm3os* and the subsequent increase in the expression of the miRNA cluster *miR-199a~214* that decreases PPAR β/δ protein levels and mitochondrial FAO. These changes facilitate a metabolic shift from predominant reliance on FAO in the healthy myocardium towards increased reliance on glucose metabolism at the onset of heart failure. Likewise, exposure of neonatal cardiomyocytes to the saturated FA palmitate, but not the monounsaturated FA oleate, downregulates the protein levels of both CPT-1 β and PPAR β/δ [57] (Fig. 2), suggesting that palmitate can exacerbate lipotoxicity by reducing FAO. Similarly, it has been reported that hyperglycemia reduces PPAR β/δ levels in cardiomyocytes through a mechanism that might involve ROS production or MAPK activation [58].

On the other hand, activation of PPAR β/δ can also improve some cardiac pathologies linked to reductions in FAO. Thus, cardiac hypertrophy is associated with an increase in glucose utilization and a decrease in FAO, which is characteristic of the fetal heart [59]. It is still a matter of controversy whether changes in intracellular substrate and metabolite levels in cardiomyocytes are a consequence or the reason for cardiac hypertrophy. However, several factors support a role for cardiac metabolism in the development of cardiac hypertrophy. Thus, defects in mitochondrial FAO enzymes cause childhood hypertrophic cardiomyopathy [60], and perturbation of FAO in animal models cause cardiac hypertrophy [61], demonstrating that substrate utilization is important in the pathogenesis of hypertrophy. We have reported that PPAR β/δ activation prevents hypertrophy in neonatal rat cardiomyocytes [62]. More recently it has been reported that PPAR β/δ activation in the adult heart improved cardiac performance and reduced fibrosis and mitochondrial abnormalities in mice subjected to pressure-overload cardiac hypertrophy [53]. Therefore, PPAR β/δ ligands might prevent cardiac hypertrophy, a process that although initially is compensatory for an increase in workload in the setting of several pathologies (hypertension, valvular heart disease, etc.), when prolonged frequently results in congestive heart failure, arrhythmia, and sudden death [63].

4. Signaling effects of lipids promoting cardiac dysfunction

Although lipids are important to meet the heart's demand for energy, allowing its function, an excess of lipids, both in amount or distribution, can also be detrimental and may lead to cardiac dysfunction, due to abnormal cardiac structure and function. This cardiac lipotoxicity can be the result of the activation of different pathological processes by several lipids (including FA, ceramide and diacylglycerol [64]), that can be regulated by PPAR β/δ .

4.1. PPAR β/δ effects in apoptosis pathways

Apoptosis, among other factors, is involved in the development of myocardial dysfunction [65]. Saturated FA can induce apoptosis by several mechanisms in isolated cardiomyocytes, including accumulation of the toxic lipid ceramide or by activating endoplasmic reticulum (ER) stress [66]. Recently it has been reported that palmitate-induced apoptosis in neonatal cardiomyocytes was prevented by PPAR β/δ ligands as well as by AMP-activated protein kinase (AMPK) activators through its ability to prevent an increase in IL-6 levels [57]. AMPK is a master regulator of mechanisms relevant to cardiac energy production by regulating glucose and fatty acid metabolism, but it also regulates mitochondrial function, ER stress, autophagy and apoptosis [67]. It is worth noting that activation of AMPK attenuates the apoptotic effect of palmitate on cardiomyocytes [68]. This effect has been attributed to the ability of AMPK to phosphorylate and inactivate acetyl-CoA carboxylase (ACC), decreasing the intracellular concentration of malonyl-CoA. Since malonyl-CoA is a negative regulator of CPT-1, AMPK promotes FAO by reducing the accumulation of toxic FA derivatives. Interestingly, we [69] and others [70] have previously reported that PPAR β/δ activates AMPK in skeletal muscle cells, but it remains to be determined whether PPAR β/δ ligands prevent palmitate-induced apoptosis in cardiac cells through a mechanism involving this kinase.

Chronic ER stress contributes to apoptotic cell death in the myocardium, thereby playing a critical role in the development of cardiomyopathy [71]. Activation of the unfolded protein response (UPR) initially aims to mitigate adverse effects of ER stress and thus enhance cell survival by halting general mRNA translation, facilitating protein degradation via the ER-associated degradation (ERAD) pathway and enhancing the production of molecular chaperones involved in protein folding. If ER stress is limited, the UPR will potentiate autophagy to protect the cells [72]. This pro-survival pathway has evolved as an alternative mechanism for saving nutrients, recycling intracellular components and eliminating abnormal protein aggregates and misfolded proteins formed during the ER stress that cannot be removed through the ERAD pathway. However, if ER stress is not mitigated within a certain time period or the disturbance is prolonged, then the UPR will turn on apoptosis to remove cells that threaten the integrity of the organism [73]. Cardiomyocytes rarely proliferate within the adult heart and, as a consequence, their loss due to apoptosis may play an essential pathogenic role during cardiovascular diseases [71].

It has been reported that exposure to a high-fat diet (HFD) induces cardiomyocyte apoptosis via the inhibition of autophagy and the promotion of ER stress [74]. Interestingly, we have reported that PPAR β/δ activation by GW501516 prevented palmitate-induced ER stress in human AC16 cardiac cells [75]. Although AMPK activation inhibits ER stress and autophagy [67], the effect of GW501516 on palmitate-induced ER stress occurred in an AMPK-independent manner. In addition, we also found that PPAR β/δ activation by GW501516 upregulated the protein levels of beclin 1 and LC3-II, two well-known markers of autophagy, in cardiac cells [75]. In accordance with this, PPAR β/δ knockout mice also displayed a reduction in autophagic markers, which indicates that this nuclear receptor plays a key role in the control of the autophagic process in cardiac cells.

Although it is believed that palmitate-induced apoptosis is not associated with increased ROS in neonatal rat cardiomyocytes [76], it has

been reported that the PPAR β/δ ligands prevent oxidative stress-induced apoptosis in cardiac cells by increasing the expression of the antioxidative enzyme catalase [77]. More recently, it has been suggested that the PPAR β/δ ligand GW0742 protects cardiac myocytes from oxidative stress-induced apoptosis through its ability to prevent the increase in the expression of the metalloproteinases 2 and 9, an effect that was blunted in the presence of the PPAR β/δ antagonist GSK0660 [78]. Since oxidative stress is an important contributing factor in the pathogenesis of ischemic heart disease and heart failure, it has been suggested that this nuclear receptor might represent a new target for oxidative stress-induced cardiac dysfunction.

Although it has been suggested that inhibition of FAO might be useful for protecting the heart from the consequences of ischemia and ischemia–reperfusion injury [1,3], *in vivo* activation of PPAR β/δ protects the heart from ischemia–reperfusion injury in Zucker fatty rats through several mechanisms, including attenuation of lipotoxicity (PPAR β/δ activation increased cardiac FAO and ameliorated the downregulation of CD36, CPT-1 and β -oxidation gene expression caused by ischemia–reperfusion injury) and upregulation of the prosurvival signaling (Akt signaling pathway and Bcl family genes) in the heart [79].

4.2. PPAR β/δ effects in lipid-induced defective insulin signaling

One of the earliest disturbances observed in the heart following exposure to a HFD is the development of insulin resistance [80], which leads to increased left-ventricle remodeling and dysfunction [81]. Lipid accumulation in the heart results in cardiomyocyte insulin resistance, which is characterized by increased FA uptake and decreased glucose uptake [82–86]. Therefore, defective insulin signaling might exacerbate lipotoxic cardiomyopathy. In human patients with type 2 diabetes mellitus and heart failure, a dramatic accumulation of lipids within the myocardium has also been observed [87]. The fact that lipid accumulation is also observed in the heart of diabetic patients with normal cardiac function suggests that metabolic disturbances precede the development of ventricular dysfunction [88]. In these patients and those with metabolic syndrome, circulating FA and triglyceride levels are significantly elevated [89]. This is the result of the consumption of high levels of FA as part of the Western diet and the presence of obesity. Under these conditions, the storage capacity of fat depots in the body is exceeded, increased lipolysis of fat releases FA to the blood, and this leads to enhanced secretion of triglyceride-enriched lipoproteins (VLDL) by the liver. In contrast to glucose, whose uptake is tightly regulated by the action of insulin, FA uptake in the heart is not hormonally regulated and depends on the availability of FA in the circulation [90]. Thus, the type 2 diabetic heart increases the rate of FA uptake, leading to reliance on FAs as the main energy source, but also provokes the accumulation of FA-derived complex lipids (mainly ceramide and diacylglycerol). In contrast to what it has been observed in cardiac hypertrophy, the accumulation of cardiac FA-derived complex lipids in the setting of diabetes is not the result of impaired mitochondrial FAO, quite the opposite, studies in animals [91,92] and humans [93,94] have shown that myocardial FAO is increased in diabetic states. Thus, in this pathology, oversupply of FA is responsible for the accumulation of lipid intermediates in the heart as the result of the incapacity of FA oxidation to compensate the high rates of FA uptake.

The mechanisms underlying the lipid-derived attenuation of the insulin signaling pathway have not been completely elucidated; however, several mechanisms have been suggested based on findings in cells other than cardiomyocytes. Thus, accumulation of FA-derivatives fatty acyl-CoA, diacylglycerol and ceramide attenuates insulin signaling through the activation of serine kinases such as protein kinase C (PKC), inhibitor κ B kinase β (IKK β), c-Jun N-terminal kinase (JNK) and mammalian target of rapamycin (mTOR) [95–99]. Binding of insulin to its receptor leads to the subsequent phosphorylation of its substrates including insulin receptor substrate 1 (IRS1) on tyrosine residues. These phosphorylated tyrosine residues provide specific docking sites for

other signaling proteins, leading to the activation of downstream signaling molecules, including phosphoinositide-3-kinase (PI3K), that finally result in Akt phosphorylation and glucose uptake. However, phosphorylation of IRS-1 on serine residues by lipid-activated kinases interferes with the functional domains of IRS1 and, for instance, reduces the binding between IRS1 and PI3K, thereby negatively regulating insulin signaling.

Ceramide-mediated insulin resistance can also be mediated by its ability to activate protein phosphatase 2A, thereby leading to dephosphorylation of Akt [99]. In a heart model of cardiac lipotoxicity induced by heart specific expression of LpL, the inhibitor of *de novo* synthesis of ceramide myriocin or heterozygosity for one of the subunits of serine palmitoyltransferase, which is involved in ceramide synthesis, improved cardiac function and corrected cardiac hypertrophy [100].

Cardiac insulin resistance is mimicked by cardiac specific overexpression of PPAR α in MHC-PPAR α mice [51]. It has been proposed that despite the increased capacity of diabetic hearts and MHC-PPAR α hearts to oxidize FA, FAO rates are insufficient to match the high rates of FA uptake and esterification, leading to accumulation of the toxic lipid derivatives diacylglycerol and ceramide. As mentioned above, MHC-PPAR β/δ did not develop myocyte lipid accumulation or cardiomyopathy, even when fed a HFD [51].

On the other hand, PPAR β/δ activation can prevent the deleterious effects of the accumulation of FA-derivatives by increasing FAO, thereby reducing the availability of FAs to be stored in the form of complex lipids. In fact, we have observed in C2C12 myotubes that PPAR β/δ activation reduced palmitate-induced diacylglycerol accumulation and insulin resistance [101].

Generation of ROS also plays a major role in the development of insulin resistance [102] and given that ROS generation can reduce PPAR β/δ levels in the heart [58], the ROS-mediated reduction of this nuclear receptor can exacerbate insulin resistance and FA accumulation.

4.3. PPAR β/δ effects in lipid-induced inflammation

Owing to its fat content, the classical Western diet has a range of adverse effects on the heart, including enhanced inflammation. Pro-inflammatory factors such as tumor necrosis factor α (TNF- α), monocyte chemoattractant protein-1 (MCP-1), and IL-6, can exert several autocrine pleiotropic effects in cardiac cells that may contribute to states that are associated with myocardial inflammation, including myocardial injury, heart failure, and dilated cardiomyopathy [103, 104]. Pro-inflammatory cytokines are under the transcriptional control of the ubiquitous inducible nuclear factor- κ B (NF- κ B), which is activated in myocarditis, congestive heart failure, and cardiac hypertrophy [105].

As mentioned above, an increase in glucose utilization and a decrease in FAO are observed during cardiac hypertrophy and congestive heart failure [106]. Interestingly, the changes that cardiac hypertrophy causes in the expression of genes involved in fatty acid metabolism were not observed when NF- κ B activity was inhibited [107–109]. These data pointed to the involvement of the pro-inflammatory transcription factor NF- κ B in the downregulation of FAO during cardiac hypertrophy. The mechanism by which activation of NF- κ B results in reduced expression of FAO genes seems to involve a dramatic reduction in the binding of PPAR β/δ to the PPRE. This reduction was partially reversed by co-incubation of the cells with NF- κ B inhibitors. Therefore, the reduced DNA-binding activity of PPAR β/δ seems to be related to the activation of NF- κ B in cardiac cells. NF- κ B is present in the cytoplasm as an inactive heterodimer that consists mostly of the p50 and p65 subunits. However, after activation, this heterodimer translocates to the nucleus and regulates the expression of genes involved in inflammatory and immune processes. Our results indicated that once the p65 subunit of NF- κ B reaches the nucleus it interacts with PPAR β/δ . This association prevents PPAR β/δ from binding to its response element, and thereby inhibits its ability to induce gene transcription (Fig. 4). It has also been

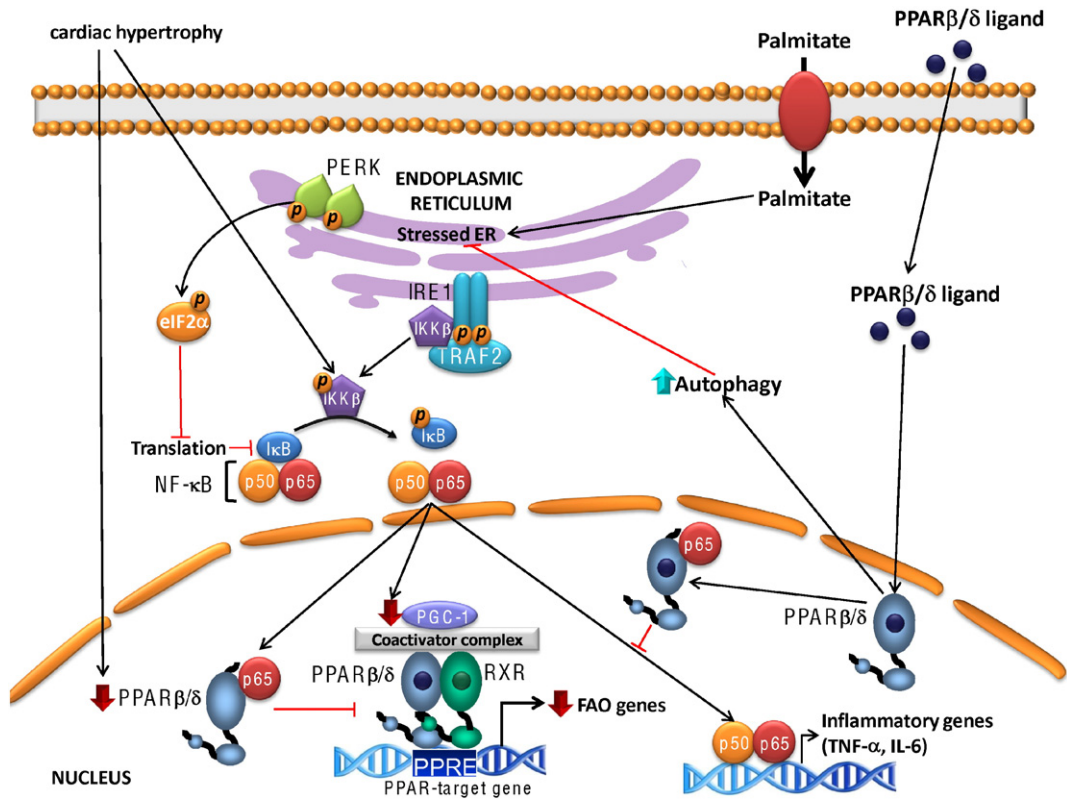


Fig. 4. Inflammation is involved in the reduction in FAO observed during cardiac hypertrophy and PPAR β/δ activation attenuates myocardial inflammatory responses. Cardiac hypertrophy activates the pro-inflammatory transcription factor NF- κ B, which in turn interacts with PPAR β/δ and reduces its DNA-binding activity causing a decrease in the expression of the genes involved in FAO. Alternatively, pressure-overload cardiac hypertrophy reduces protein levels of PPAR β/δ . Inflammatory and hypertrophic stimuli, such as TNF- α , can reduce the expression of FAO genes by decreasing the levels of the transcriptional co-activator PGC-1 α through NF- κ B activation. FA overload results in the induction of ER stress and the subsequent activation of inflammatory pathways. Thus, during ER stress, protein kinase R (PKR)-like ER kinase (PERK)–eukaryotic initiation factor 2 α (eIF2 α) pathway activation and, thus, protein translation inhibition, together with the shorter half-life of I κ B α compared with that of NF- κ B, results in a reduction in the I κ B α /NF- κ B ratio, leading to nuclear NF- κ B translocation and a consequent increase in the expression of pro-inflammatory genes. In addition, following activation of ER stress, the cytoplasmic domain of phosphorylated inositol-requiring enzyme 1 α (IRE-1 α) recruits TNF- α receptor-associated factor 2 (TRAF2), forming a complex that interacts and activates I κ B kinase (IKK β), leading to NF- κ B activation. PPAR β/δ activation prevents lipid-induced NF- κ B activation by interacting with the p65 subunit of NF- κ B, thereby reducing its availability to increase the expression of pro-inflammatory genes. It also prevents palmitate-induced ER stress and inflammation by increasing the expression of autophagic markers. PPRE, peroxisome proliferator response element.

reported that PPAR β/δ ligands and overexpression of this nuclear receptor suppressed myocardial inflammatory responses, such as the lipopolysaccharide-mediated production of TNF α . This had beneficial effects on animals that had undergone ischemia/reperfusion injury or cardiac hypertrophy [110].

The shift in glucose metabolism observed during cardiac hypertrophy induced by the TNF- α may also involve PPAR β/δ through the down-regulation of the transcriptional co-activator PGC-1 α [111]. In the myocardium, PGC-1 α may co-activate PPAR α and PPAR β/δ subtypes, although it also interacts with and co-activates the estrogen-related receptor α (ERR α) [112]. We have reported that exposure of cardiac cells to TNF- α activates both p38 MAPK and NF- κ B, causing PGC-1 α down-regulation (Fig. 4). This results in an elevated glucose oxidation rate, which involves a reduction in pyruvate dehydrogenase kinase 4, an inhibitor of the key glycolytic enzyme pyruvate dehydrogenase, caused by the reduction of the DNA-binding activity of both PPAR β/δ and estrogen-related receptor α (ERR α).

We have also evaluated whether PPAR β/δ activation prevents the inflammatory processes induced in the heart of mice fed a HFD for 3 weeks [113]. This short period of exposure was selected to study the specific effects of lipid-induced inflammation on the heart, while avoiding other confounding factors such as obesity and established insulin resistance. The HFD induced the expression of TNF- α , MCP-1 and IL-6, and promoted the activity of NF- κ B in the heart of mice. Interestingly, the PPAR β/δ agonist GW501516 abrogated this enhanced inflammatory profile. Moreover, since many inconsistencies have been observed when results obtained with murine models have been

extrapolated to humans, we used AC16 cells, a cardiac cell line of human origin, and exposed them to palmitate. This is of interest, given that PPARs are known to be expressed at lower levels in human cells than in rodent cells [114], and gene expression is also differentially regulated by PPARs in human versus rodent cells [115]. When human cardiac AC16 cells were incubated with palmitate in the presence of GW501516, similar results were obtained to those reported in the heart of mice exposed to the HFD. Activation of PPAR β/δ in AC16 cells enhanced the physical interaction between PPAR β/δ and the p65 subunit of NF- κ B, suggesting that this was the mechanism that interferes with NF- κ B transactivation in the heart of mice exposed to a HFD.

Accumulation of FAs has been linked to the induction of ER stress and this process intersects with many different inflammatory signaling pathways, including the NF- κ B pathway [116]. Thus, UPR activation results in a general repression of mRNA translation. Since inhibitor of κ B (I κ B), which inhibits NF- κ B, has a shorter half-life than NF- κ B, UPR activation shifts the I κ B/NF- κ B ratio, thereby releasing NF- κ B, which translocates to the nucleus and increases the expression of its target genes, such as IL-6 and TNF- α [117]. In addition, in response to ER stress, the cytoplasmic domain of phosphorylated inositol-requiring enzyme 1 α (IRE-1 α) can recruit TNF- α receptor-associated factor 2, forming a complex that interacts with and activates I κ B kinase, leading to NF- κ B activation [117,118]. In AC16 cells we have reported that the PPAR β/δ agonist GW501516 attenuated palmitate-induced ER stress [75]. Although we have recently reported that PPAR β/δ activation by GW501516 prevents palmitate-induced ER stress by activating AMPK in myotubes [69], in cardiac cells the effect of GW501516 seems to be

independent of AMPK. In addition, ER stress induced by an HFD in the heart of mice was exacerbated in PPAR β/δ -deficient mice. As mentioned above, PPAR β/δ activation by GW501516 upregulated markers of autophagy in cardiac cells and PPAR β/δ knockout mice also displayed a reduction in autophagic markers [75]. Based on these findings and considering our previous data showing that PPAR β/δ can limit myocardial inflammation by NF- κ B inhibition [113], we hypothesized that GW501516 might prevent palmitate-induced ER stress and inflammation in human cardiac cells by inducing autophagy (Fig. 3). In fact, studies performed in mice fed an HFD reported that autophagy is down-regulated in adipose tissue [119] and in the heart [120]. The former study also demonstrated that suppression of autophagy induces the inflammatory response via ER stress activation, while the opposite, that is activation of autophagy with rapamycin, decreases inflammatory gene expression [119]. These effects of PPAR β/δ on autophagy have important implications in cardiac disease since suppression of autophagy favors the development of heart failure during diabetes [121], whereas its induction may reduce myocardial ischemia/reperfusion-induced lethal injury [72].

5. Concluding remarks

Cardiac energy metabolism to assure constant pumping of the heart mainly relies on the oxidation of FAs. The reduction in cardiac FAO promotes the accumulation of FA derivatives that can alter cellular structures and activate downstream pathways leading to cardiac inflammation and toxicity. Moreover, despite its preference for FAs, the heart is also vulnerable to the pathological effects of FA overload. Therefore, dysregulation in cardiac FA metabolism leads to cardiac dysfunction.

PPAR β/δ is endowed with the dual capacity to modulate both FA metabolism and inflammation. A reduction in the activity of this nuclear receptor might be involved in the development of several cardiac disorders, whereas its activation by ligands may offer a therapeutic approach to attenuate both cardiac disorders caused by FAO inhibition and lipid-activated signaling pathways that promote cardiac dysfunction. Despite the abundance of preclinical data supporting the notion that treatment with PPAR β/δ ligands offers protection to the heart in several cardiac disorders, there is still a gap to bridge between preclinical data and clinical trials that needs filling in the future to clearly demonstrate the beneficial effects of these ligands in the clinical setting.

Transparency document

The [Transparency document](#) associated with this article can be found, in online version.

Acknowledgments

Funding support for the authors is from the Ministerio de Economía y Competitividad of the Spanish Government (SAF2012-30708) and CIBER de Diabetes y Enfermedades Metabólicas Asociadas (CIBERDEM) (ISCIII CB07/08/0003). CIBERDEM is an initiative of the Instituto de Salud Carlos III (ISCIII) – Ministerio de Economía y Competitividad. We thank the University of Barcelona's Language Advisory Service for editing the manuscript.

References

- G.D. Lopaschuk, J.R. Ussher, C.D. Folmes, J.S. Jaswal, W.C. Stanley, Myocardial fatty acid metabolism in health and disease, *Physiol. Rev.* 90 (2010) 207–258.
- P.M. Barger, D.P. Kelly, PPAR signaling in the control of cardiac energy metabolism, *Trends Cardiovasc. Med.* 10 (2000) 238–245.
- G.W. Goodwin, C.S. Taylor, H. Taegtmeyer, Regulation of energy metabolism of the heart during acute increase in heart work, *J. Biol. Chem.* 273 (1998) 29530–29539.
- F. Di Lisa, M. Canton, R. Menabò, N. Kaludercic, P. Bernardi, Mitochondria and cardioprotection, *Heart Fail. Rev.* 12 (2007) 249–260.
- H. Taegtmeyer, P. McNulty, M.E. Young, Adaptation and maladaptation of the heart in diabetes: part I: general concepts, *Circulation* 105 (2002) 1727–1733.
- M.E. Young, P. McNulty, H. Taegtmeyer, Adaptation and maladaptation of the heart in diabetes: part II: potential mechanisms, *Circulation* 105 (2002) 1861–1870.
- I. Issemann, S. Green, Activation of a member of the steroid hormone receptor superfamily by peroxisome proliferators, *Nature* 347 (1990) 645–650.
- L. Cheng, G. Ding, Q. Qin, Y. Huang, W. Lewis, et al., Cardiomyocyte-restricted peroxisome proliferator-activated receptor- δ deletion perturbs myocardial fatty acid oxidation and leads to cardiomyopathy, *Nat. Med.* 10 (2004) 1245–1250.
- Nuclear Receptors Nomenclature Committee, A unified nomenclature system for the nuclear receptor superfamily, *Cell* 97 (1999) 161–163.
- A. Schmidt, N. Endo, S.J. Rutledge, R. Vogel, D. Shinar, et al., Identification of a new member of the steroid hormone receptor superfamily that is activated by a peroxisome proliferator and fatty acids, *Mol. Endocrinol.* 6 (1992) 1634–1641.
- F. Chen, S.W. Law, B.W. O'Malley, Identification of two mPPAR related receptors and evidence for the existence of five subfamily members, *Biochem. Biophys. Res. Commun.* 196 (1993) 671–677.
- S.A. Klierer, B.M. Forman, B. Blumberg, E.S. Ong, U. Borgmeyer, D.J. Mangelsdorf, et al., Differential expression and activation of a family of murine peroxisome proliferator-activated receptors, *Proc. Natl. Acad. Sci. U. S. A.* 91 (1994) 7355–7359.
- C.K. Glass, Going nuclear in metabolic and cardiovascular disease, *J. Clin. Invest.* 116 (2006) 556–560.
- O. Braissant, F. Fougère, C. Scotto, M. Dauca, W. Wahli, Differential expression of peroxisome proliferator-activated receptors (PPARs): tissue distribution of PPAR- α , - β , and - γ in the adult rat, *Endocrinology* 137 (1996) 354–366.
- S. Kersten, J. Seydoux, J.M. Peters, F.J. Gonzalez, B. Desvergne, et al., Peroxisome proliferator-activated receptor α mediates the adaptive response to fasting, *J. Clin. Invest.* 103 (1999) 1489–1498.
- B. Desvergne, W. Wahli, Peroxisome proliferator-activated receptors: nuclear control of metabolism, *Endocr. Rev.* 20 (1999) 649–688.
- A.J. Gilde, K.A. van der Lee, P.H. Willemssen, G. Chinetti, F.R. van der Leij, G.J. van der Vusse, et al., Peroxisome proliferator-activated receptor (PPAR) α and PPAR β/δ , but not PPAR γ , modulate the expression of genes involved in cardiac lipid metabolism, *Circ. Res.* 92 (2003) 518–524.
- B.E. Teunissen, P.J. Smeets, P.H. Willemssen, L.J. De Windt, G.J. Van der Vusse, et al., Activation of PPAR δ inhibits cardiac fibroblast proliferation and the transdifferentiation into myofibroblasts, *Cardiovasc. Res.* 75 (2007) 519–529.
- J.N. Feige, L. Gelman, L. Michalik, B. Desvergne, W. Wahli, From molecular action to physiological outputs: peroxisome proliferator-activated receptors are nuclear receptors at the crossroads of key cellular functions, *Prog. Lipid Res.* 45 (2006) 120–159.
- G. Chinetti, J.C. Fruchart, B. Staels, Peroxisome proliferator-activated receptors (PPARs): nuclear receptors at the crossroads between lipid metabolism and inflammation, *Inflamm. Res.* 49 (2000) 497–505.
- P. Puigserver, B.M. Spiegelman, Peroxisome proliferator-activated receptor- γ coactivator 1 α (PGC-1 α): transcriptional coactivator and metabolic regulator, *Endocr. Rev.* 24 (2003) 78–90.
- R.A. Daynes, D.C. Jones, Emerging roles of PPARs in inflammation and immunity, *Nat. Rev. Immunol.* 2 (2002) 748–759.
- M. Li, G. Pascual, C.K. Glass, Peroxisome proliferator-activated receptor γ -dependent repression of the inducible nitric oxide synthase gene, *Mol. Cell. Biol.* 20 (2000) 4699–4707.
- Y. Kamei, L. Xu, T. Heinzel, J. Torchia, R. Kurokawa, B. Gloss, et al., A CBP integrator complex mediates transcriptional activation and AP-1 inhibition by nuclear receptors, *Cell* 85 (1996) 403–414.
- P. Delerive, K. De Bosscher, S. Besnard, W. Vandenberghe, J.M. Peters, F.J. Gonzalez, et al., Peroxisome proliferator-activated receptor α negatively regulates the vascular inflammatory gene response by negative cross-talk with transcription factors NF- κ B and AP-1, *J. Biol. Chem.* 274 (1999) 32048–32054.
- P. Delerive, F. Martin-Nizard, G. Chinetti, F. Trottein, J.C. Fruchart, J. Najib, et al., Peroxisome proliferator-activated receptor activators inhibit thrombin-induced endothelin-1 production in human vascular endothelial cells by inhibiting the activator protein-1 signaling pathway, *Circ. Res.* 85 (1999) 394–402.
- P. Desreumaux, L. Dubuquoy, S. Nutten, M. Peuchmaur, W. Englaro, K. Schoonjans, et al., Attenuation of colon inflammation through activators of the retinoid X receptor (RXR)/peroxisome proliferator-activated receptor γ (PPAR γ) heterodimer. A basis for new therapeutic strategies, *J. Exp. Med.* 193 (2001) 827–838.
- T.E. Johnson, M.K. Holloway, R. Vogel, S.J. Rutledge, J.J. Perkins, et al., Structural requirements and cell-type specificity for ligand activation of peroxisome proliferator-activated receptors, *J. Steroid Biochem. Mol. Biol.* 63 (1997) 1–8.
- I. Takada, R.T. Yu, H.E. Xu, M.H. Lambert, V.G. Montana, et al., Alteration of a single amino acid in peroxisome proliferator-activated receptor- α (PPAR α) generates a PPAR δ phenotype, *Mol. Endocrinol.* 14 (2000) 733–740.
- H.E. Xu, M.H. Lambert, V.G. Montana, D.J. Parks, S.G. Blanchard, et al., Molecular recognition of fatty acids by peroxisome proliferator-activated receptors, *Mol. Cell* 3 (1999) 397–403.
- B.M. Forman, B. Ruan, J. Chen, G.J. Schroeffer Jr., R.M. Evans, The orphan nuclear receptor LXR α is positively and negatively regulated by distinct products of mevalonate metabolism, *Proc. Natl. Acad. Sci. U. S. A.* 94 (1997) 10588–10593.
- K. Yu, W. Bayona, C.B. Kallen, H.P. Harding, C.P. Ravera, et al., Differential activation of peroxisome proliferator-activated receptors by eicosanoids, *J. Biol. Chem.* 270 (1995) 23975–23983.
- G. Krey, O. Braissant, F. L'Horsset, E. Kalkhoven, M. Perroud, et al., Fatty acids, eicosanoids, and hypolipidemic agents identified as ligands of peroxisome proliferator-activated receptors by coactivator-dependent receptor ligand assay, *Mol. Endocrinol.* 11 (1997) 779–791.
- N. Shaw, M. Elholm, N. Noy, Retinoic acid is a high affinity selective ligand for the peroxisome proliferator-activated receptor β/δ , *J. Biol. Chem.* 278 (2003) 41589–41592.

- [35] A. Chawla, C.-H. Lee, Y. Barak, W. He, J. Rosenfeld, et al., PPAR δ is a very low-density lipoprotein sensor in macrophages, *Proc. Natl. Acad. Sci. U. S. A.* 100 (2003) 1268–1273.
- [36] M.L. Sznajdman, C.D. Haffner, P.R. Maloney, A. Fivush, E. Chao, et al., Novel selective small molecule agonists for peroxisome proliferator-activated receptor δ (PPAR δ)-synthesis and biological activity, *Bioorg. Med. Chem. Lett.* 13 (2003) 1517–1521.
- [37] J. Berger, M.D. Leibowitz, T.W. Doebber, A. Elbrecht, B. Zhang, et al., Novel peroxisome proliferator-activated receptor (PPAR) γ and PPAR δ ligands produce distinct biological effects, *J. Biol. Chem.* 274 (1999) 6718–6725.
- [38] B.G. Shearer, D.J. Steger, J.M. Way, T.B. Stanley, D.C. Lobe, et al., Identification and characterization of a selective peroxisome proliferator-activated receptor β/δ (NR1C2) antagonist, *Mol. Endocrinol.* 22 (2008) 523–529.
- [39] A.N. Billin, PPAR-beta/delta agonists for Type 2 diabetes and dyslipidemia: an adopted orphan still looking for a home, *Expert Opin. Investig. Drugs* 17 (2008) 1465–1471.
- [40] K. Iwasaki, M. Haimerl, Y.H. Paik, K. Taura, Y. Kodama, et al., Protection from liver fibrosis by a peroxisome proliferator-activated receptor δ agonist, *Proc. Natl. Acad. Sci. U. S. A.* 109 (2012) E1369–E1376.
- [41] B.G. Shearer, R.W. Wiethe, A. Ashe, A.N. Billin, J.M. Way, et al., Identification and characterization of 4-chloro-N-(2-[[5-(trifluoromethyl)-2-pyridyl]sulfonyl]ethyl)benzamide (GSK3787), a selective and irreversible peroxisome proliferator-activated receptor delta (PPARdelta) antagonist, *J. Med. Chem.* 53 (2010) 1857–1861.
- [42] P.S. Palkar, M.G. Borland, S. Naruhn, C.H. Ferry, C. Lee, et al., Cellular and pharmacological selectivity of the peroxisome proliferator-activated receptor-beta/delta antagonist GSK3787, *Mol. Pharmacol.* 78 (2010) 419–430.
- [43] G.M.P. Giordano Attianese, B. Desvergne, Integrative and systemic approaches for evaluating PPAR β/δ (PPARD) function, *Nucl. Recept. Signal.* 13 (2015), e001.
- [44] G.J. van der Vusse, M. van Bilsen, J.F. Glatz, Cardiac fatty acid uptake and transport in health and disease, *Cardiovasc. Res.* 45 (2000) 279–293.
- [45] B. Razani, H. Zhang, P.C. Schulze, J.D. Schilling, J. Verbsky, et al., Fatty acid synthase modulates homeostatic responses to myocardial stress, *J. Biol. Chem.* 286 (2011) 30949–30961.
- [46] D.D. Habets, W.A. Coumans, P.J. Voshol, M.A. den Boer, M. Febbraio, et al., AMPK-mediated increase in myocardial long-chain fatty acid uptake critically depends on sarcolemmal CD36, *Biochem. Biophys. Res. Commun.* 355 (2007) 204–210.
- [47] G.D. Lopaschuk, D.D. Belke, J. Gamble, T. Itoi, B.O. Schönekeess, Regulation of fatty acid oxidation in the mammalian heart in health and disease, *Biochim. Biophys. Acta* 1213 (1994) 263–276.
- [48] V.A. Kurien, M.F. Oliver, Free fatty acids during acute myocardial infarction, *Prog. Cardiovasc. Dis.* 13 (1971) 361–373.
- [49] H. Yagyu, G. Chen, M. Yokoyama, K. Hirata, A. Augustus, et al., Lipoprotein lipase (LpL) on the surface of cardiomyocytes increases lipid uptake and produces a cardiomyopathy, *J. Clin. Invest.* 111 (2003) 419–426.
- [50] P. Wang, J. Liu, Y. Li, S. Wu, J. Luo, et al., Peroxisome proliferator-activated receptor δ is an essential transcriptional regulator for mitochondrial protection and biogenesis in adult heart, *Circ. Res.* 106 (2010) 911–919.
- [51] E.M. Burkart, N. Sambandam, X. Han, R.W. Gross, M. Courtois, et al., Nuclear receptors PPARbeta/delta and PPARalpha direct distinct metabolic regulatory programs in the mouse heart, *J. Clin. Invest.* 117 (2007) 3930–3939.
- [52] A. Georgiadi, L. Lichtenstein, T. Degenhardt, M.V. Boekschoten, M. van Bilsen, et al., Induction of cardiac Angptl4 by dietary fatty acids is mediated by peroxisome proliferator-activated receptor beta/delta and protects against fatty acid-induced oxidative stress, *Circ. Res.* 106 (2010) 1712–1721.
- [53] J. Liu, P. Wang, J. Luo, Y. Huang, et al., Peroxisome proliferator-activated receptor β/δ activation in adult hearts facilitates mitochondrial function and cardiac performance under pressure-overload condition, *Hypertension* 57 (2011) 223–230.
- [54] L. Cheng, G. Ding, Q. Qin, Y. Xiao, D. Woods, et al., Peroxisome proliferator-activated receptor delta activates fatty acid oxidation in cultured neonatal and adult cardiomyocytes, *Biochem. Biophys. Res. Commun.* 313 (2004) 277–286.
- [55] H.E. Azzouzi, S. Leptidis, P.A. Doevendans, L.J. De Windt, HypoxamiRs: regulators of cardiac hypoxia and energy metabolism, *Trends Endocrinol. Metab.* 26 (2015) 502–508.
- [56] H. el Azzouzi, S. Leptidis, E. Dirckx, J. Hoeks, B. van Bree, et al., The hypoxia-inducible microRNA cluster miR-199a~214 targets myocardial PPAR δ and impairs mitochondrial fatty acid oxidation, *Cell Metab.* 18 (2013) 341–354.
- [57] T. Haffar, F.A. Bérubé-Simard, N. Boussette, Cardiomyocyte lipotoxicity is mediated by IL-6 and causes down-regulation of PPARs, *Biochem. Biophys. Res. Commun.* 459 (2015) 54–59.
- [58] B.C. Yu, C.K. Chang, H.Y. Ou, K.C. Cheng, J.T. Cheng, Decrease of peroxisome proliferator-activated receptor delta expression in cardiomyopathy of streptozotocin-induced diabetic rats, *Cardiovasc. Res.* 80 (2008) 78–87.
- [59] M.N. Sack, T.A. Rader, S. Park, J. Bastin, S.A. McCune, et al., Fatty acid oxidation enzyme gene expression is downregulated in the failing heart, *Circulation* 94 (1996) 2837–2842.
- [60] D.P. Kelly, A.W. Strauss, Inherited cardiomyopathies, *N. Engl. J. Med.* 330 (1994) 913–919.
- [61] H.C. Chiu, A. Kovacs, D.A. Ford, F.F. Hsu, R. Garcia, et al., A novel mouse model of lipotoxic cardiomyopathy, *J. Clin. Invest.* 107 (2001) 813–822.
- [62] A. Planavila, R. Rodríguez-Calvo, M. Jové, L. Michalik, W. Wahli, et al., Peroxisome proliferator-activated receptor beta/delta activation inhibits hypertrophy in neonatal rat cardiomyocytes, *Cardiovasc. Res.* 65 (2005) 832–841.
- [63] B.H. Lorell, B.A. Carabello, Left ventricular hypertrophy: pathogenesis, detection, and prognosis, *Circulation* 102 (2000) 470–479.
- [64] K. Drosatos, P.C. Schulze, Cardiac lipotoxicity: molecular pathways and therapeutic implications, *Curr. Heart Fail. Rep.* 10 (2013) 109–121.
- [65] K. Konstantinidis, R.S. Whelan, R.N. Kitsis, Mechanisms of cell death in heart disease, *Arterioscler. Thromb. Vasc. Biol.* 32 (2012) 1552–1562.
- [66] M. Park, A. Sabetski, Y. Kwan Chan, S. Turdi, G. Sweeney, Palmitate induces ER stress and autophagy in H9c2 cells: implications for apoptosis and adiponectin resistance, *J. Cell. Physiol.* 230 (2015) 630–639.
- [67] D. Qi, L.H. Young, AMPK: energy sensor and survival mechanism in the ischemic heart, *Trends Endocrinol. Metab.* 26 (2015) 422–429.
- [68] D.L. Hickson-Bick, L.M. Buja, J.B. McMillin, Palmitate-mediated alterations in the fatty acid metabolism of rat neonatal cardiac myocytes, *J. Mol. Cell. Cardiol.* 32 (2000) 511–519.
- [69] L. Salvadó, E. Barroso, A.M. Gómez-Foix, X. Palomer, L. Michalik, et al., PPAR β/δ prevents endoplasmic reticulum stress-associated inflammation and insulin resistance in skeletal muscle cells through an AMPK-dependent mechanism, *Diabetologia* 57 (2014) 2126–2135.
- [70] D.K. Krämer, L. Al-Khalili, B. Guigas, Y. Leng, P.M. Garcia-Roves, et al., Role of AMP kinase and PPARdelta in the regulation of lipid and glucose metabolism in human skeletal muscle, *J. Biol. Chem.* 282 (2007) 19313–19320.
- [71] T. Minamino, I. Komuro, M. Kitakaze, Endoplasmic reticulum stress as a therapeutic target in cardiovascular disease, *Circ. Res.* 107 (2010) 1071–1082.
- [72] G. Petrovski, S. Das, B. Juhasz, A. Kertesz, A. Tosaki, et al., Cardioprotection by endoplasmic reticulum stress-induced autophagy, *Antioxid. Redox Signal.* 14 (2011) 2191–2200.
- [73] H. Zhao, Y. Liao, T. Minamino, Y. Asano, M. Asakura, et al., Inhibition of cardiac remodeling by pravastatin is associated with amelioration of endoplasmic reticulum stress, *Hypertens. Res.* 31 (2008) 1977–1987.
- [74] H.C. Hsu, C.Y. Chen, B.C. Lee, M.F. Chen, High-fat diet induces cardiomyocyte apoptosis via the inhibition of autophagy, *Eur. J. Nutr.* (Sep 10 2015).
- [75] X. Palomer, E. Capdevila-Busquets, G. Botteri, L. Salvadó, E. Barroso, et al., PPAR β/δ attenuates palmitate-induced endoplasmic reticulum stress and induces autophagic markers in human cardiac cells, *Int. J. Cardiol.* 174 (2014) 110–118.
- [76] D.L. Hickson-Bick, G.C. Sparagna, L.M. Buja, J.B. McMillin, Palmitate-induced apoptosis in neonatal cardiomyocytes is not dependent on the generation of ROS, *Am. J. Physiol. Heart Circ. Physiol.* 282 (2002) H656–H664.
- [77] M. Pesant, S. Sueur, P. Dutartre, M. Tallandier, P.A. Grimaldi, et al., Peroxisome proliferator-activated receptor delta (PPARdelta) activation protects H9c2 cardiomyoblasts from oxidative stress-induced apoptosis, *Cardiovasc. Res.* 69 (2006) 440–449.
- [78] E. Barlaka, A. Görbe, R. Gáspár, J. Pálóczi, P. Ferdinandy, et al., Activation of PPAR β/δ protects cardiac myocytes from oxidative stress-induced apoptosis by suppressing generation of reactive oxygen/nitrogen species and expression of matrix metalloproteinases, *Pharmacol. Res.* 95–96 (2015) 102–110.
- [79] T.L. Yue, S.S. Nerurkar, W. Bao, B.M. Jucker, L. Sarov-Blat, et al., In vivo activation of peroxisome proliferator-activated receptor-delta protects the heart from ischemia/reperfusion injury in Zucker fatty rats, *J. Pharmacol. Exp. Ther.* 325 (2008) 466–474.
- [80] S.Y. Park, Y.R. Cho, H.J. Kim, T. Higashimori, C. Danton, et al., Unraveling the temporal pattern of diet-induced insulin resistance in individual organs and cardiac dysfunction in C57BL/6 mice, *Diabetes* 54 (2005) 3530–3540.
- [81] M.J. Raheer, H.B. Thibault, E.S. Buys, D. Kuruppu, N. Shimizu, et al., A short duration of high-fat diet induces insulin resistance and predisposes to adverse left ventricular remodeling after pressure overload, *Am. J. Physiol. Heart Circ. Physiol.* 295 (2008) H2495–H2502.
- [82] P. Iozzo, P. Chareonthaitawee, D. Dutka, D.J. Betteridge, E. Ferrannini, et al., Independent association of type 2 diabetes and coronary artery disease with myocardial insulin resistance, *Diabetes* 51 (2002) 3020–3024.
- [83] P.K. Mazumder, B.T. O'Neill, M.W. Roberts, J. Buchanan, U.J. Yun, et al., Impaired cardiac efficiency and increased fatty acid oxidation in insulin-resistant ob/ob mouse hearts, *Diabetes* 53 (2004) 2366–2374.
- [84] M.E. Young, P.H. Guthrie, P. Razeghi, B. Leightner, S. Abbasi, et al., Impaired long-chain fatty acid oxidation and contractile dysfunction in the obese Zucker rat heart, *Diabetes* 51 (2002) 2587–2595.
- [85] O.J. How, E. Aasum, D.L. Severson, W.Y. Chan, M.F. Essop, et al., Increased myocardial oxygen consumption reduces cardiac efficiency in diabetic mice, *Diabetes* 55 (2006) 466–473.
- [86] D.D. Belke, S. Betuing, M.J. Tuttle, C. Graveleau, M.E. Young, et al., Insulin signaling coordinately regulates cardiac size, metabolism, and contractile protein isoform expression, *J. Clin. Invest.* 109 (2002) 629–639.
- [87] S. Sharma, J.V. Adrogue, L. Golfman, I. Uray, J. Lemm, et al., Intramyocardial lipid accumulation in the failing human heart resembles the lipotoxic rat heart, *FASEB J.* 18 (2004) 1692–1700.
- [88] H.E. Lebovitz, B. Ludvik, I. Yaniv, W. Haddad, T. Schwartz, et al., Fasting plasma triglycerides predict the glycaemic response to treatment of type 2 diabetes by gastric electrical stimulation. A novel lipotoxicity paradigm, *Diabet. Med.* 30 (2013) 687–693.
- [89] R.M. Krauss, Lipids and lipoproteins in patients with type 2 diabetes, *Diabetes Care* 27 (2004) 1496–1504.
- [90] D. An, B. Rodrigues, Role of changes in cardiac metabolism in development of diabetic cardiomyopathy, *Am. J. Physiol. Heart Circ. Physiol.* 291 (2006) H1489–H1506.
- [91] A. Onay-Besikci, S. Guner, E. Arioglu, I. Ozakca, A.T. Ozelcikay, et al., The effects of chronic trimetazidine treatment on mechanical function and fatty acid oxidation in diabetic rat hearts, *Can. J. Physiol. Pharmacol.* 85 (2007) 527–535.
- [92] V. Sharma, P. Dhillon, R. Wambolt, H. Parsons, R. Brownsey, et al., Metoprolol improves cardiac function and modulates cardiac metabolism in the streptozotocin-diabetic rat, *Am. J. Physiol. Heart Circ. Physiol.* 294 (2008) H1609–H1620.
- [93] L.R. Peterson, P. Herrero, K.B. Schechtman, S.B. Racette, A.D. Waggoner, et al., Effect of obesity and insulin resistance on myocardial substrate metabolism and efficiency in young women, *Circulation* 109 (2004) 2191–2196.

- [94] L.J. Rijzewijk, R.W. van der Meer, H.J. Lamb, H.W. de Jong, M. Lubberink, et al., Altered myocardial substrate metabolism and decreased diastolic function in nonischemic human diabetic cardiomyopathy: studies with cardiac positron emission tomography and magnetic resonance imaging, *J. Am. Coll. Cardiol.* 54 (2009) 1524–1532.
- [95] G.P. Sykiotis, A.G. Papavassiliou, Serine phosphorylation of insulin receptor substrate-1: a novel target for the reversal of insulin resistance, *Mol. Endocrinol.* 15 (2001) 1864–1869.
- [96] J.F. Tanti, J. Jager, Cellular mechanisms of insulin resistance: role of stress-regulated serine kinases and insulin receptor substrates (IRS) serine phosphorylation, *Curr. Opin. Pharmacol.* 9 (2009) 753–762.
- [97] J.K. Kim, J.J. Fillmore, M.J. Sunshine, B. Albrecht, et al., PKC- θ knockout mice are protected from fat-induced insulin resistance, *J. Clin. Invest.* 114 (2004) 823–827.
- [98] M. Yuan, N. Konstantopoulos, J. Lee, L. Hansen, et al., Reversal of obesity- and diet-induced insulin resistance with salicylates or targeted disruption of I κ B β , *Science* 293 (2001) 1673–1677.
- [99] B. Chaurasia, S.A. Summers, Ceramides – lipotoxic inducers of metabolic disorders, *Trends Endocrinol. Metab.* 26 (2015) 538–550.
- [100] T.S. Park, Y. Hu, H.L. Noh, K. Drosatos, K. Okajima, et al., Ceramide is a cardiotoxin in lipotoxic cardiomyopathy, *J. Lipid Res.* 49 (2008) 2101–2112.
- [101] T. Coll, D. Alvarez-Guardia, E. Barroso, A.M. Gómez-Foix, X. Palomer, et al., Activation of peroxisome proliferator-activated receptor- δ by GW501516 prevents fatty acid-induced nuclear factor- κ B activation and insulin resistance in skeletal muscle cells, *Endocrinology* 151 (2010) 1560–1569.
- [102] N. Houstis, E.D. Rosen, E.S. Lander, Reactive oxygen species have a causal role in multiple forms of insulin resistance, *Nature* 440 (2006) 944–948.
- [103] F.J. Neumann, I. Ott, M. Gawaz, G. Richardt, H. Holzapfel, et al., Cardiac release of cytokines and inflammatory responses in acute myocardial infarction, *Circulation* 92 (1995) 748–755.
- [104] A. Matsumori, T. Yamada, H. Suzuki, Y. Matoba, S. Sasayama, Increased circulating cytokines in patients with myocarditis and cardiomyopathy, *Br. Heart J.* 72 (1994) 561–566.
- [105] W.K. Jones, M. Brown, X. Ren, S. He, M. McGuinness, NF- κ B as an integrator of diverse signaling pathways: the heart of myocardial signaling? *Cardiovasc. Toxicol.* 3 (2003) 229–254.
- [106] Y. Kagaya, Y. Kanno, D. Takeyama, N. Ishide, Y. Maruyama, et al., Effects of long-term pressure overload on regional myocardial glucose and free fatty acid uptake in rats. A quantitative autoradiographic study, *Circulation* 81 (1990) 1353–1361.
- [107] A. Planavila, J.C. Laguna, M. Vázquez-Carrera, Nuclear factor- κ B activation leads to down-regulation of fatty acid oxidation during cardiac hypertrophy, *J. Biol. Chem.* 280 (2005) 17464–17471.
- [108] A. Planavila, J.C. Laguna, M. Vázquez-Carrera, Atorvastatin improves peroxisome proliferator-activated receptor signaling in cardiac hypertrophy by preventing nuclear factor- κ B activation, *Biochim. Biophys. Acta* 1687 (2005) 76–83.
- [109] P.J. Smeets, B.E. Teunissen, A. Planavila, H. de Vogel-van den Bosch, P.H. Willemsen, et al., Inflammatory pathways are activated during cardiomyocyte hypertrophy and attenuated by peroxisome proliferator-activated receptors PPAR α and PPAR δ , *J. Biol. Chem.* 283 (2008) 29109–29118.
- [110] G. Ding, L. Cheng, Q. Qin, S. Frontin, Q. Yang, et al., PPAR δ modulates lipopolysaccharide-induced TNF α inflammation signaling in cultured cardiomyocytes, *J. Mol. Cell. Cardiol.* 40 (2006) 821–828.
- [111] X. Palomer, D. Alvarez-Guardia, R. Rodríguez-Calvo, T. Coll, J.C. Laguna, et al., TNF- α reduces PGC-1 α expression through NF- κ B and p38 MAPK leading to increased glucose oxidation in a human cardiac cell model, *Cardiovasc. Res.* 81 (2009) 703–712.
- [112] B.N. Finck, D.P. Kelly, Peroxisome proliferator-activated receptor gamma coactivator-1 (PGC-1) regulatory cascade in cardiac physiology and disease, *Circulation* 115 (2007) 2540–2548.
- [113] D. Alvarez-Guardia, X. Palomer, T. Coll, L. Serrano, R. Rodríguez-Calvo, et al., PPAR β / δ activation blocks lipid-induced inflammatory pathways in mouse heart and human cardiac cells, *Biochim. Biophys. Acta* 1811 (2011) 59–67.
- [114] C.N. Palmer, M.H. Hsu, K.J. Griffin, J.L. Raucy, E.F. Johnson, Peroxisome proliferator activated receptor- α expression in human liver, *Mol. Pharmacol.* 53 (1998) 14–22.
- [115] J.W. Lawrence, Y. Li, S. Chen, J.G. DeLuca, J.P. Berger, et al., Differential gene regulation in human versus rodent hepatocytes by peroxisome proliferator-activated receptor (PPAR) α . PPAR α fails to induce peroxisome proliferation-associated genes in human cells independently of the level of receptor expression, *J. Biol. Chem.* 276 (2001) 31521–31527.
- [116] G.S. Hotamisligil, Endoplasmic reticulum stress and the inflammatory basis of metabolic disease, *Cell* 140 (2010) 900–917.
- [117] K. Zhang, R.J. Kaufman, From endoplasmic-reticulum stress to the inflammatory response, *Nature* 454 (2008) 455–462.
- [118] L. Salvadó, X. Palomer, E. Barroso, M. Vázquez-Carrera, Targeting endoplasmic reticulum stress in insulin resistance, *Trends Endocrinol. Metab.* 26 (2015) 438–448.
- [119] T. Yoshizaki, C. Kusunoki, M. Kondo, M. Yasuda, S. Kume, et al., Autophagy regulates inflammation in adipocytes, *Biochem. Biophys. Res. Commun.* 417 (2012) 352–357.
- [120] R. Guo, Y. Zhang, S. Turdi, J. Ren, Adiponectin knockout accentuates high fat diet-induced obesity and cardiac dysfunction: role of autophagy, *Biochim. Biophys. Acta* 1382 (2013) 1136–1148.
- [121] C. He, H. Zhu, H. Li, M.H. Zou, Z. Xie, Dissociation of Bcl-2–Beclin1 complex by activated AMPK enhances cardiac autophagy and protects against cardiomyocyte apoptosis in diabetes, *Diabetes* 62 (2013) 1270–1281.